Supporting Information

Photoswitchable azobenzene-appended iridium(III) complexes

J. Pérez-Miqueo,[a] A. Altube,[b] E. García-Lecina,[b] A. Tron,[c] N. McClenaghan,[c] Z. Freixa.*[a,d]

[a]Department of Applied Chemistry, Faculty of Chemistry, University of the Basque Country (UPV-EHU), San Sebastián, Spain. E-mail: Zoraida_freixa@ehu.eus
[b]Surfaces Division, IK4-CIDETEC, San Sebastián, Spain.
[c]Institut des Sciences Moléculaires, CNRS UMR 5255, University of Bordeaux, 33405 Talence, France .
[d]IKERBASQUE, Basque Foundation for Science, Bilbao, Spain.

Compound d. Synthesis and characterization.

SYNTHESIS

4-(Phenylazo)phenol (2.00 g, 10.1 mmol), (4-bromomethylphenyl)boronic acid pinacol ester (3.58 g, 12.1 mmol) and NaOH (0.80 g, 20.0 mmol) were dissolved in 170 mL of a degassed mixture of CH_3CN/CH_2Cl_2 (20:3, v/v). The solution was then stirred and refluxed (95 °C) for 2 days under N_2. The solution was cooled to room temperature and gravity-filtered to remove NaBr. After concentrating *in vacuo*, the resulting solid was purified by column chromatography (silica, CH_2Cl_2, Rf = 0.7). The title compound was obtained as an orange solid (2.70 g, 65%).

Elemental Analysis: calculated for $C_{25}H_{27}F_3BN_2O_3$: C, 72.48; H, 6.57; N, 6.76. Found: C, 72.52; H, 6.73; N, 6.41.

Exact mass (MALDI) - m/z: 415.2186 for $[M + H]^+$.

^{1}H NMR (300 MHz, $CDCl_3$): δ 7.97-7.88 (m, 6H), 7.57-7.47 (m, 5H), 7.12 (d, *J* = 9.0, 2H, C_6H_4 ($C_{12}H_9N_2$)), 5.22 (s, 2H, CH_2), 1.40 (s, 12H, CH_3).

^{13}C NMR (75 MHz, $CDCl_3$): δ 161.12 (1C, $C_{quat.}$), 152.75 (1C, $C_{quat.}$), 147.15 (1C, $C_{quat.}$), 139.54 (1C, $C_{quat.}$), 135.10 (2C, CH), 130.35 (1C, CH, C_6H_4 ($C_{12}H_9N_2$)), 129.00 (2C, CH), 126.52 (2C, CH), 124.72 (2C, CH), 122.55 (2C, CH), 115.13 (2C, CH), 83.84 (2C, $C_{quat.}$), 70.14 (1C, CH_2), 24.85 (4C, CH_3), (C-B not seen)

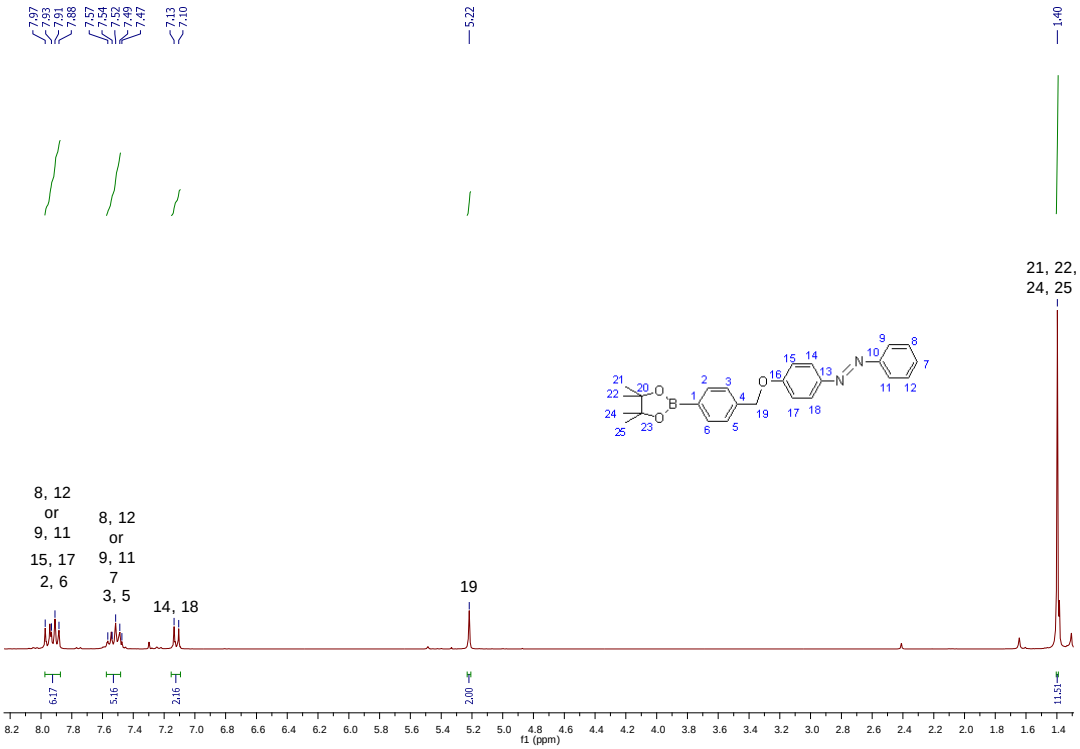

Fig. S1. ^{1}H NMR spectrum of compound **d** in $CDCl_3$, 300 MHz.

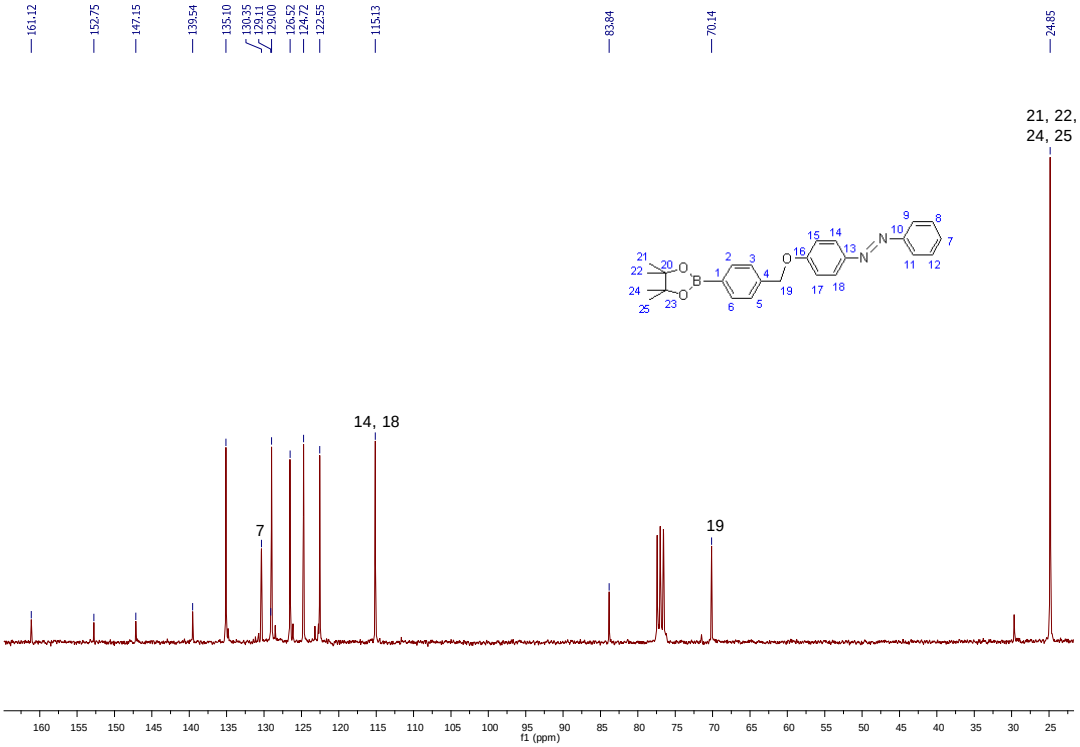

Fig. S2. ^{13}C NMR spectrum of compound **d** in $CDCl_3$, 75 MHz.

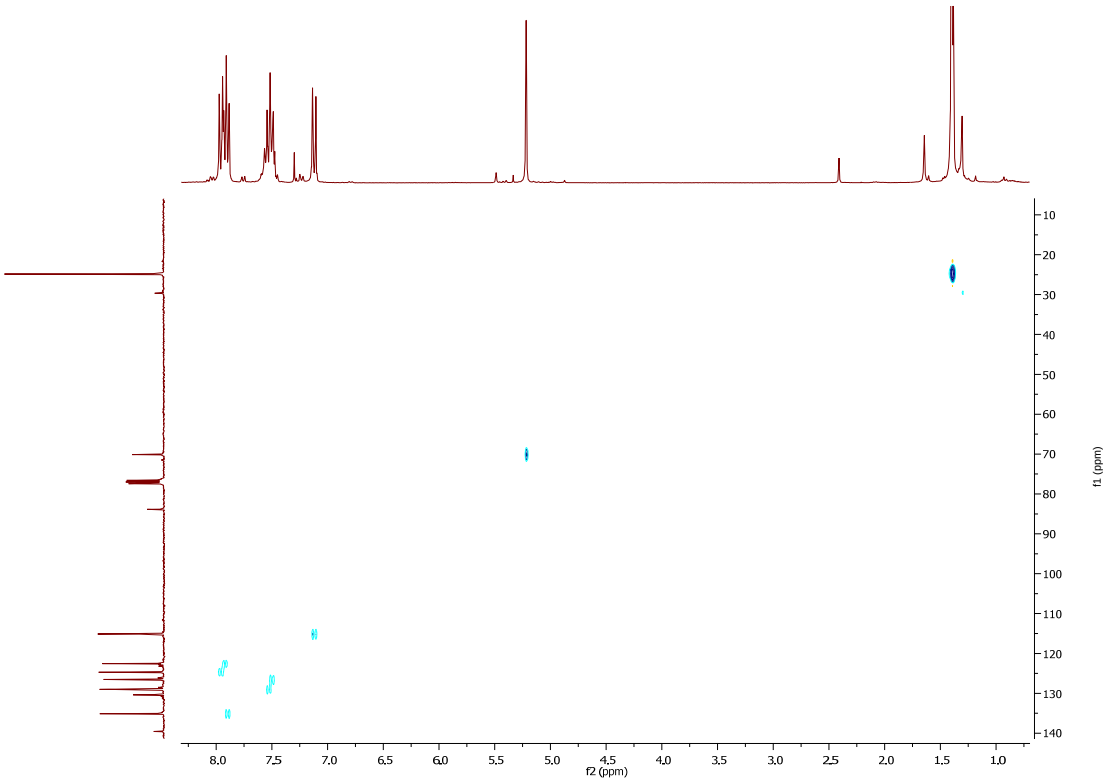

Fig. S3. HSQC spectrum of compound **d** in $CDCl_3$.

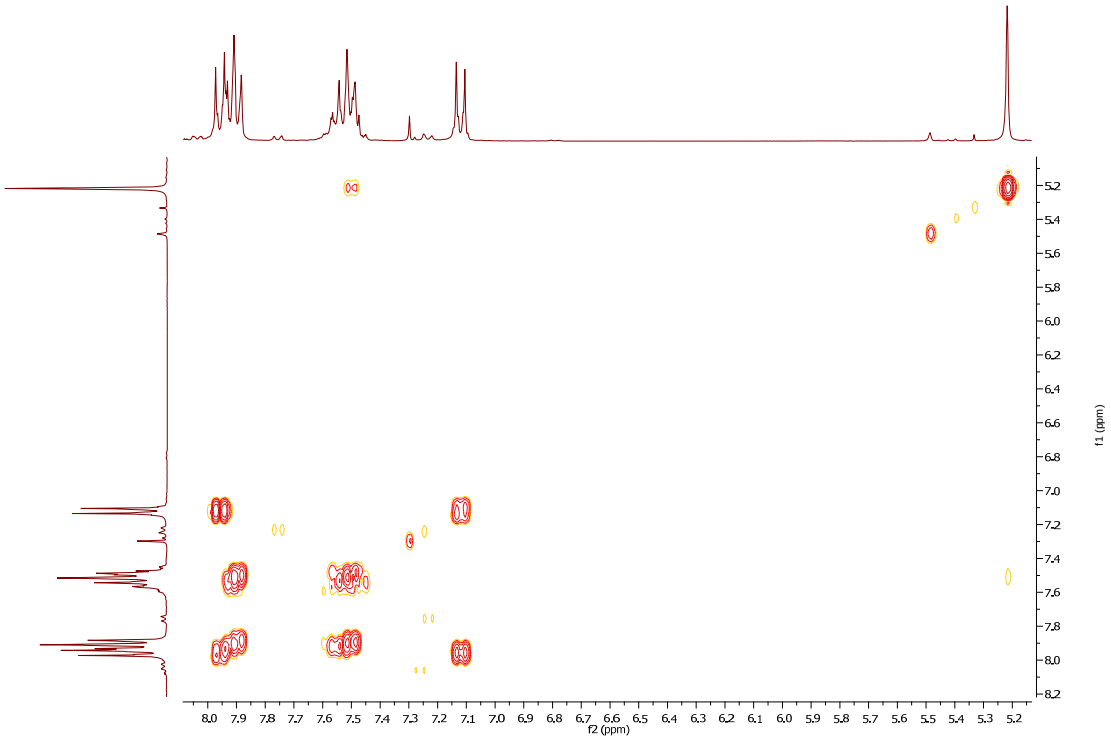

Fig. S4. COSY spectrum of compound **d** in $CDCl_3$.

Ligand 1. Synthesis, characterization and photoisomerization studies.

SYNTHESIS

The compound **d** (2.65 g, 6.3 mmol) was dissolved in 38 mL of degassed THF. To this mixture, 2-bromopyridine (1.11 g, 0.67 mL, 7.0 mmol), $Pd(PPh_3)_4$ (2 mol%, 0.15 g, 1.3 mmol), and Na_2CO_3 (1 M aq., 19 mL) were added successively under nitrogen, and heated overnight at 80 °C. The reaction was cooled to room temperature and 60 ml of water was added. The resulting mixture was extracted with ethyl acetate (5 × 10 mL), dried ($MgSO_4$), filtered and evaporated *in vacuo*. The resulting solid was washed with ethanol and dried *in vacuo*; the product was obtained as an orange powder (2.22 g, 95%).

Elemental Analysis: calculated for $C_{24}H_{19}N_3O \cdot 0.9CH_2Cl_2$: C, 67.51; H, 4.74; N, 9.48. Found: C, 67.51; H, 4.69; N, 8.98.

Exact mass (EI) - m/z: 366.1603 for $[M + H]^+$.

^{1}H NMR (300 MHz, $CDCl_3$): δ 8.74 (d, J = 4.6, 1H, C_5H_4N), 8.08 (d, J = 8.3, 2H, C_6H_4 ($C_{11}H_8N$)), 7.96 (d, J = 9.0, 2H, C_6H_4 ($C_{12}H_9N_2$)), 7.93 – 7.90 (m, 2H, C_6H_5), 7.82 – 7.78 (m, 2H, C_5H_4N), 7.60 (d, J = 8.4, 2H, C_6H_4 ($C_{11}H_8N$)), 7.57 – 7.44 (m, 3H, C_6H_5), 7.29 – 7.26 (m, 1H, C_5H_4N), 7.15 (d, J = 9.0, 2H, C_6H_4 ($C_{12}H_9N_2$)), 5.26 (s, 2H, CH_2).

^{13}C NMR (75 MHz, $CDCl_3$): δ 161.10 (1C, $C_{quat.}$), 156.96 (1C, $C_{quat.}$), 152.71 (1C, $C_{quat.}$), 149.62 (1C, CH, C_5H_4N), 147.15 (1C, $C_{quat.}$), 139.18 (1C, $C_{quat.}$), 137.22 (1C, $C_{quat.}$), 136.85 (1C, CH, C_5H_4N), 130.36 (1C, CH, C_6H_5), 128.98 (2C, CH, C_6H_5), 127.76 (2C, CH, C_6H_4 ($C_{11}H_8N$), 127.20 (2C, CH, C_6H_4 ($C_{11}H_8N$), 124.72 (2C, CH, C_6H_4 ($C_{12}H_9N_2$), 122.52 (2C, CH, C_6H_5), 122.24 (1C, CH, C_5H_4N), 120.63 (1C, CH, C_5H_4N), 115.13 (2C, CH, C_6H_4 ($C_{12}H_9N_2$)), 69.92 (1C, CH_2).

UV/Vis (CH_3CN, λ, nm (ε, L mol^{-1} cm^{-1})): 345 ($1.7 \cdot 10^4$), 444 ($0.6 \cdot 10^3$).

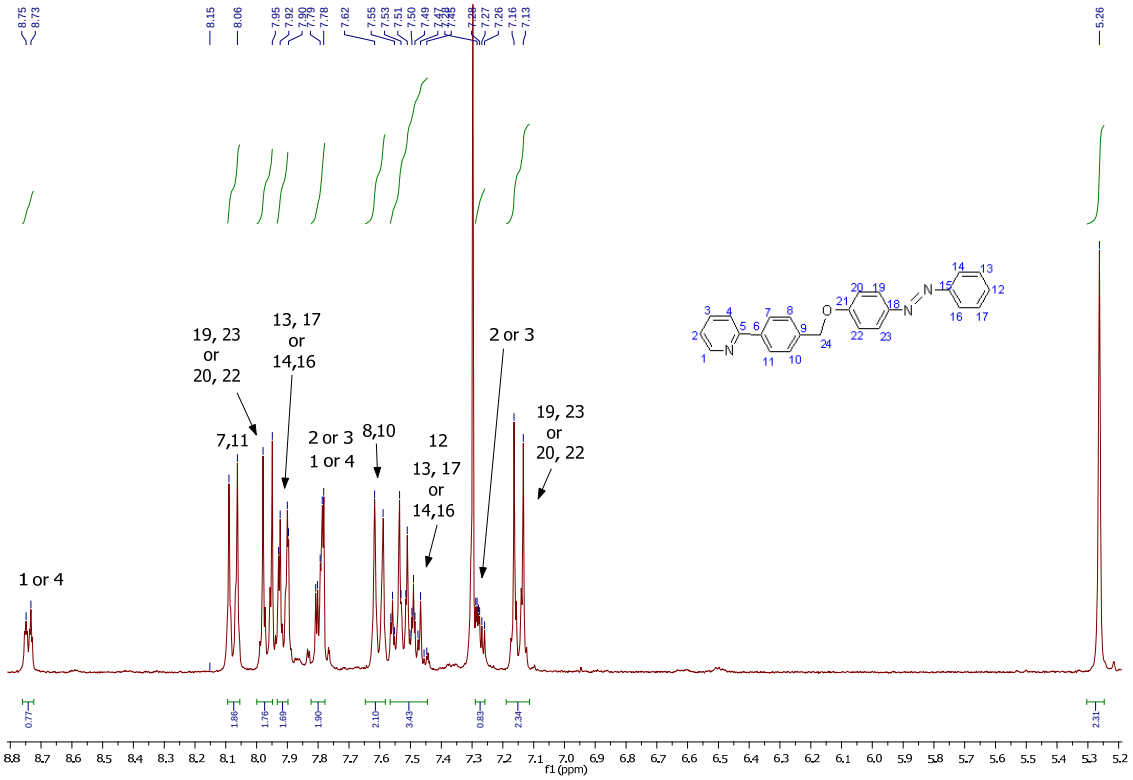

Fig. S5. ^{1}H NMR spectrum of ligand **1** in $CDCl_3$, 300 MHz.

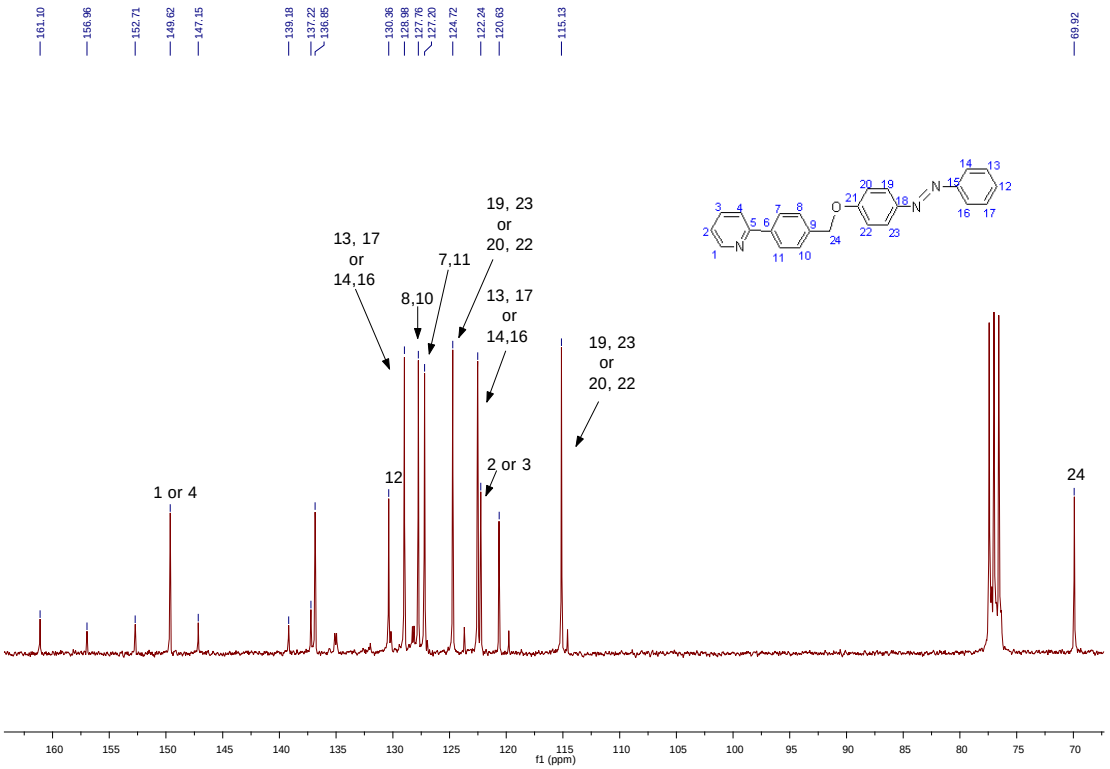

Fig. S6. ^{13}C NMR spectrum of ligand **1** in $CDCl_3$,75 MHz.

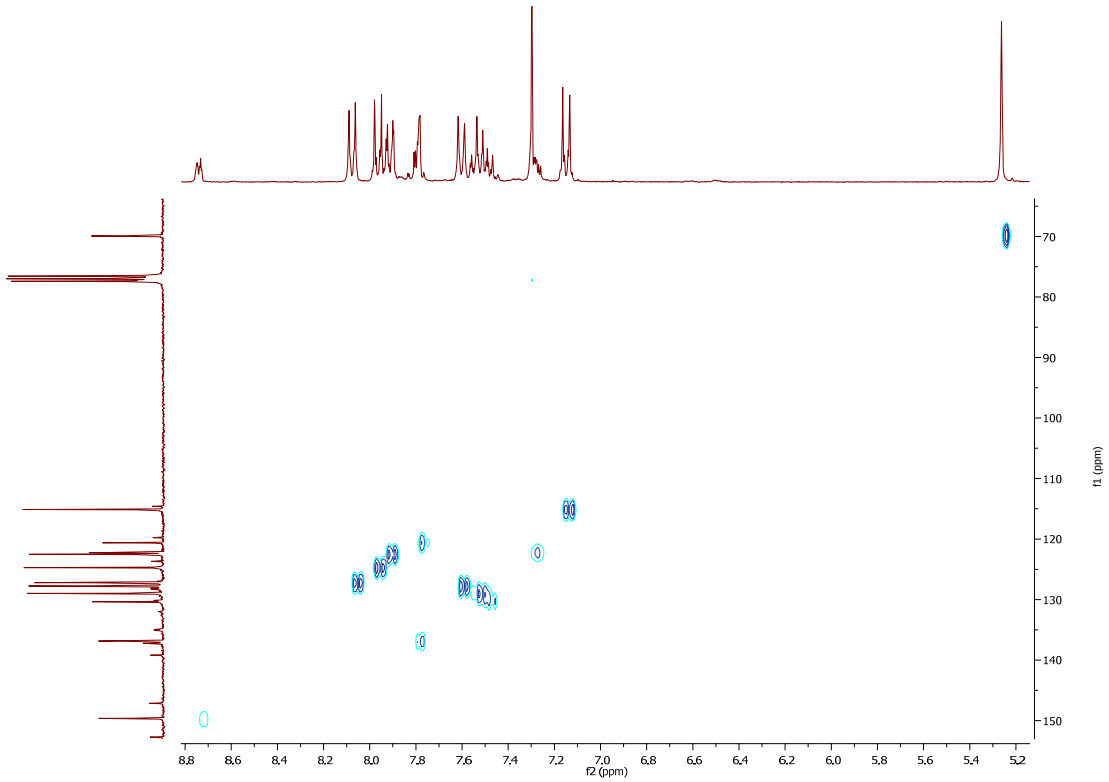

Fig. S7. HSQC NMR spectrum of ligand **1** in $CDCl_3$.

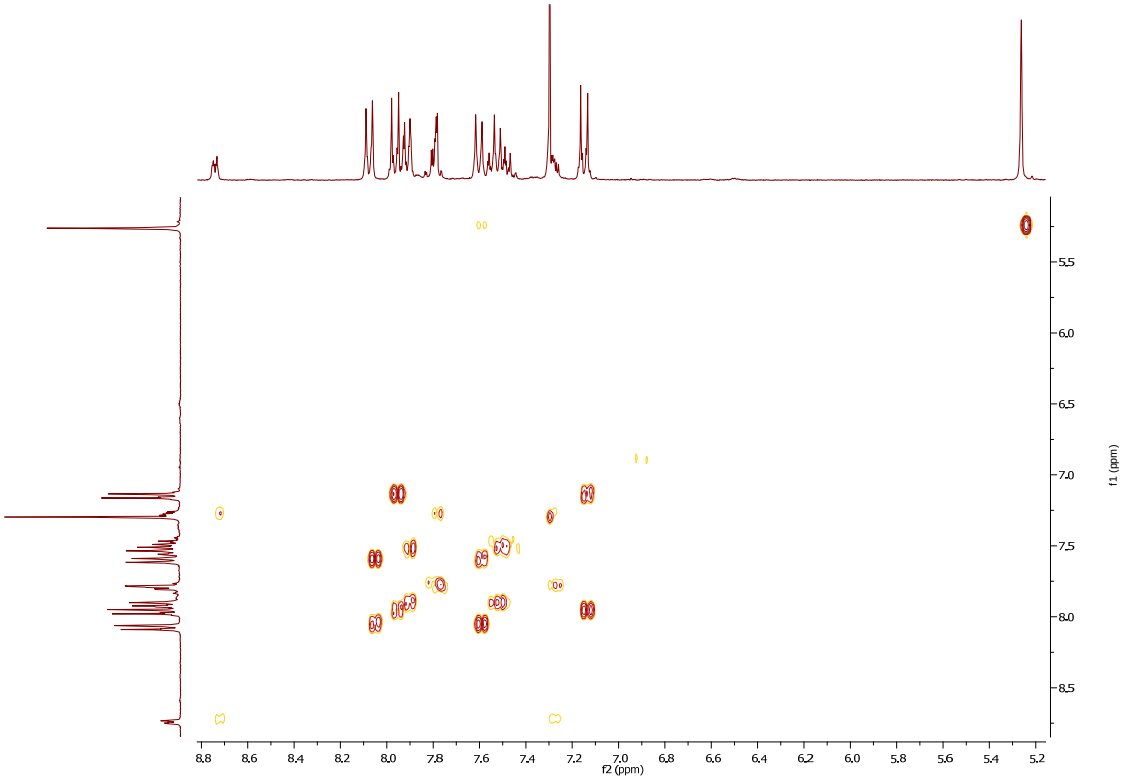

Fig. S8. COSY NMR spectrum of ligand **1** in $CDCl_3$.

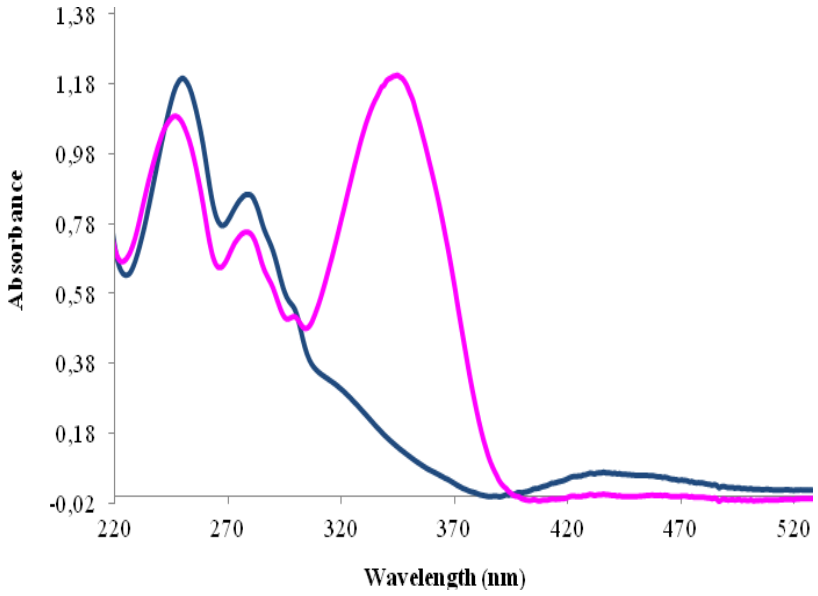

Fig. S9. UV/Vis spectra of ligand **1** in CH_3CN. Before (pink line) and after (blue line) irradiation at 347nm, $2.50 \cdot 10^{-5}$ M.

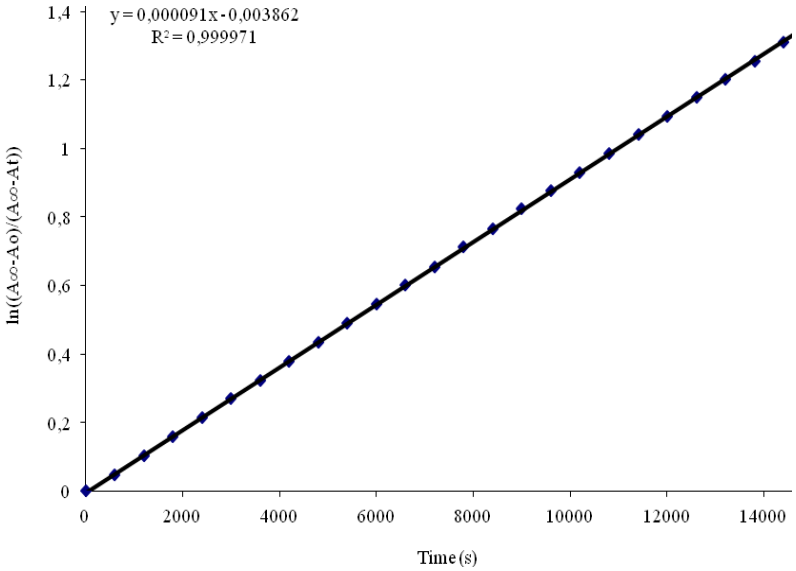

Fig. S10. *Cis* to *trans* thermal isomerization kinetics of ligand **1**. All k values were calculated from the first-order plots of absorption change of the band 345 nm at 328 K in CH_3CN after irradiation at 347 nm ($2.50 \cdot 10^{-5}$M). *Cis* to *trans* thermal isomerization of this complex is slow, and the A_∞ (1.200) value obtained in the kinetic measure does not correspond to A_∞ value (1.256) obtained as maximum of absorbance before the photoisomerization. We have used A_∞ = 1.256 as maximum of absorbance corresponding to *trans* isomer. k (s^{-1}) = $0.9 \cdot 10^{-4}$. Half-life (s) = 7600.

(6-Phenyl-3-pyridyl)-boronic acid. Synthesis and characterization.

SYNTHESIS

5-Bromo-2-phenylpyridine (2.00 g, 8.6 mmol) was dissolved in 13 mL of distilled toluene and 4 mL of distilled THF: Triisopropyl borate (2.30 mL, 10.2 mmol) and n-BuLi (1.6 M in hexane, 6.40 mL, 10.2 mmol) were added at -40 °C under N_2 atmosphere, and the reaction mixture was stirred for 1 hour at this temperature. The reaction mixture was allowed to warm up to -20 °C and 10 mL of $HCl_{(aq.)}$ (2 M) were added. When the reaction mixture reached r.t., it was quenched with water and treated with a NaOH aqueous solution (5 M) until a neutral pH was reached. The mixture was saturated with NaCl and it was extracted with THF (3 × 50 mL). The combined organic layers were dried over $MgSO_4$. The solvent was removed *in vacuo* and the residue was washed with ether and dichloromethane. The product was obtained as a white solid (1.60 g, 95%).

Elemental Analysis: calculated for $C_{11}H_{10}BNO_2 \cdot 1.75CH_2Cl_2$: C, 44.05; H, 3.91; N, 4.03. Found: C, 43.80; H, 3.47; N, 4.42.

Exact mass (EI) - m/z: 200.0884 for $[M + H]^+$.

^{1}H NMR (300 MHz, MeOD): δ 8.82 (s, 1H, C_5H_3N), 8.38 (d, J = 7.9, 1H, C_5H_3N), 8.03 – 7.95 (m, 3H), 7.60 – 7.55 (m, 3H, C_6H_5).

^{13}C NMR (75 MHz, MeOD): δ 157.00 (1C, $C_{quat.}$), 152.02 (1C, CH, C_5H_3N), 147.08 (1C, CH, C_5H_3N), 137.99 (1C, $C_{quat.}$), 131.23 (1C, CH, C_6H_5), 130.20 (2C, CH, C_6H_5), 128.73 (2C, CH, C_6H_5), 122.88 (1C, CH, C_5H_3N), (C-B not seen).

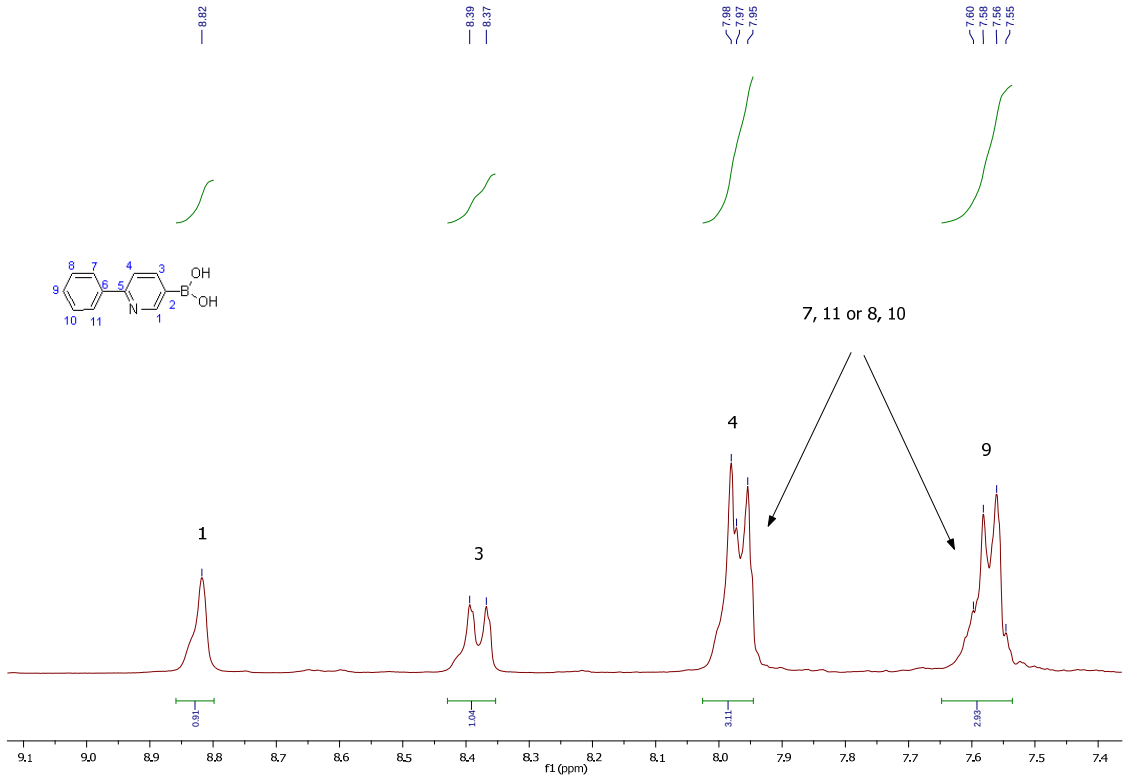

Fig. S11. ^{1}H NMR spectrum of (6-phenyl-3-pyridyl)-boronic acid in MeOD, 300 MHz.

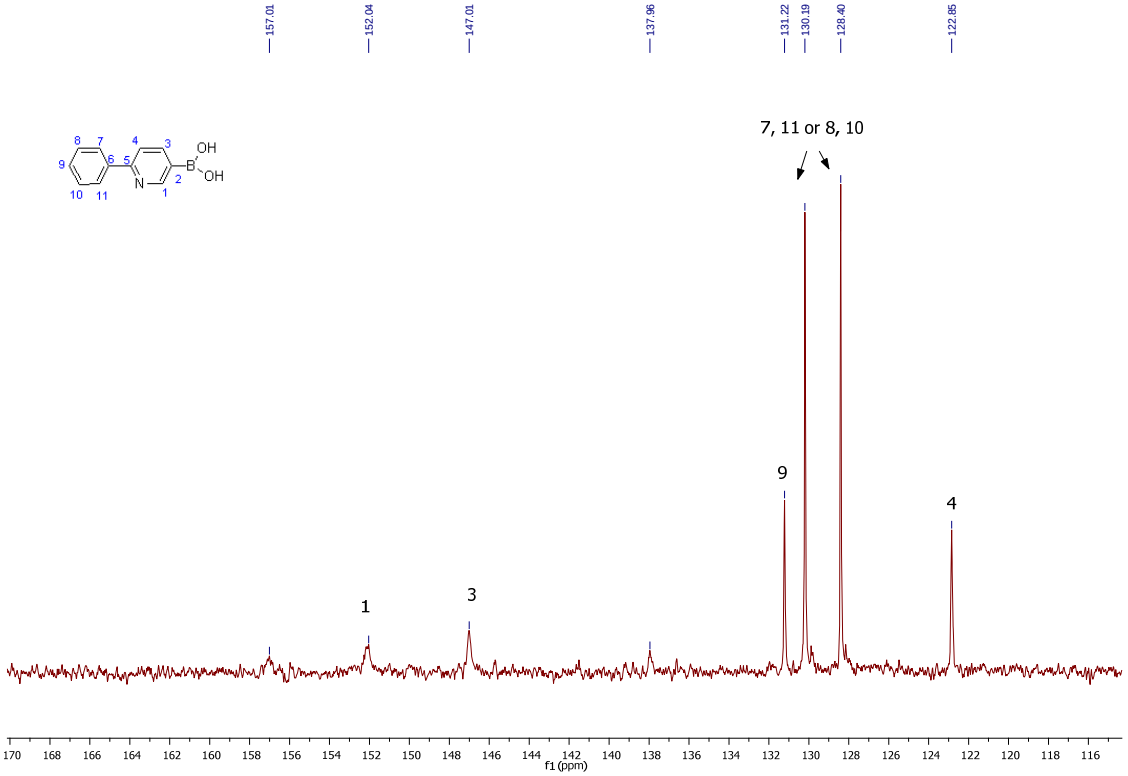

Fig. S12. ^{13}C NMR spectrum of (6-phenyl-3-pyridyl)-boronic acid in MeOD, 75 MHz.

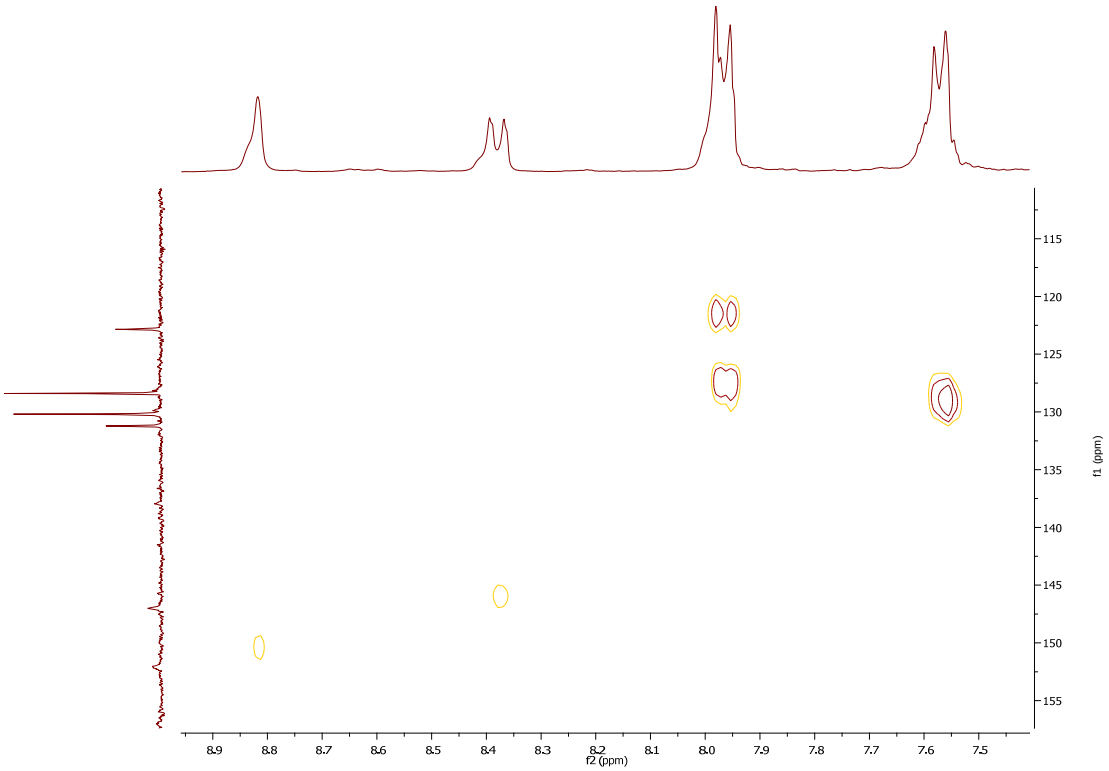

Fig. S13. HSQC NMR spectrum of (6-phenyl-3-pyridyl)-boronic acid in MeOD.

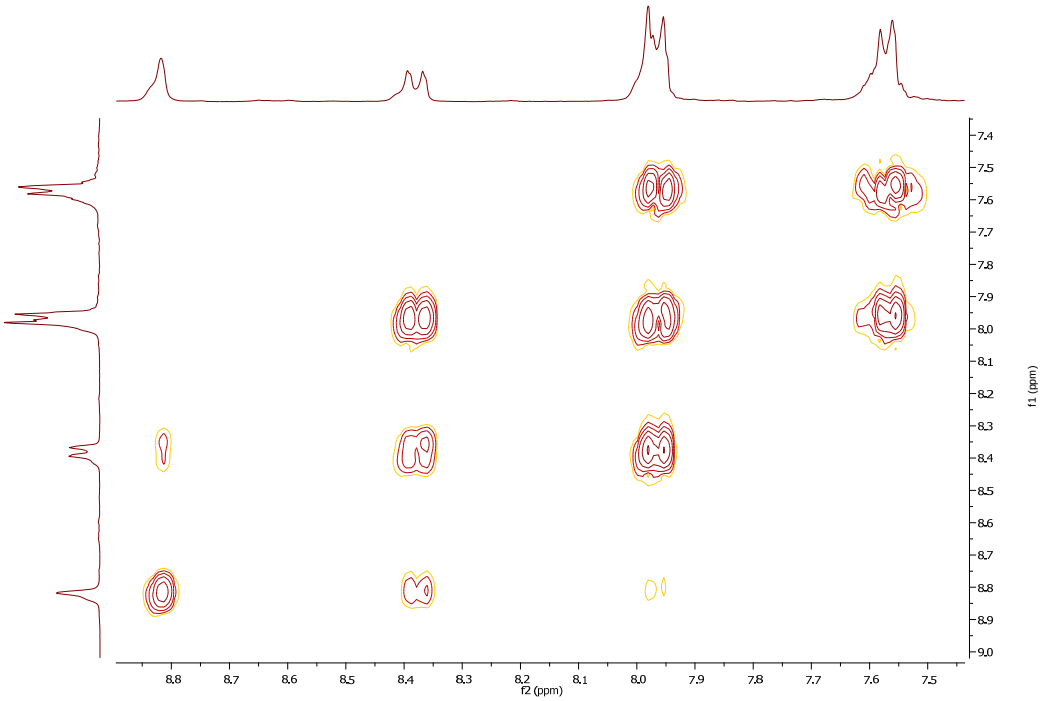

Fig. S14. COSY NMR spectrum of (6-phenyl-3-pyridyl)-boronic acid in MeOD.

.

Ligand 2. Synthesis, characterization and photoisomerization studies.

SYNTHESIS.

(6-Phenyl-3-pyridyl)-boronic acid (300 mg, 1.50 mmol) and $Pd(PPh_3)_4$ (3 mol%, 35 mg, 0.03 mmol) were dissolved in 10 mL of DME. The mixture was stirred under N_2 at 50 °C for 10 min. To this solution, *4*-(phenylazo)benzyl bromide (280 mg, 1.00 mmol) dissolved in 3mL of DME/ethanol (2:1, v/v) and Na_2CO_3 (2 M aq., 2.0 mL) were added successively under nitrogen, and heated overnight at 110 °C with continuous stirring. The reaction was cooled to room temperature and 50 mL of water were added. The resulting mixture was extracted with ethyl acetate (5 × 10 mL), dried ($MgSO_4$), filtered and the solvent removed *in vacuo*. The resulting solid was purified on by column chromatography (silica, CH_2Cl_2, Rf = 0.4); the product was obtained as a red crystalline solid (140 mg, 40%).

Elemental Analysis: calculated for $C_{24}H_{19}N_3$: C, 82.49; H, 5.48; N, 12.03. Found: C, 82.63; H, 5.22; N, 11.94.

Exact mass (MALDI) - m/z: 350.1646 for $[M + H]^+$.

^{1}H NMR (300 MHz, $CDCl_3$): δ 8.66 (d, *J* = 1.8, 1H, C_5H_3N), 8.03 (d, *J* = 6.9, 2H), 7.98 – 7.91 (m, 4H), 7.71 (dd, *J* = 8.1, 0.4, 1H, C_5H_3N), 7.61 – 7.44 (m, 7H), 7.40 (d, *J* = 8.5, 2H, C_6H_4), 4.14 (s, 2H, CH_2).

^{13}C NMR (75 MHz, $CDCl_3$): δ 155.68 (1C, $C_{quat.}$), 152.64 (1C, $C_{quat.}$), 151.37 (1C, $C_{quat.}$), 149.95 (1C, CH, C_5H_3N), 143.11 (1C, $C_{quat.}$), 139.10 (1C, $C_{quat.}$), 137.13 (1C, CH), 134.30 (1C, $C_{quat.}$), 130.90 (1C, CH), 129.57 (2C, CH), 129.05 (2C, CH), 128.80 (1C, CH), 128.71 (2C, CH), 126.75 (2C, CH), 123.21 (2C, CH), 122.78 (2C, CH), 120.35 (1C, CH, C_5H_3N), 38.57 (1C, CH_2).

UV/Vis (CH_3CN, λ, nm (ε, L mol^{-1} cm^{-1})): 326 ($2.2 \cdot 10^4$), 435 ($0.9 \cdot 10^3$).

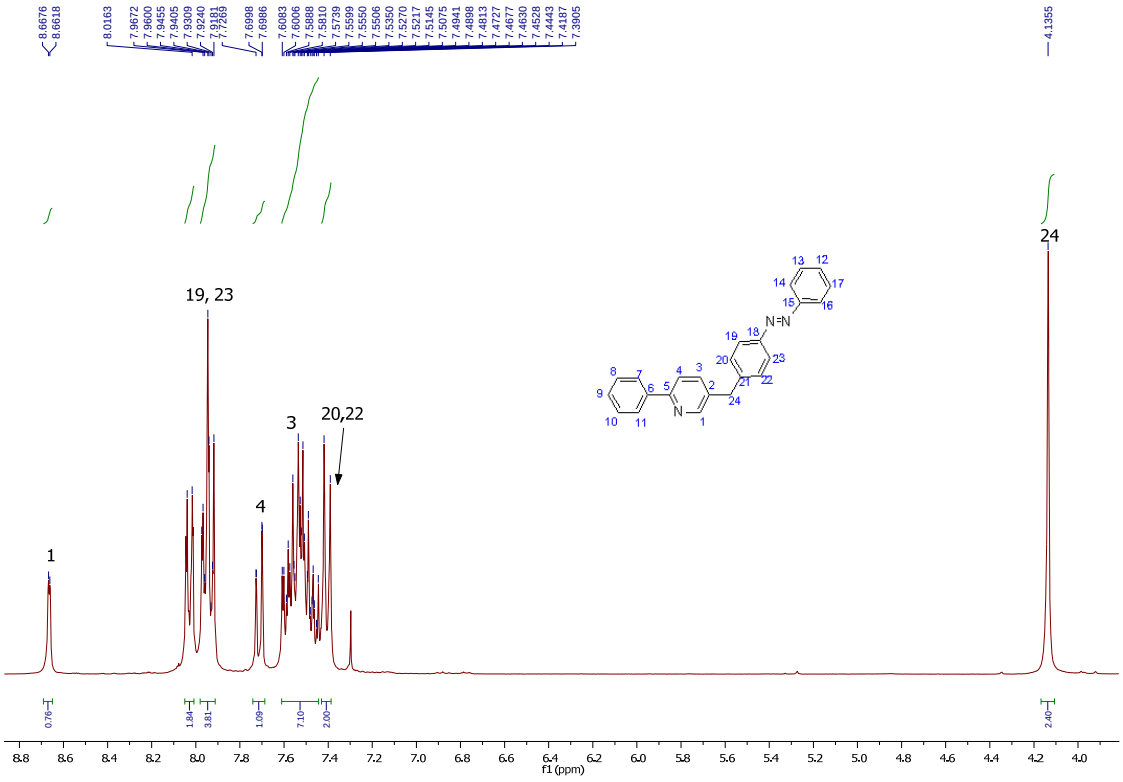

Fig. S15. ^{1}H NMR spectrum of ligand **2** in $CDCl_3$, 300 MHz.

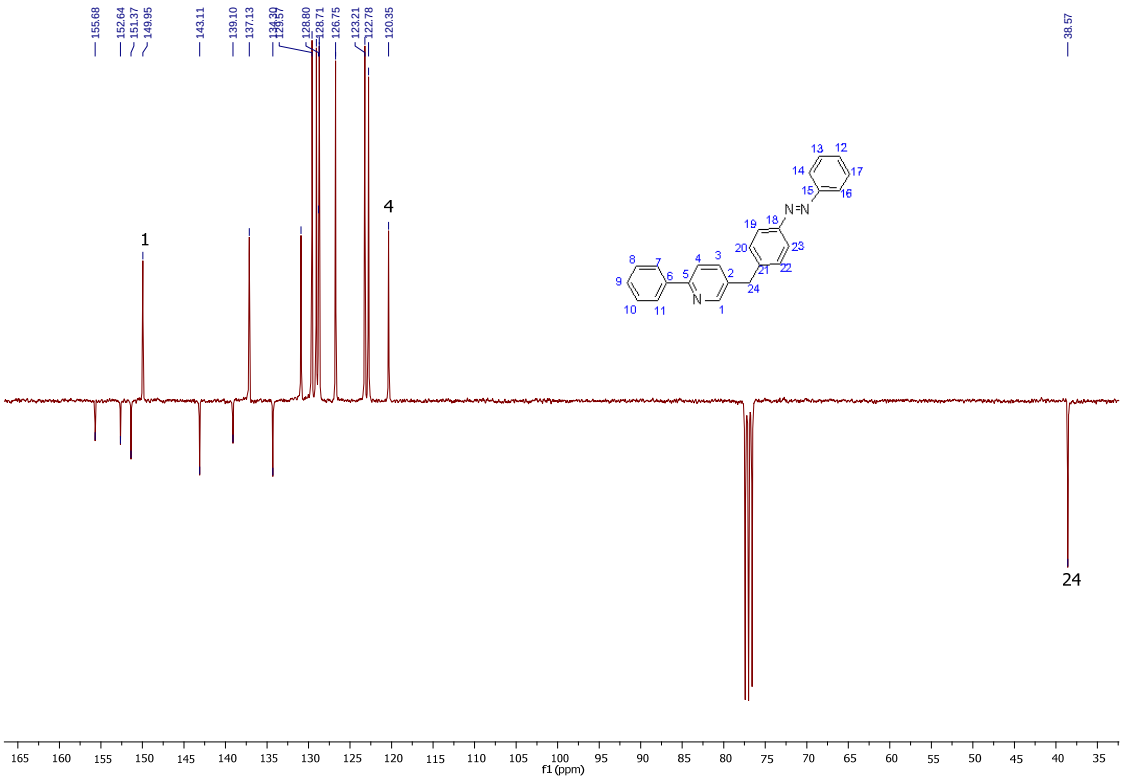

Fig. S16. ^{13}C APT NMR spectrum of ligand **2** in $CDCl_3$, 75 MHz.

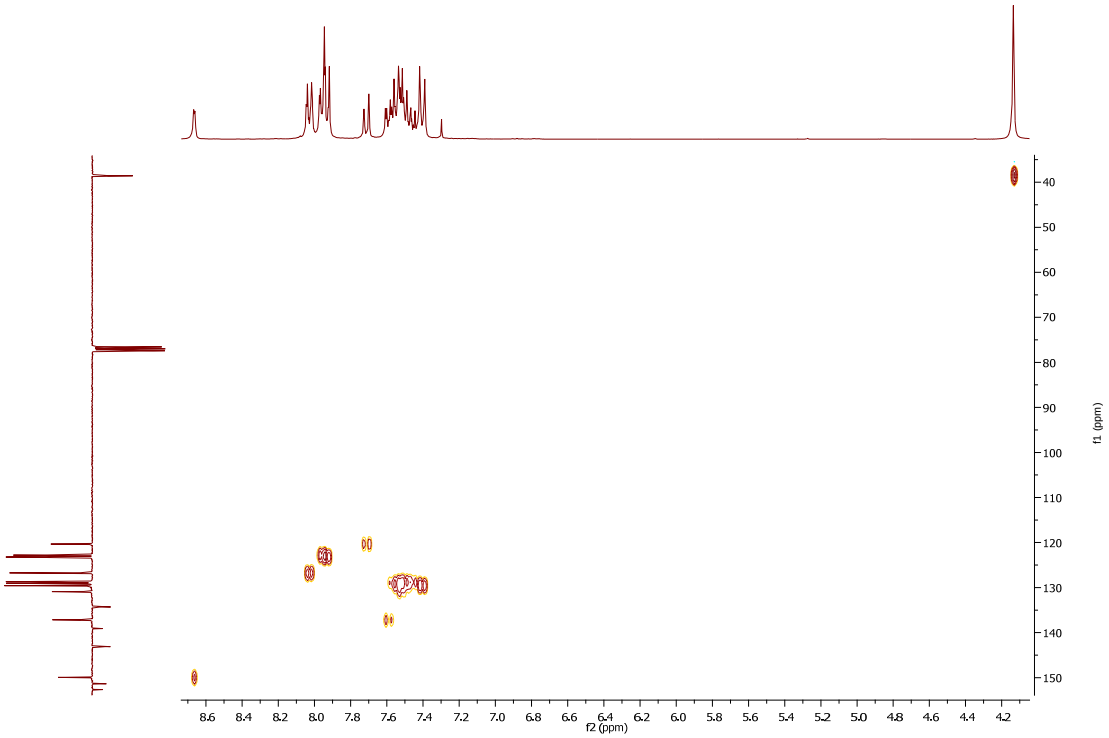

Fig. S17. HSQC NMR spectrum of ligand **2** in $CDCl_3$.

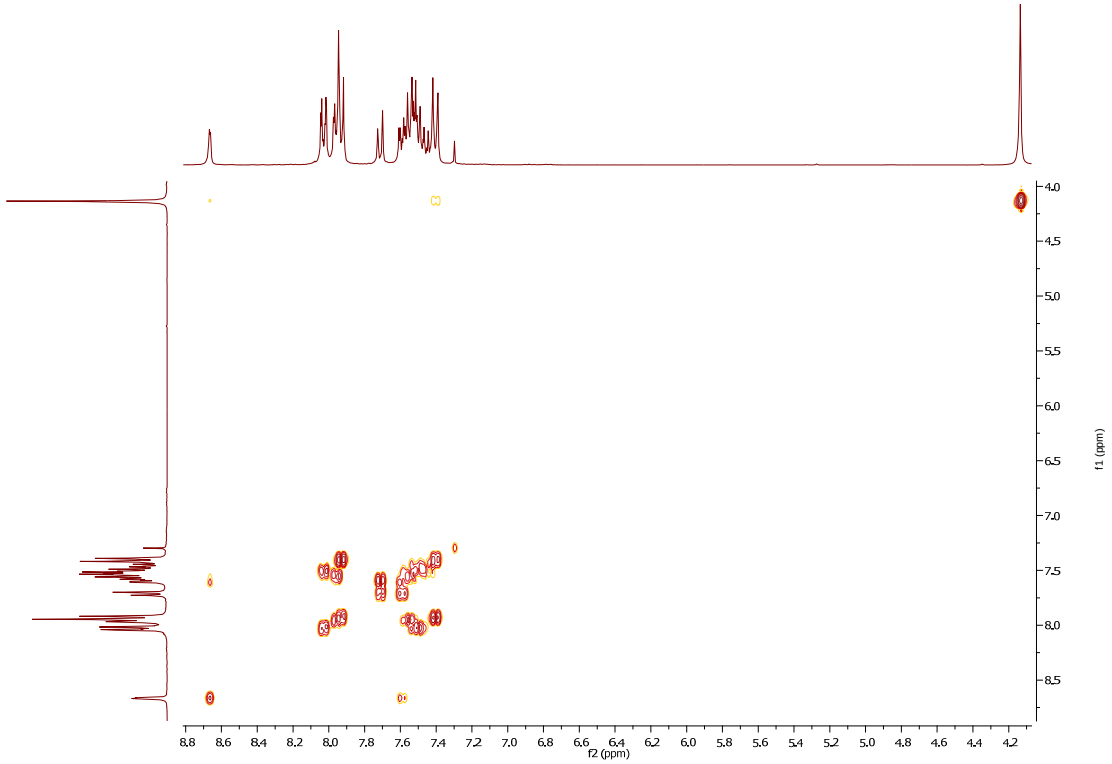

Fig. S18. COSY NMR spectrum of ligand **2** in $CDCl_3$.

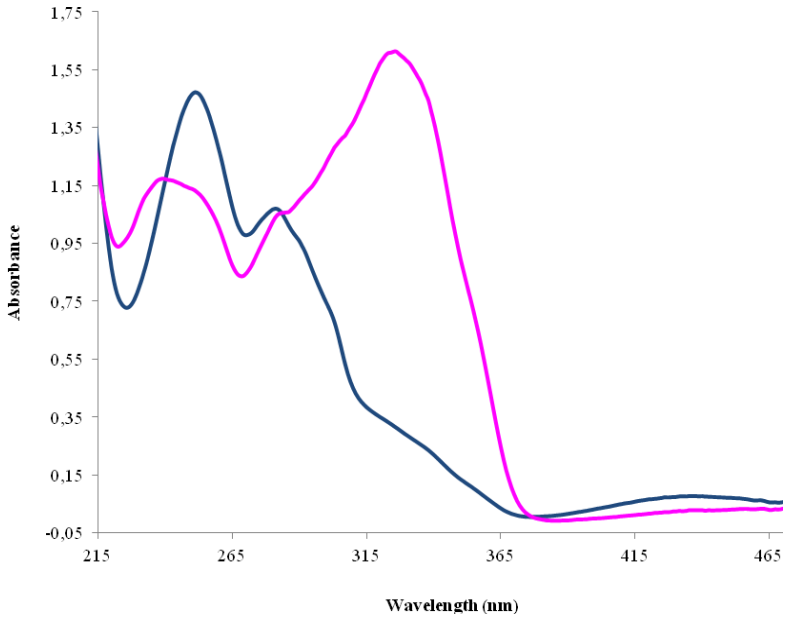

Fig. S19. UV/Vis spectra of ligand **2** in CH_3CN. Before (pink line) and after (blue line) irradiation at 326 nm, $2.50 \cdot 10^{-5}$ M.

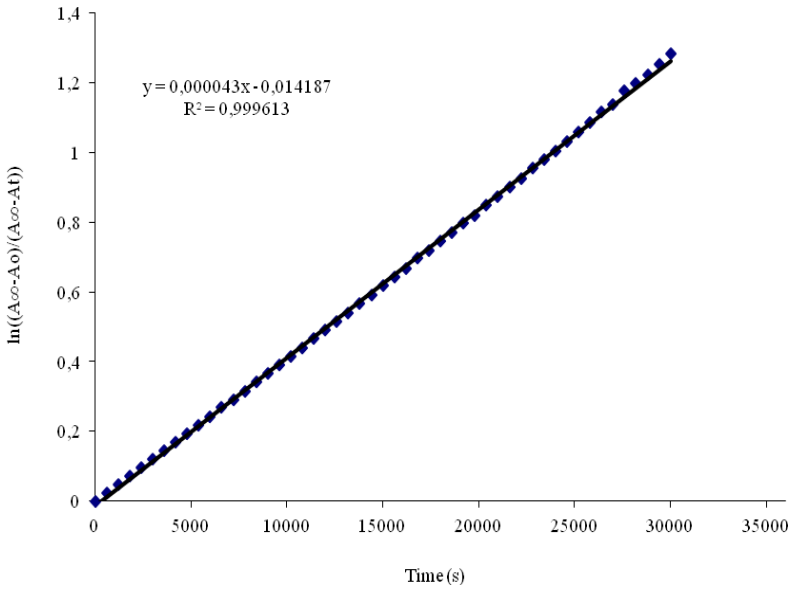

Fig. S20. *Cis* to *trans* thermal isomerization kinetics of ligand **2**. All k values were calculated from the first-order plots of absorption change of the band 326 nm at 328 K in CH_3CN after irradiation at 327 nm ($2.50 \cdot 10^{-5}$ M). *Cis* to *trans* thermal isomerization of this complex is slow, and the A_∞ (1.339) value obtained in the kinetic measure does not correspond to A_∞ value (1.616) obtained as maximum of absorbance before the photoisomerization. We have used A_∞ = 1.616 as maximum of absorbance corresponding to *trans* isomer. k (s^{-1}) = $0.4 \cdot 10^{-4}$. Half-life (s) = 16000.

Ligand 3. Synthesis, characterization and photoisomerization studies.

SYNTHESIS

4-(phenylazo)iodobenzene (0.77 g, 2.5 mmol) was dissolved in 10 mL of DMSO. To this mixture, acetylacetone (0.75 g, 0.77 mL, 7.50 mmol), K_2CO_3 (1.38 g, 10.0 mmol), CuI (0.05 g, 0.3 mmol) and *L*-proline (0.06 g, 0.5 mmol) were added successively under nitrogen, and heated at 90 °C for 6 h. The reaction mixture was quenched with HCl (1 M, 100 mL) and it was extracted with EtOAc (3 × 25 mL). $MgSO_4$ was added to the organic fraction, filtered and evaporated *in vacuo*. The resulting solid was purified by column chromatography (silica) eluting with hexane/dichloromethane (5:1, v/v) (Rf = 0.3); the product was obtained as a red crystalline solid (0.25 g, 36%).

Elemental Analysis: calculated for $C_{17}H_{16}N_2O_2$: C, 72.84; H, 5.75; N, 9.99. Found: C, 72.76; H, 5.52; N, 9.88.

Exact mass (MALDI) - m/z: 281.1277 for $[M + H]^+$.

^{1}H NMR (300 MHz, $CDCl_3$): δ 16.76 (s, 1H, CH*), 8.01–7.96 (m, 4H), 7.61–7.52 (m, 3H, C_6H_5), 7.40–7.36 (m, 2H, C_6H_4), 1.98 (s, 6H, CH_3).

^{13}C NMR (75 MHz, $CDCl_3$): δ 190.78 (2C, $C_{quat.C=O*}$), 152.60 (1C, $C_{quat.}$), 151.87 (1C, $C_{quat.}$), 139.78 (1C, $C_{quat.}$), 131.94 (2C, CH, C_6H_4), 131.17 (1C, CH, C_6H_5), 129.12 (2C, CH, C_6H_5), 123.21 (2C, CH), 122.87 (2C, CH), 114.59 (1C, $C_{quat.}$), 24.20 (2C, CH_3).

UV/Vis (CH_3CN, λ, nm (ε, L mol^{-1} cm^{-1})): 326 ($2.0 \cdot 10^4$), 439 ($0.8 \cdot 10^3$).

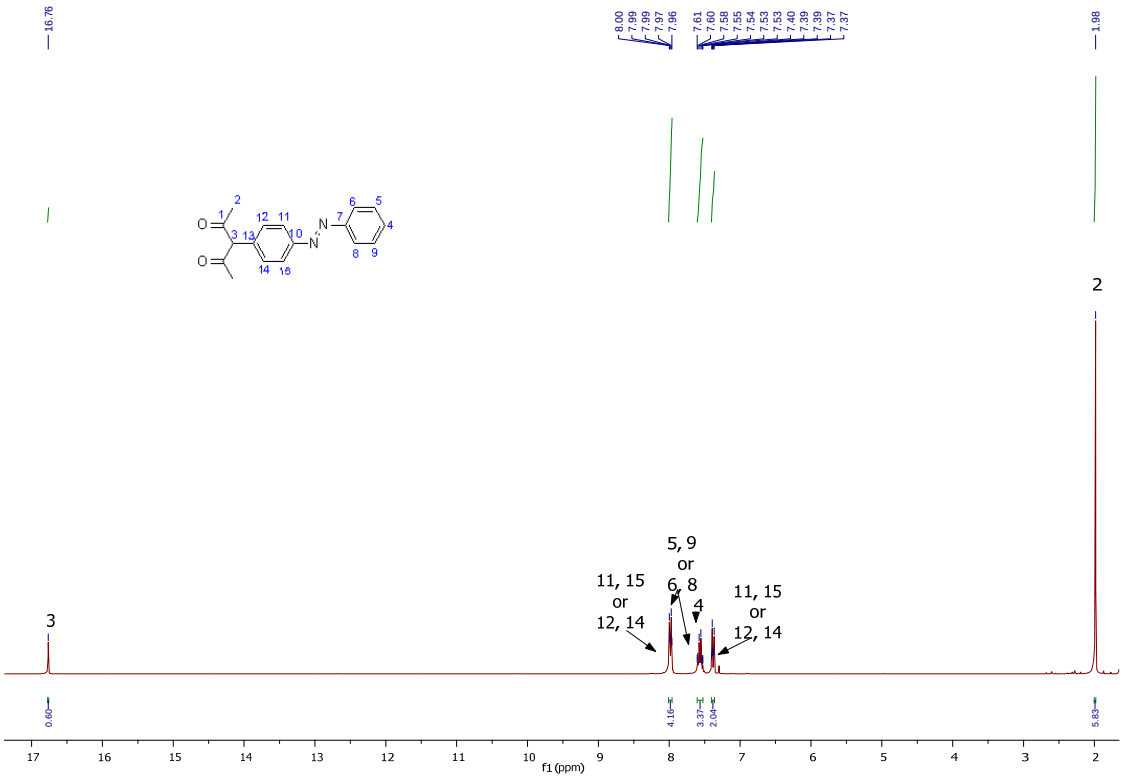

Fig. S21. ^{1}H NMR spectrum of ligand **3** in $CDCl_3$, 300 MHz.

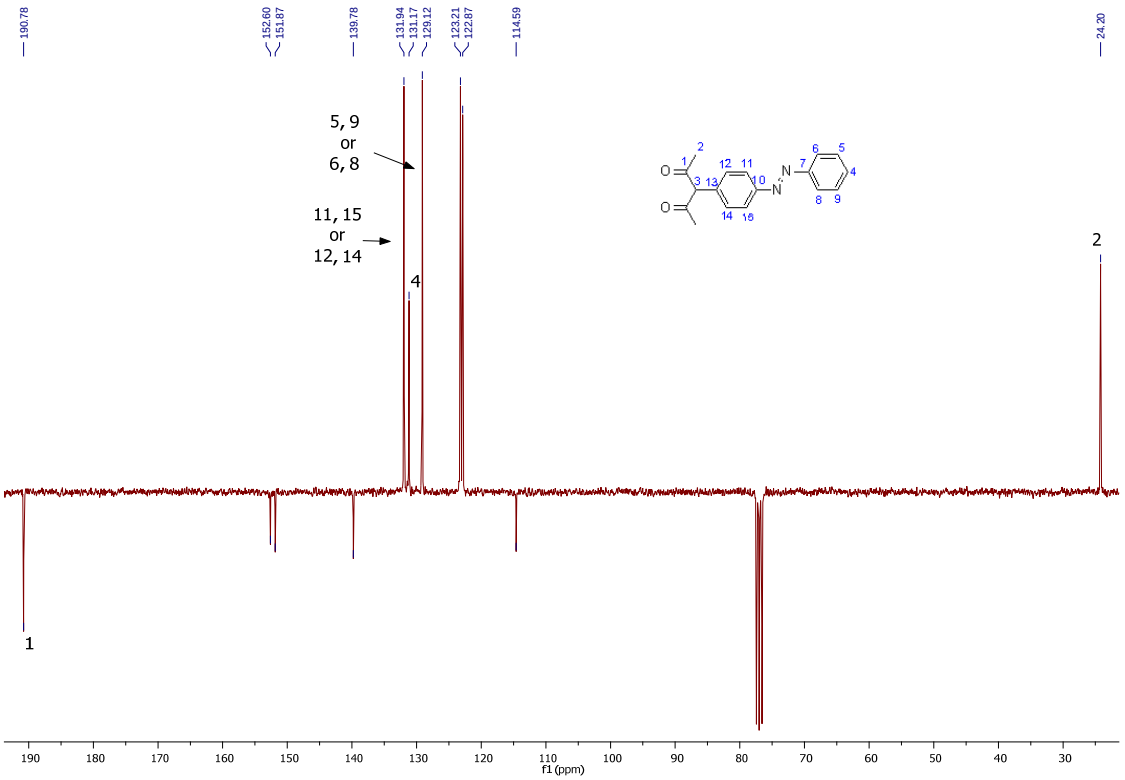

Fig. S22. ^{13}C APT NMR spectrum of ligand **3** in $CDCl_3$, 75 MHz.

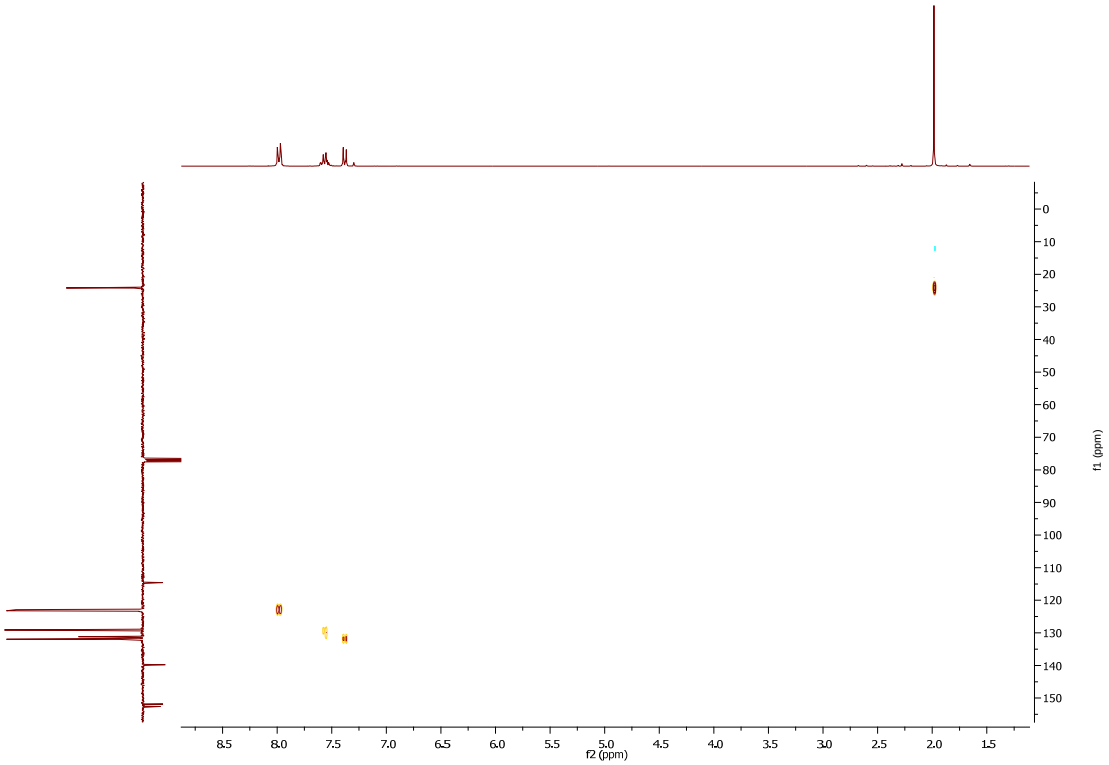

Fig. S23. HSQC NMR spectrum of ligand **3** in $CDCl_3$.

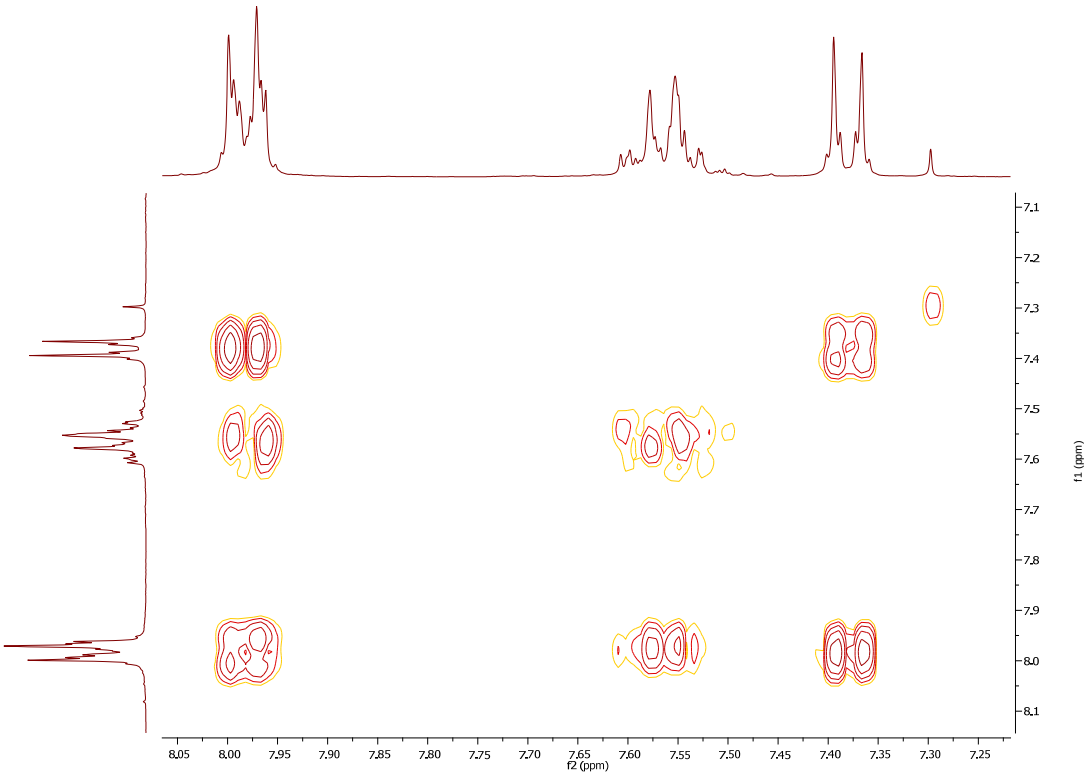

Fig. S24. COSY NMR spectrum of ligand **3** in $CDCl_3$.

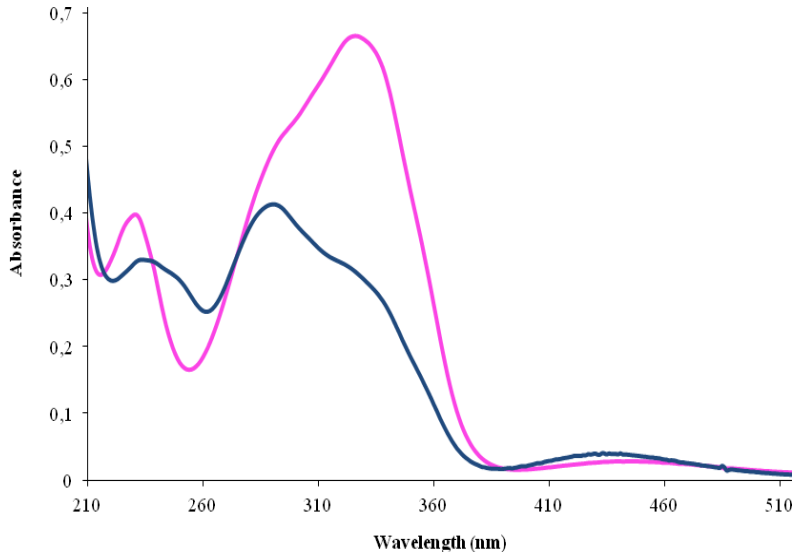

Fig. S25. UV/Vis spectra of ligand **3** in CH_3CN. Before (pink line) and after (blue line) irradiation at 332 nm, 2.50×10^{-5} M.

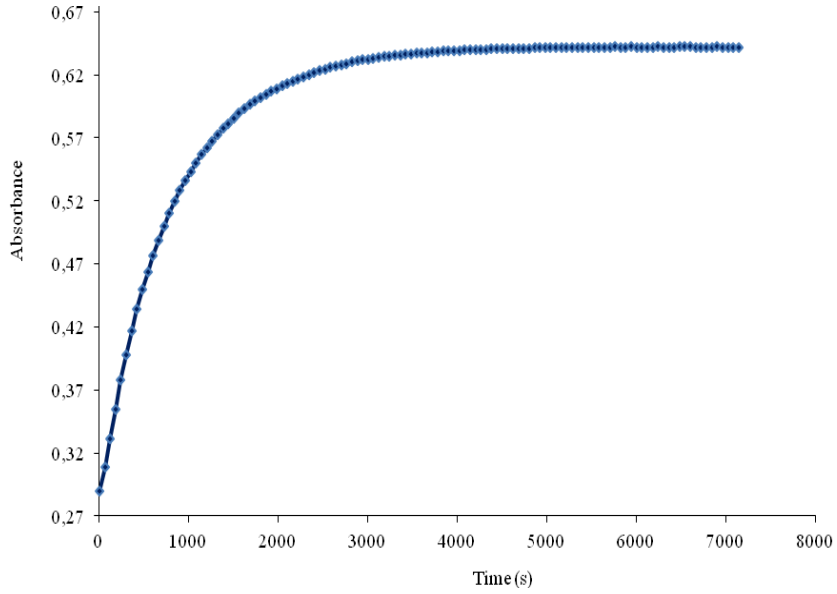

Fig. S26. *Cis* to *trans* thermal isomerization kinetics of ligand **3**. Absorption change of the band 326 nm at 328 K in CH_3CN after irradiation at 332 nm ($2.50 \cdot 10^{-5}$ M).

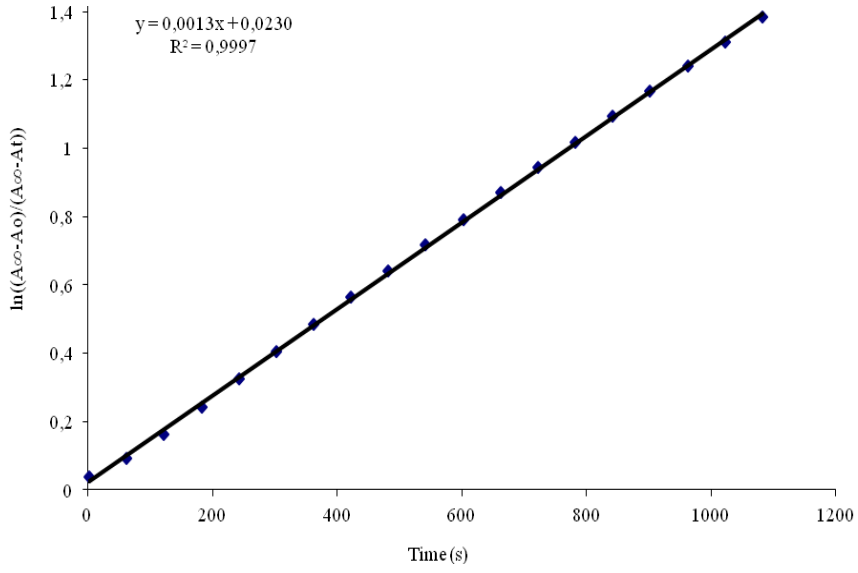

Fig. S27. *Cis* to *trans* thermal isomerization kinetics of ligand **3**. First-order plot. k (s^{-1}) = $1.2 \cdot 10^{-3}$. Half-life (s) = 530.

Ligand 5. Synthesis, characterization and photoisomerization studies.

SYNTHESIS

5-Bromo-2-phenylpyridine (300 mg, 0.130 mmol) was dissolved in 4 mL of degassed THF. To this mixture, 4-(phenylazo)phenyl boronic acid pinacol ester (430 mg, 0.140 mmol), $Pd(PPh_3)_4$ (2 mol%, 3 mg, 0.003 mmol), Na_2CO_3 (1 M aq., 2 mL) were added successively under nitrogen, and heated overnight at 80 °C with continuous stirring. The reaction mixture was heated overnight at 80 °C with continuous stirring. The reaction was cooled to room temperature and 50 mL of water was added. The resulting mixture was extracted with CH_2Cl_2 (5 × 20 mL), dried over $MgSO_4$, filtered and evaporated *in vacuo*. The product was washed with dichloromethane (2 mL) and dried *in vacuo*. The product was obtained as an orange powder (380 mg, 88%).

Elemental Analysis: calculated for $C_{23}H_{17}N_3 \cdot 0.5CH_2Cl_2$: C, 74.70; H, 4.80; N, 11.12. Found: C, 74.83; H, 4.77; N, 11.04.

Exact mass (MALDI) - m/z: 336.1495 for $[M+H]^+$.

^{1}H NMR (300 MHz, $CDCl_3$): δ 9.06 (d, *J* = 1.9, 1H, C_5H_3N), 8.13 – 8.06 (m, 5H), 8.00 (d, *J* = 8.0, 1.4, 2H), 7.89 (d, *J* = 8.3, 1H, C_5H_3N), 7.85 (d, *J* = 8.5, 2H, C_6H_4), 7.61 – 7.50 (m, 6H).

^{13}C NMR (75 MHz, $CDCl_3$): δ 156.27 (1C, $C_{quat.}$), 152.28 (1C, $C_{quat.}$), 151.79 (1C, $C_{quat.}$), 147.66 (1C, CH, C_5H_3N), 139.64 (1C, $C_{quat.}$), 138.41 (1C, $C_{quat.}$), 134.67 (1C, CH, C_5H_3N), 133.54 (1C, $C_{quat.}$), 130.75 (1C, CH, C_6H_5), 128.74 (1C, CH, C_6H_5), 128.71 (2C, CH, C_6H_5), 128.42 (2C, CH, C_6H_5), 127.20 (2C, CH, C_6H_4), 126.47 (2C, CH), 123.25 (2C, CH), 122.52 (2C, CH, C_6H_5), 119.99 (1C, CH, C_5H_3N).

UV/Vis (CH_3CN, λ, nm (ε, L mol^{-1} cm^{-1})): 347 ($3.3 \cdot 10^4$), 436 ($1.5 \cdot 10^3$).

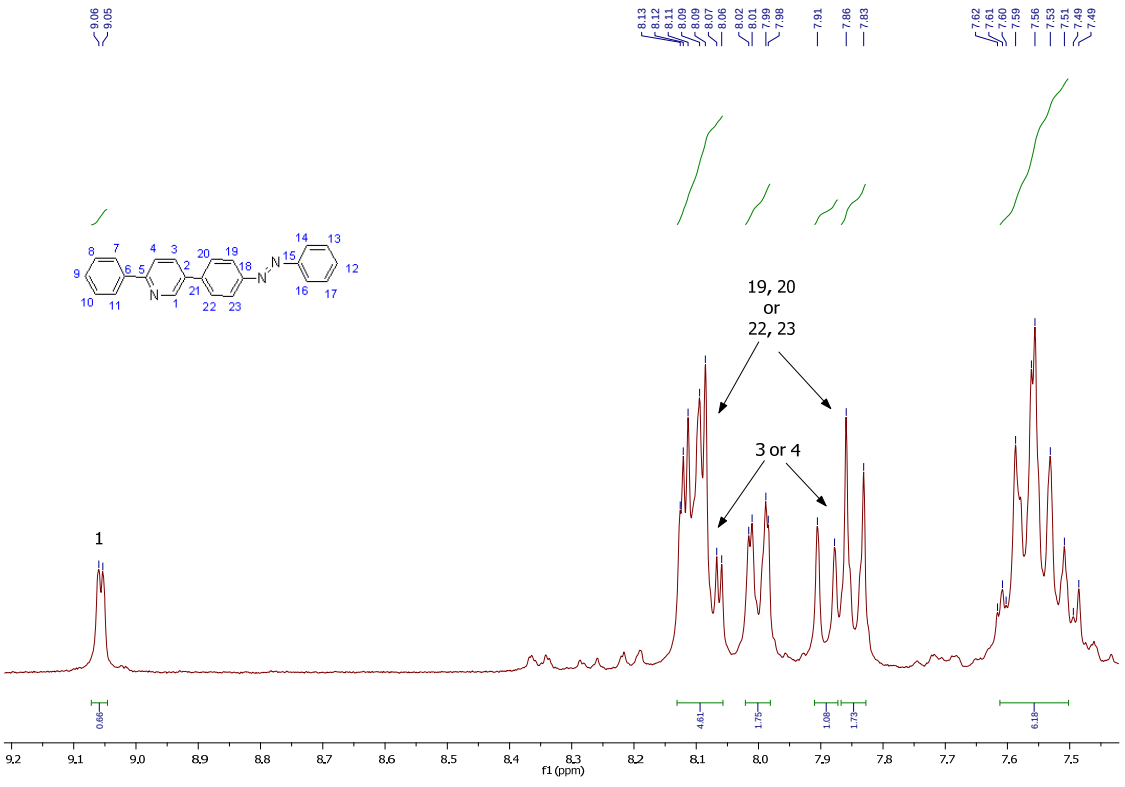

Fig. S28. ^{1}H NMR spectrum of ligand **5** in $CDCl_3$, 300 MHz.

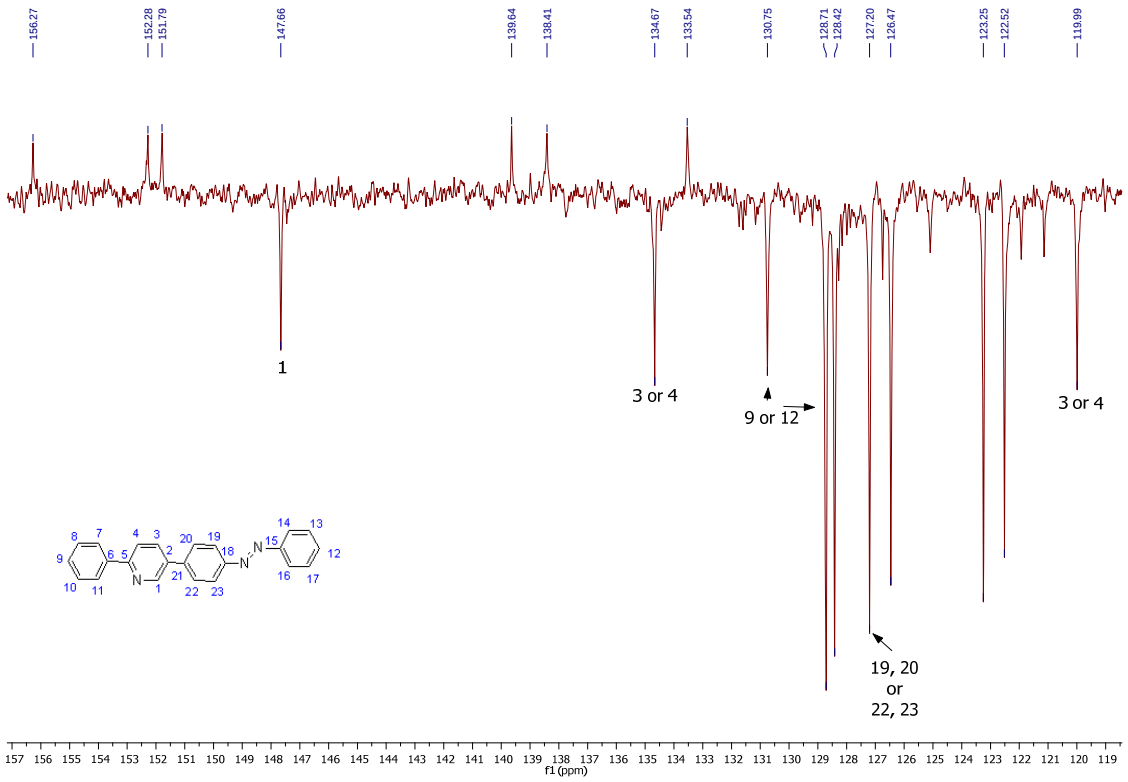

Fig. S29. ^{13}C APT NMR spectrum of ligand **5** in $CDCl_3$, 75 MHz.

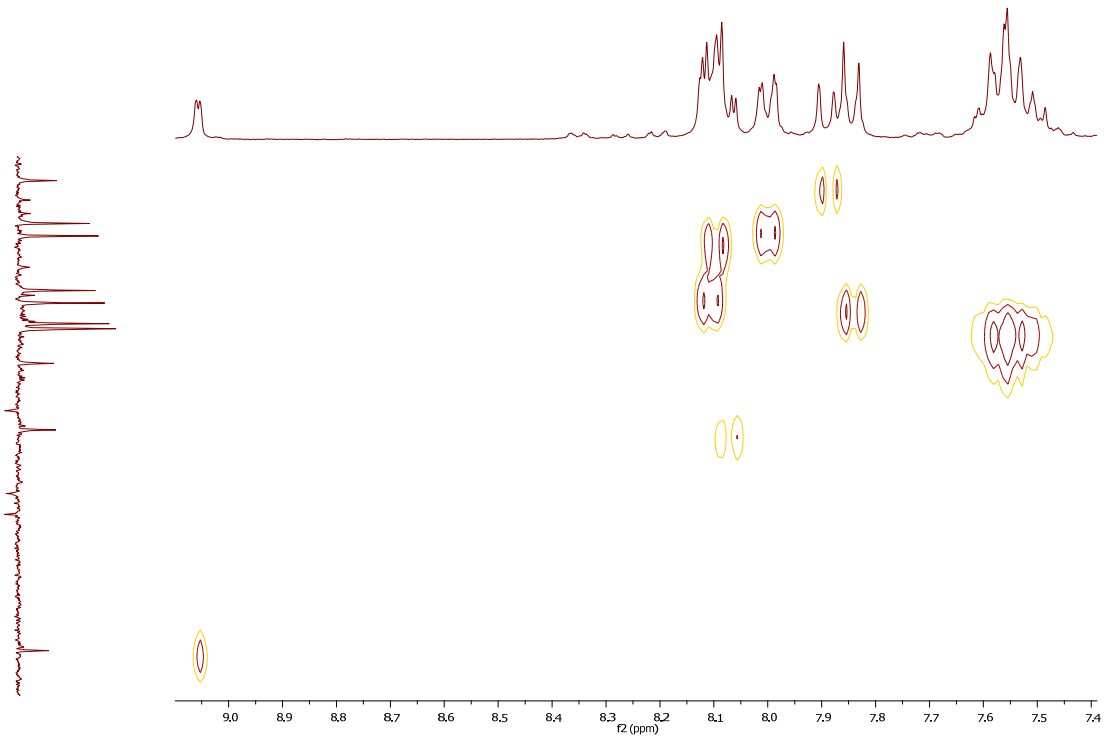

Fig. S30. HSQC NMR spectrum of ligand **5** in $CDCl_3$.

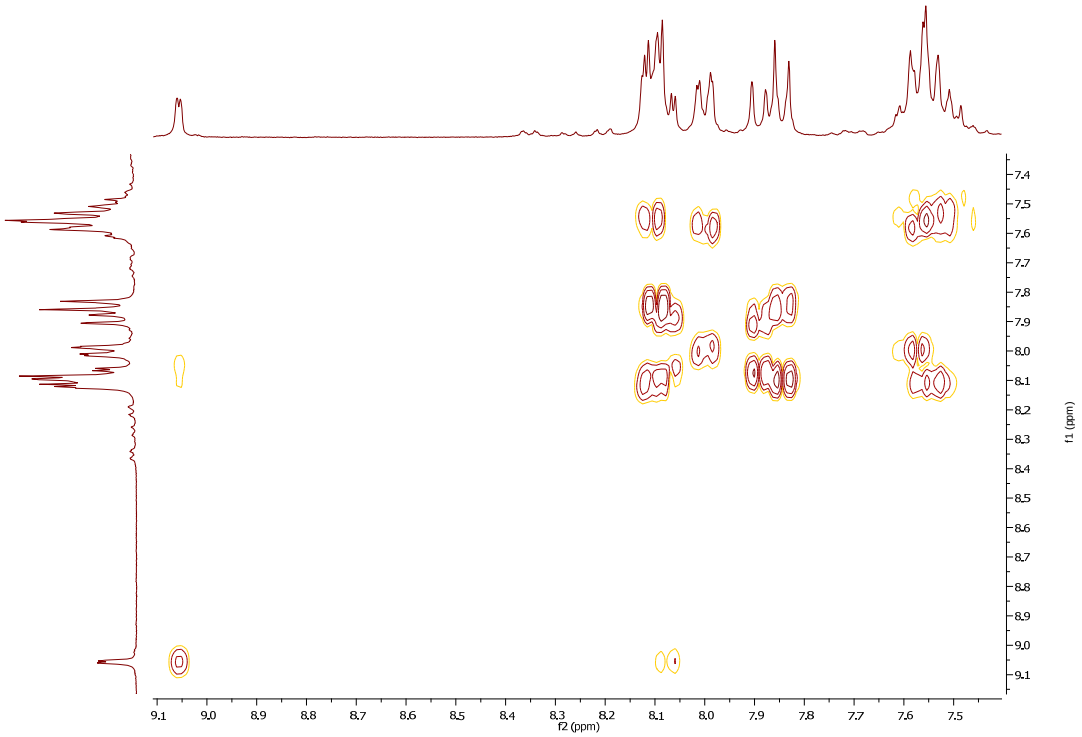

Fig. S31. COSY NMR spectrum of ligand **5** in $CDCl_3$.

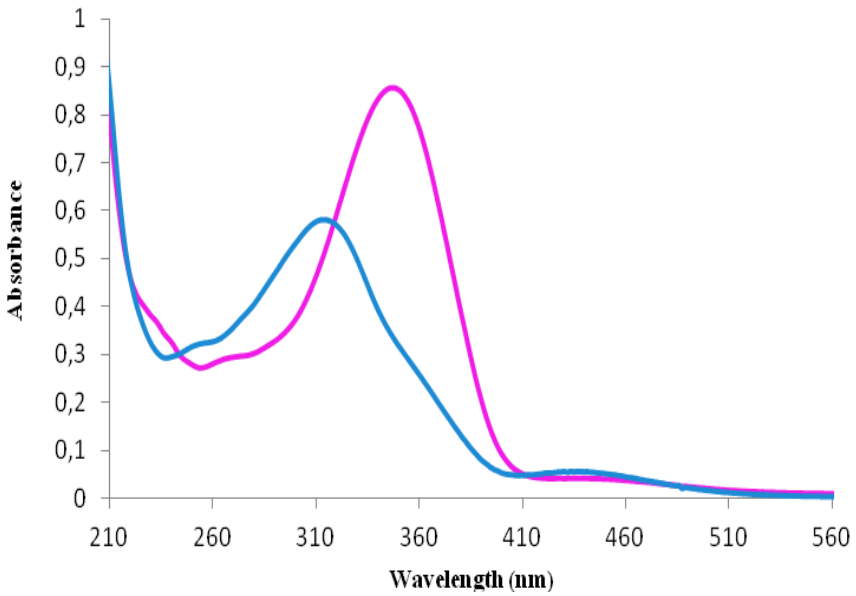

Fig. S32. UV/Vis spectra of ligand **5** in CH_3CN. Before (pink line) and after (blue line) irradiation at 353 nm, 2.50×10^{-5} M.

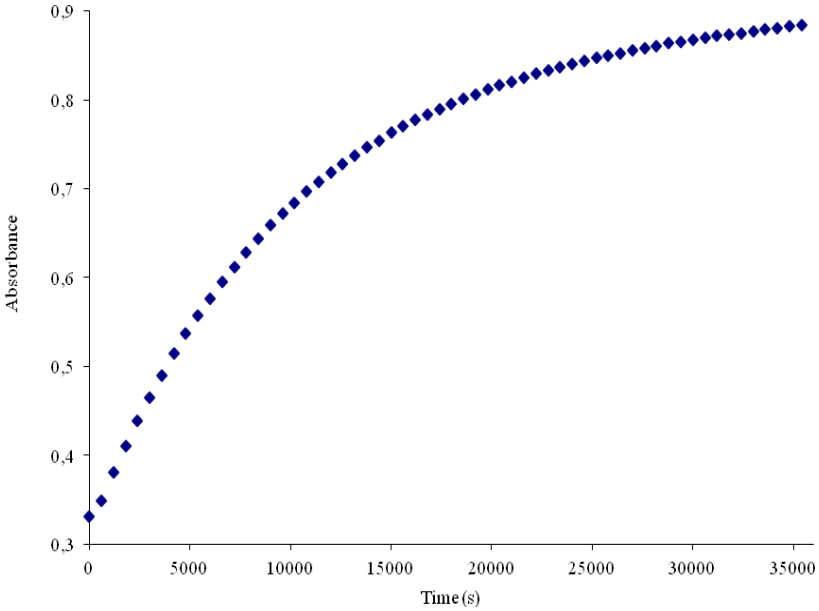

Fig. S33. *Cis* to *trans* thermal isomerization kinetics of ligand **5**. Absorption change of the band 347 nm at 328 K in CH_3CN after irradiation at 353 nm (2.50×10^{-5} M).

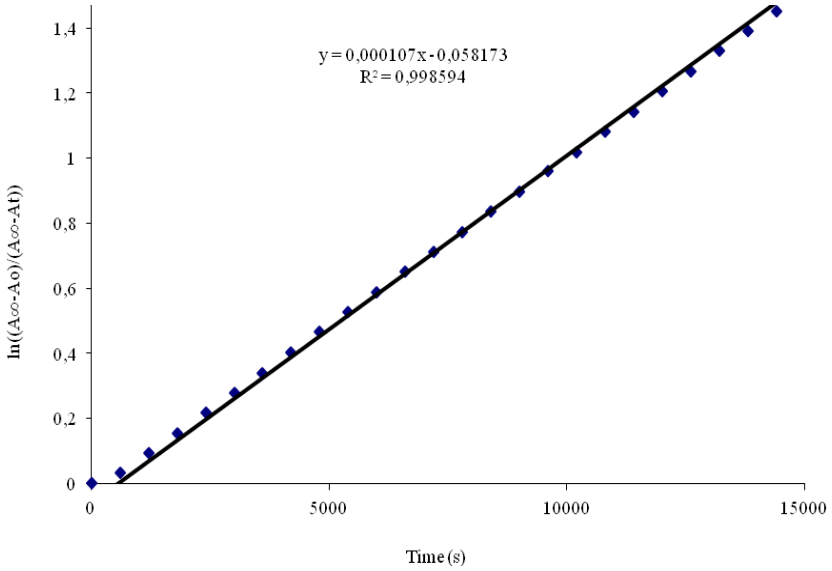

Fig. S34. *Cis* to *trans* thermal isomerization kinetics of ligand **5**. First-order plot. k (s^{-1}) = 1.1×10^{-4}. Half-life (s) = 6500.

[Ir((ppyBr)$_2$Cl]$_2$. Synthesis and characterization.

SYNTHESIS

To a solution of 5-bromo-2-phenylpyridine (3.00 g, 12.8 mmol) in 2-ethoxyethanol : H_2O (3:1, v/v; 60 mL) was added $IrCl_3 \cdot 3H_2O$ (1.80 g, 5.10 mmol) and the reaction mixture was heated to 120 °C for 24 h. The reaction was cooled to room temperature and 50 mL of water were added to precipitate the formed compound. The solution was gravity filtered and the solid was washed with 20 mL of hexane, 20 mL of ethanol and 50 mL of diethyl ether. The product obtained was rather insoluble in all the solvents assayed (i.e. solubility is less than 0.1 mg in 10 mL of $CDCl_3$), it was a light-orange powder (3.40 g, 96%). Low solubility hampered a complete NMR characterization.

Elemental Analysis: calculated for $C_{44}H_{28}Br_4Cl_2Ir2N_4$: C, 38.08; H, 2.03; N, 4.04. Found: C, 38.29; H, 2.44; N, 3.92.

[Ir(ppyBr)$_2$(acac)]. Synthesis and characterization.

SYNTHESIS

$[Ir(ppyBr)_2Cl]_2$, (150 mg, 0.11 mmol) and AgOTf (84 mg, 0.32 mmol) were dissolved in degassed acetone (8 mL) and refluxed (55 °C) under nitrogen for 2 h. The solution was cooled to room temperature and gravity-filtered to remove AgCl. The filtrate was refluxed (55 °C) under nitrogen for 1 h and added to a 1 h refluxed solution of acetylacetone (45 µL, 0.43 mmol) and triethylamine (113 µL, 0.81 mmol) dissolved in degassed acetone (4 mL). The resulting solution was refluxed overnight under nitrogen. After removing the solvent, the residue was purified by column chromatography: silica/CH_2Cl_2 (Rf = 0.8). It was obtained as a light-orange powder (106 mg, 65%)

Elemental Analysis: calculated for $C_{27}H_{21}Br_2IrN_2O_2 \cdot 2\ C_3H_6O$: C, 45.37; H, 3.81; N, 3.21. Found: C, 45.52; H, 4.14; N, 3.29.

Exact mass (MALDI) - m/z: 755.9575 for $[M]^+$ with (^{193}Ir)(^{79}Br).

^{1}H NMR (300 MHz, $CDCl_3$): δ 8.60 (d, *J* = 1.9, 2H, C_5H_3NBr), 7.87 (dd, *J* = 8.7, 2.1, 2H, C_5H_3NBr), 7.75 (d, *J* = 8.7, 2H, C_5H_3NBr), 7.54 (dd, *J* = 7.6, 1.2, 2H, C_6H_4), 6.87 (td, 7.5, 1.3, 2H, C_6H_4), 6.77 (td, 7.4, 1.4, 2H, C_6H_4), 6.30 (d, *J* = 7.5, 2H, C_6H_4), 5.31 (s, 1H, HAcac), 1.87 (s, 6H, HAcac).

^{13}C NMR (75 MHz, $CDCl_3$): δ 185.11 (2C, $C_{quat.}$), 167.58 (2C, $C_{quat.}$), 148.75 (2C, CH, C_5H_3NBr), 147.31 (2C, $C_{quat.}$), 143.49 (2C, $C_{quat.}$), 139.68 (2C, CH, C_5H_3NBr), 132.99 (2C, CH, C_6H_4), 129.61 (2C, CH, C_6H_4), 124.22 (2C, CH, C_6H_4), 121.10 (2C, CH, C_6H_4), 119.16 (2C, CH, C_5H_3NBr), 115.78 (2C, $C_{quat.}$), 100.78 (1C, CH, HAcac), 28.77 (2C, CH_3, Hacac).

UV/Vis (CH_3CN, λ, nm (ε, L mol^{-1} cm^{-1})): 265 ($4.5 \cdot 10^4$), 312 ($1.9 \cdot 10^4$), 347 ($8.6 \cdot 10^3$), 380 ($5.3 \cdot 10^3$), 416 ($3.9 \cdot 10^3$), 470 ($2.5 \cdot 10^3$), 503 ($1.0 \cdot 10^3$).

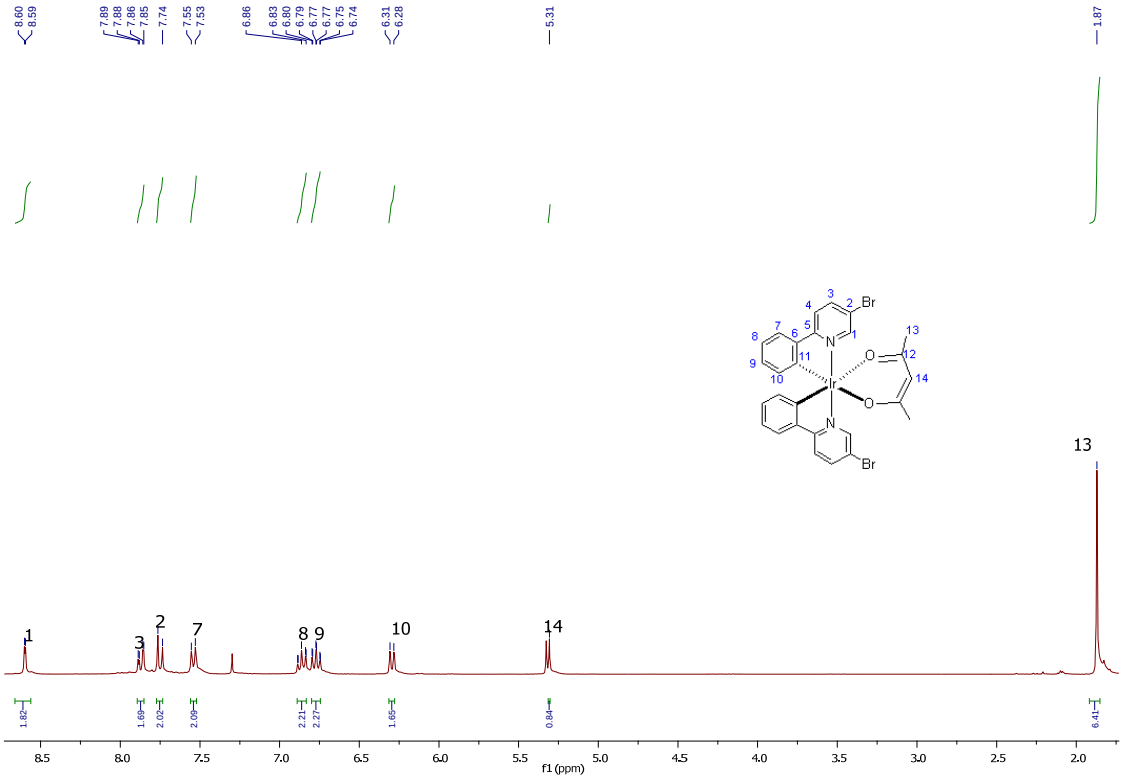

Fig. S35. ^{1}H NMR spectrum of $[Ir(ppyBr)_2(acac)]$ in $CDCl_3$, 300 MHz.

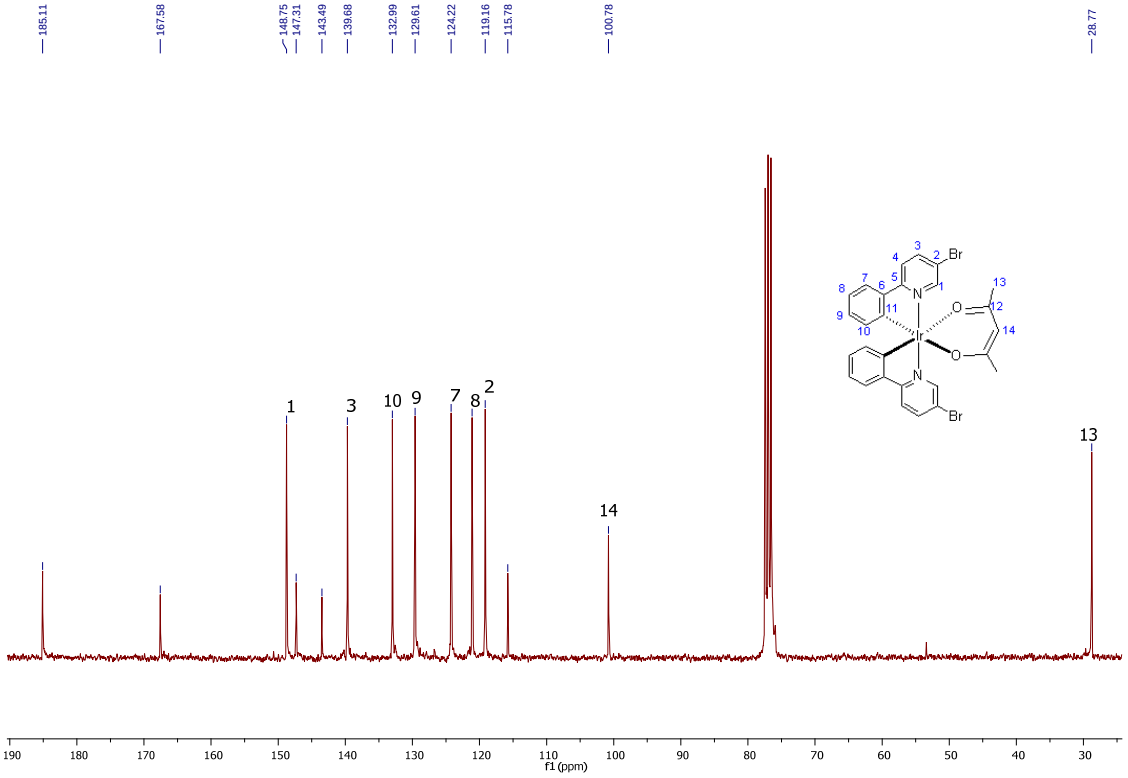

Fig. S36. ^{13}C NMR spectrum of $[Ir(ppyBr)_2(acac)]$ in $CDCl_3$, 75 MHz.

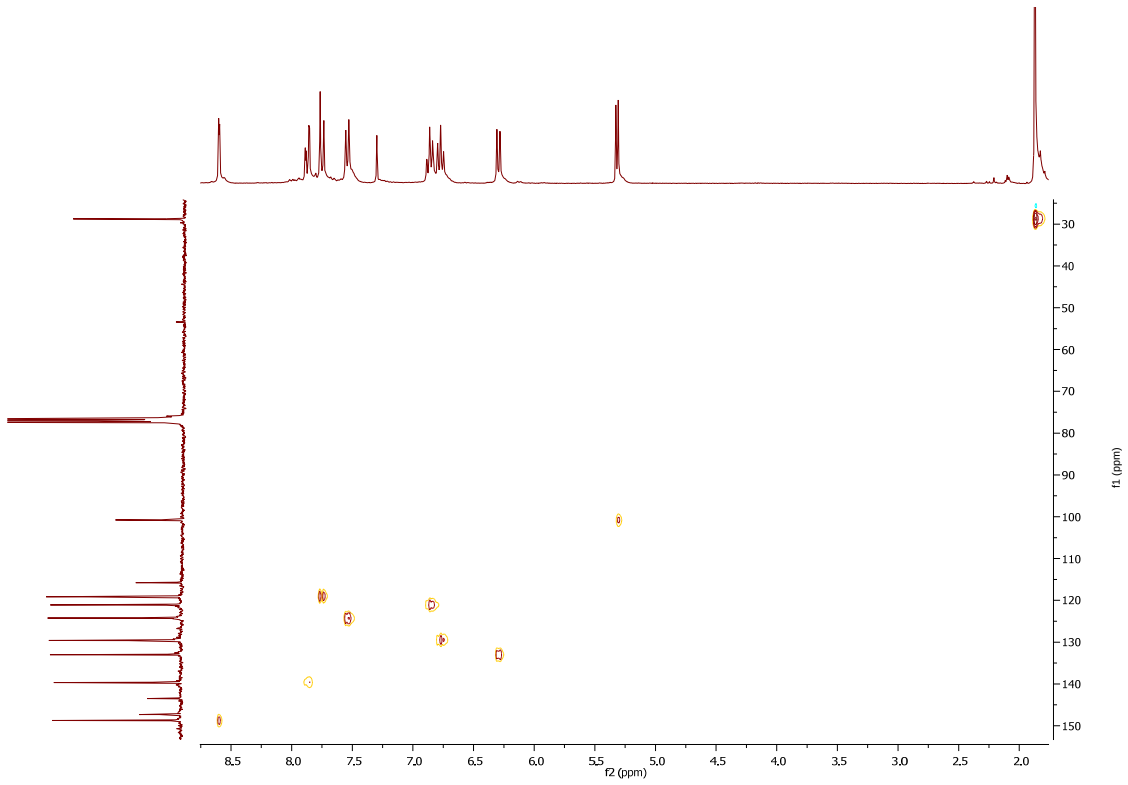

Fig. S37. HSQC spectrum of $[Ir(ppyBr)_2(acac)]$ in $CDCl_3$.

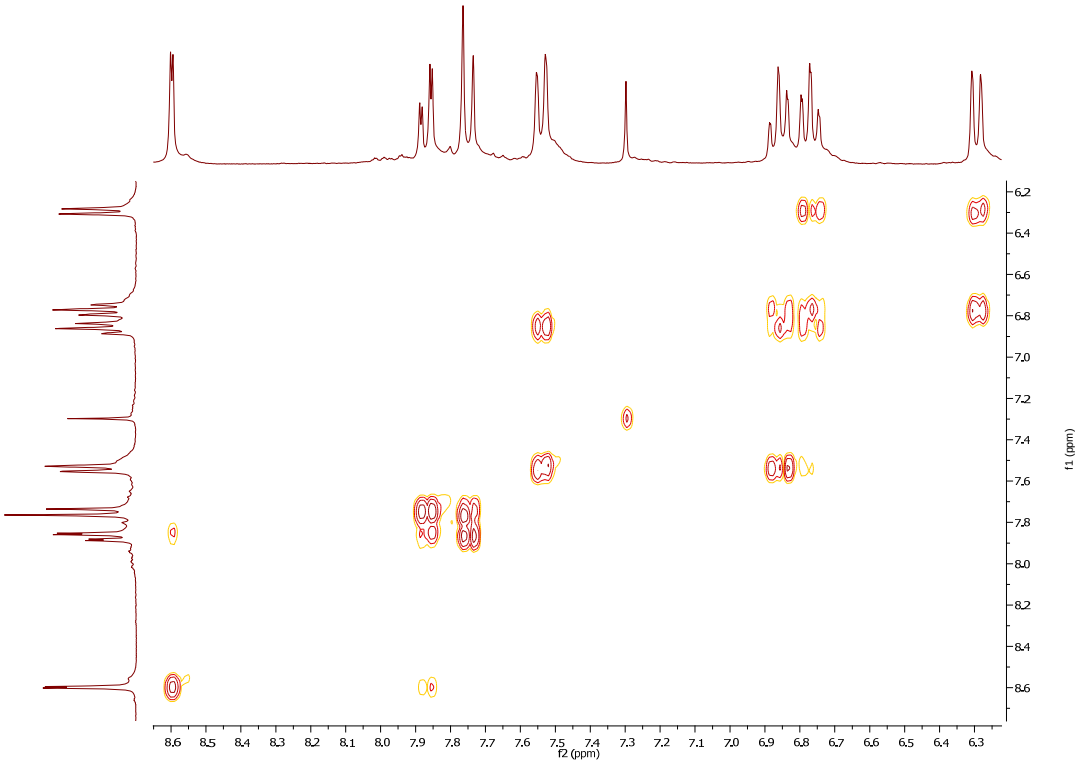

Fig. S38. COSY spectrum of $[Ir(ppyBr)_2(acac)]$ in $CDCl_3$.

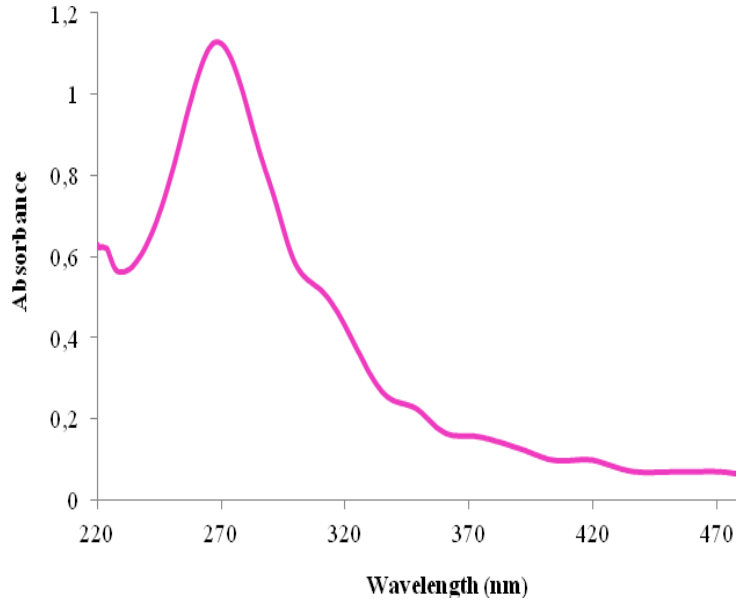

Fig. S39. UV/Vis spectra of $[Ir(ppyBr)_2(acac)]$ in CH_3CN, $2.50 \cdot 10^{-5}$M.

[Ir(5)$_2$(acac)]. Synthesis, characterization and photoisomerization studies.

SYNTHESIS

[Ir(ppyBr)$_2$(acac)] (60 mg, 0.079 mmol) was dissolved in 4 mL of degassed THF. To this mixture, 4-(phenylazo)phenyl boronic acid pinacol ester (54 mg, 0.174 mmol), Pd(PPh$_3$)$_4$ (2 mol%, 3 mg, 0.002 mmol), and Na_2CO_3 (1 M aq., 2 mL) were added successively under nitrogen. The reaction mixture was heated overnight at 80 °C with continuous stirring. The reaction was cooled to room temperature and 50 mL of water were added to precipitate the formed compound. The solution was gravity filtered and the solid was washed with hexane (20 mL). The resulting solid was purified by column chromatography (silica) eluting with dichloromethane (Rf = 0.7), obtaining 65 mg of the title compound (86% yield) as a red powder.

Elemental Analysis: calculated for $C_{51}H_{39}IrN_6O_2 \cdot 1C_6H_{14}$: C, 65.43; H, 5.11; N, 8.03. Found: C, 65.10; H, 4.89; N, 7.91.

Exact mass (MALDI) - m/z: 960.2776 for $[M]^+$ with (^{193}Ir).

^{1}H NMR (300 MHz, $CDCl_3$): δ 8.93 (d, *J* = 1.9, 2H, C_5H_3N), 8.12 – 8.08 (m, 6H), 8.00 (m, 6H), 7.84 (d, *J* = 8.6, 4H, C_6H_4 ($C_{12}H_9N_2$)), 7.66 (dd, *J* = 8.1, 1.2, 2H, C_6H_4 ($C_{11}H_7$)), 7.59 – 7.53 (m, 6H, C_6H_5), 6.91 (dt, *J* = 7.4, 1.1, 2H, C_6H_4 ($C_{11}H_7$)), 6.78 (dt, *J* = 7.5, 1.3, 2H, C_6H_4 ($C_{11}H_7$)), 6.43 (dd, J=7.5, 0.8, 2H, C_6H_4 ($C_{11}H_7$)), 5.37 (s, 1H, HAcac), 1.89 (s, 6H, HAcac).

^{13}C NMR (75 MHz, $CDCl_3$): δ 184.55 (2C, $C_{quat.}$), 167.33 (2C, $C_{quat.}$), 152.25 (2C, $C_{quat.}$), 151.88 (2C, $C_{quat.}$), 147.45 (2C, $C_{quat.}$), 145.87 (2C, CH, C_5H_3N), 143.87 (2C, $C_{quat.}$), 138.55 (2C, $C_{quat.}$), 134.76 (2C, CH, C_5H_3N), 133.04 (2C, $C_{quat.}$), 132.86 (2C, CH, C_6H_4 ($C_{11}H_7$)), 130.83 (2C, CH, C_6H_5), 128.93 (2C, CH, C_6H_4 ($C_{11}H_7$)), 128.72 (4C, CH, C_6H_5), 126.89 (4C, CH, C_6H_4 ($C_{12}H_9N_2$)), 123.76 (2C, CH, C_6H_4 ($C_{11}H_7$)), 123.37 (4C, CH, , C_6H_4 ($C_{12}H_9N_2$)), 122.54, (4C, CH, C_6H_5) 120.60 (2C, CH, C_6H_4 ($C_{11}H_7$)), 117.97 (2C, CH, C_5H_3N), 100.34 (1C, CH, HAcac), 28.34 (2C, CH_3, HAcac).

UV/Vis (CH_3CN, λ, nm (ε, L mol^{-1} cm^{-1})): 349 (7.9×10^4), 486 (6.9×10^3).

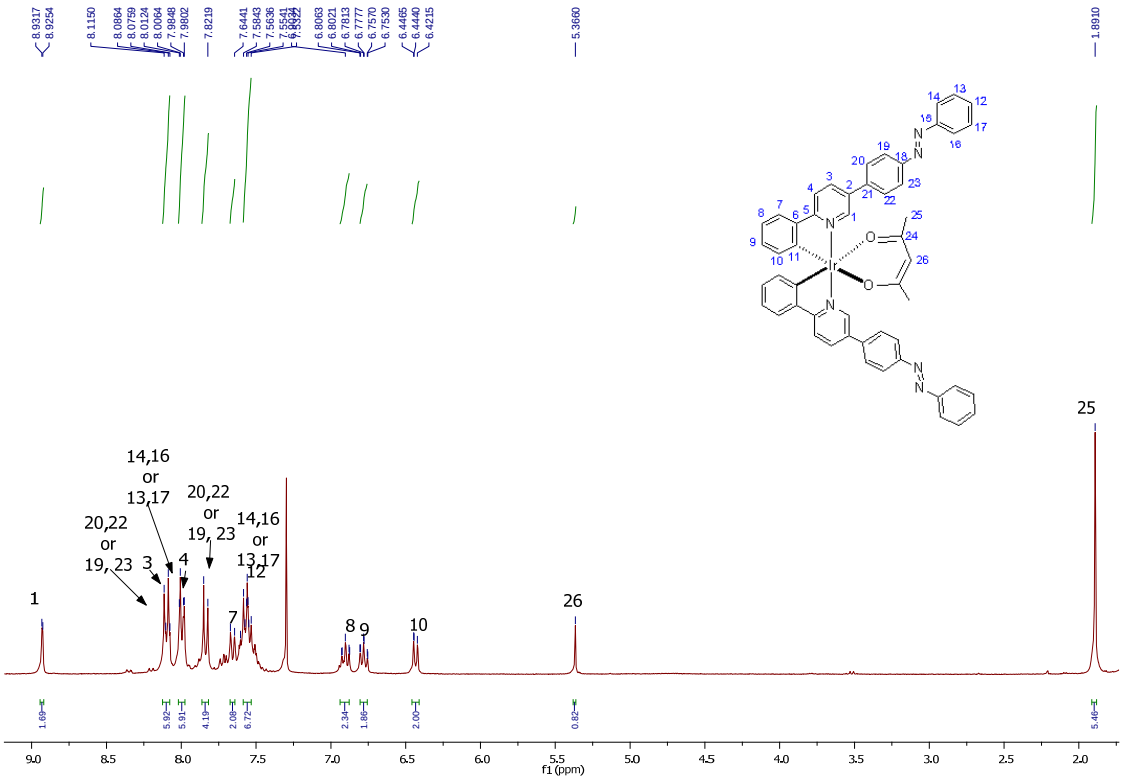

Fig. S40. ^{1}H NMR spectrum of [Ir(**5**)$_2$(acac)] in $CDCl_3$, 300 MHz.

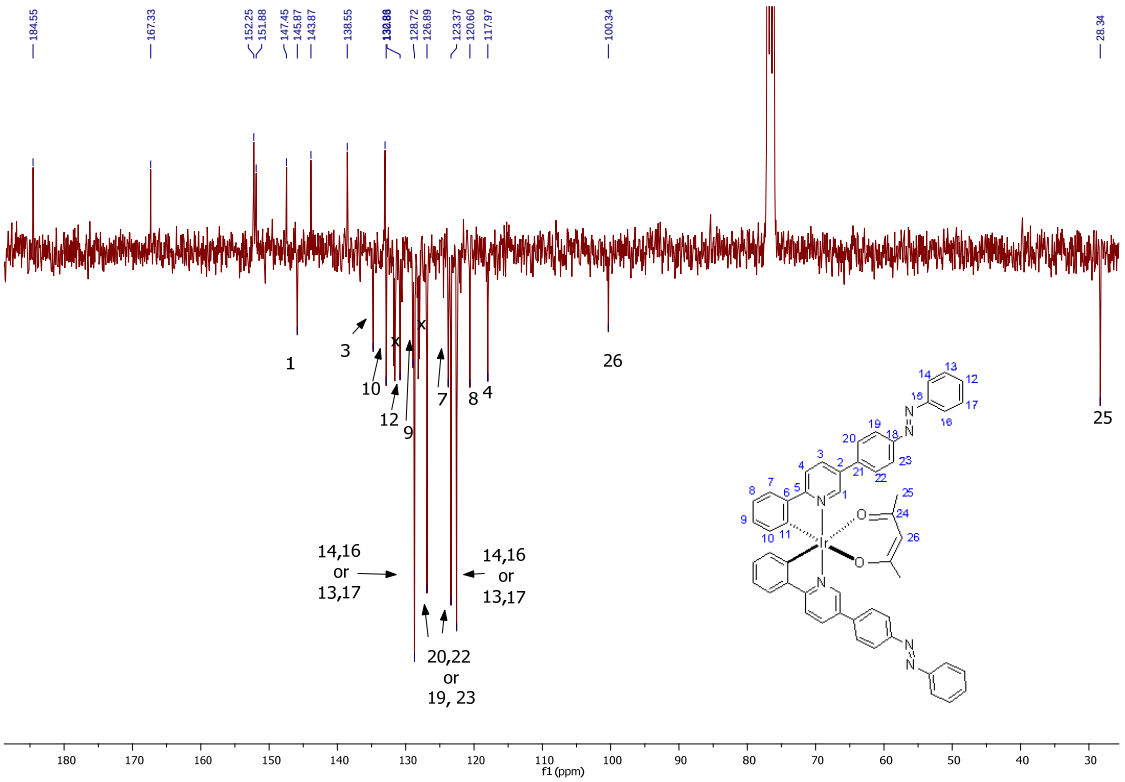

Fig. S41. ^{13}C APT NMR spectrum of [Ir(**5**)$_2$(acac)] in $CDCl_3$, 75 MHz.

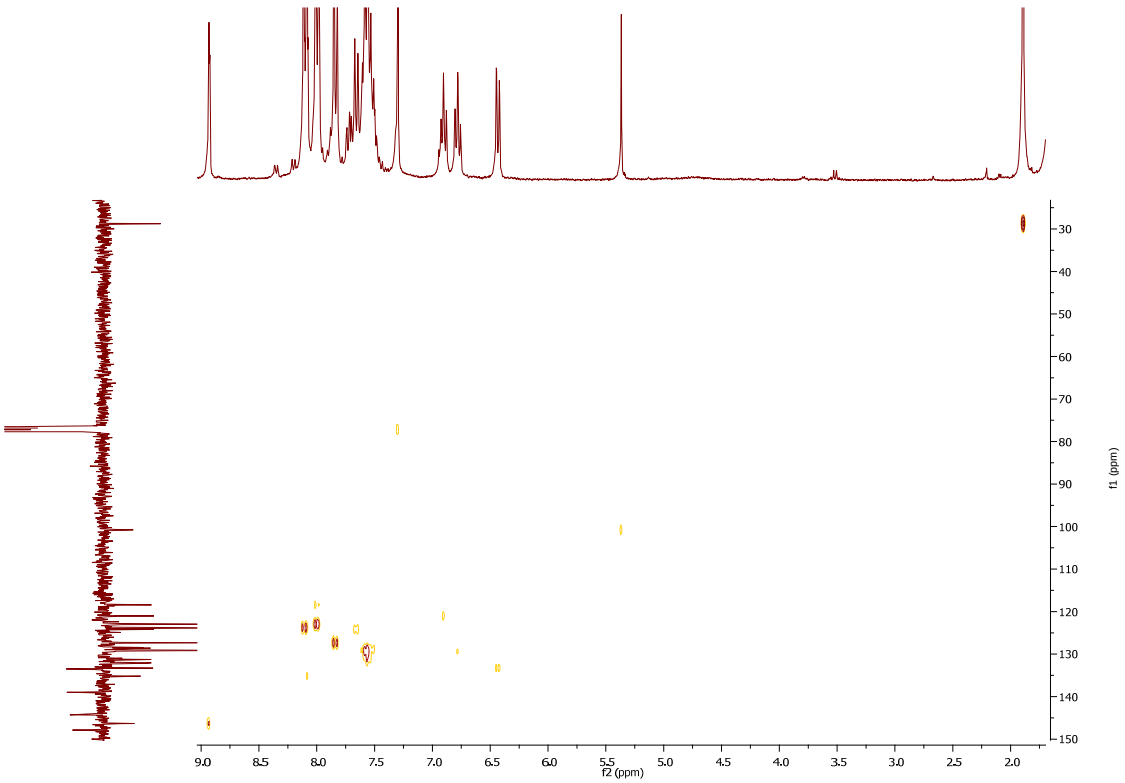

Fig. S42. HSQC NMR spectrum of [Ir(**5**)$_2$(acac)] in $CDCl_3$.

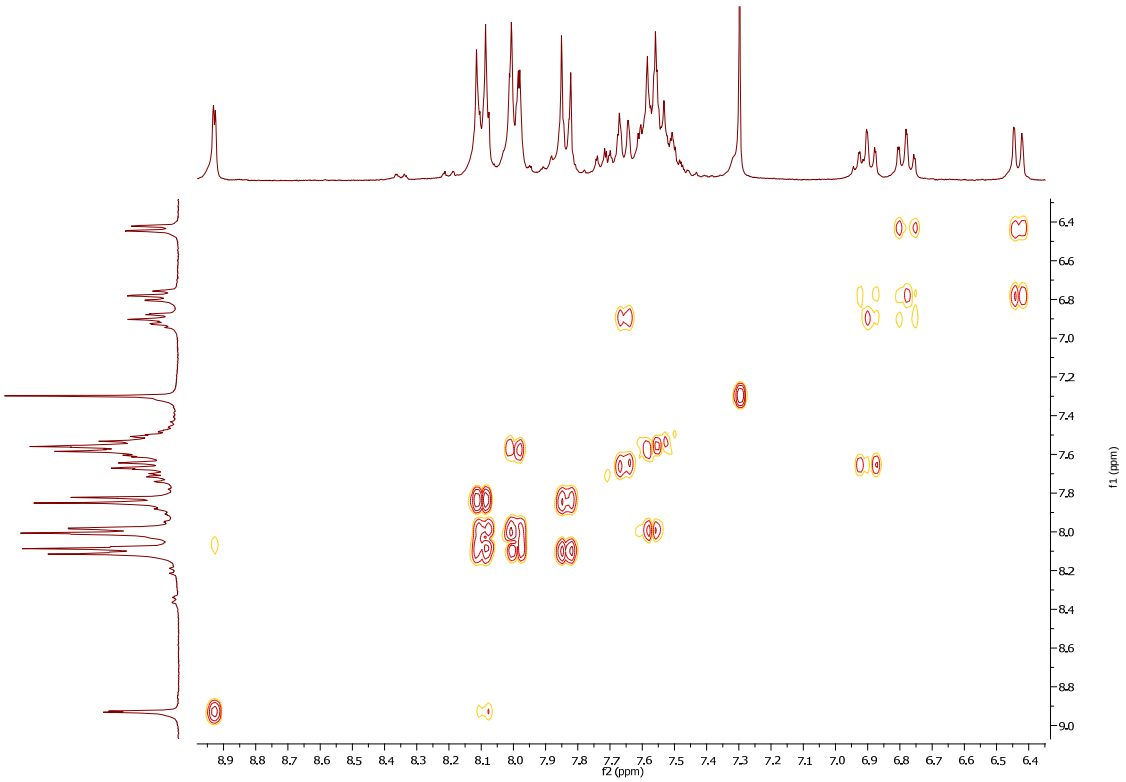

Fig. S43. COSY NMR spectrum of [Ir(**5**)$_2$(acac)] in $CDCl_3$.

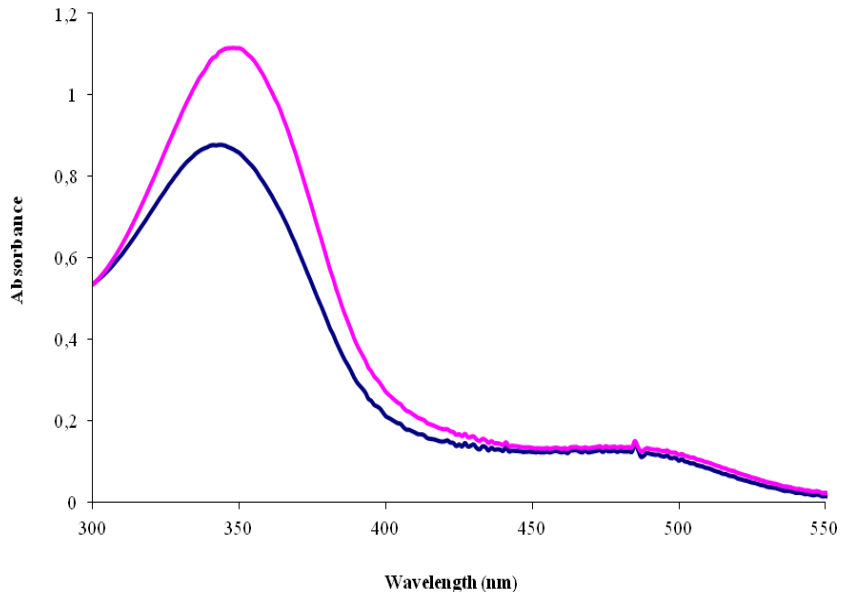

Fig. S44. UV/Vis spectra of [Ir(**5**)$_2$(acac)] in CH_3CN. Before (pink line) and after (blue line) irradiation at 359 nm, 2.50×10^{-5} M.

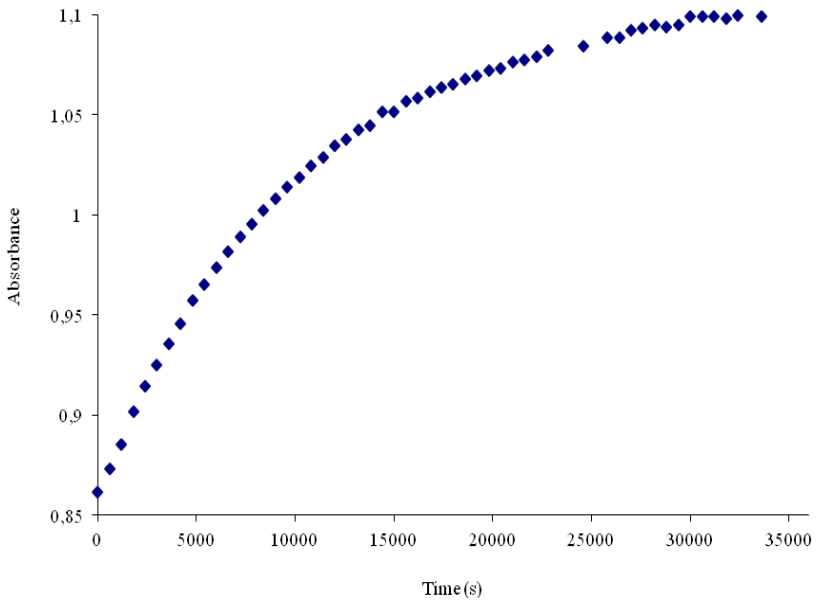

Fig. S45. *Cis* to *trans* thermal isomerization kinetics of [Ir(**5**)$_2$(acac)]. Absorption change of the band 349 nm at 328 K in CH_3CN after irradiation at 359 nm (2.50×10^{-5} M).

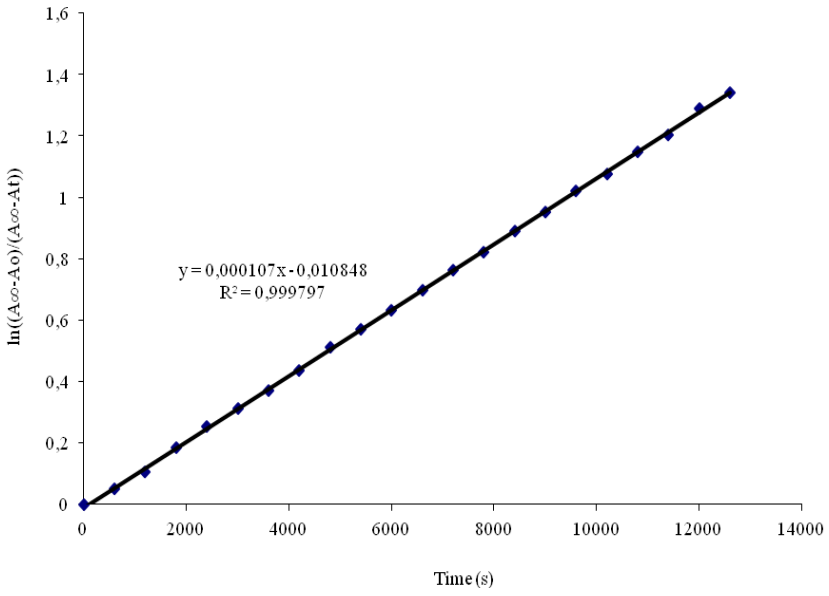

Fig. S46. *Cis* to *trans* thermal isomerization kinetics of [Ir(**5**)$_2$(acac)]. First-order plot. k (s^{-1}) = $1.1 \cdot 10^{-4}$. Half-life (s) = 6500.

[Ir(ppy)$_2$(1)]. Synthesis, characterization and photoisomerization studies.

SYNTHESIS

$[Ir(ppy)_2Cl]_2$ (150 mg, 0.14 mmol) and AgOTf (108 mg, 0.42 mmol) were dissolved in degassed acetone (8 mL) and refluxed under nitrogen for 2 h. The solution was cooled to room temperature and gravity-filtered to remove AgCl. The filtrate was refluxed under nitrogen (55 °C) for 1 h and added to a 1 h refluxed solution of ligand **1** (205 mg, 0.56 mmol) and NEt_3 (147 µL, 1.05 mmol) in degassed acetone (4 mL). The resulting solution was refluxed overnight (55 °C) under nitrogen. After removing the solvent, the residue was purified by column chromatography: silica/CH_2Cl_2 (Rf = 0.8). It was obtained as an orange powder (120 mg, 50%).

Elemental Analysis: calculated for $C_{46}H_{34}IrN_5O$: C, 63.87; H, 3.96; N, 8.10. Found: C, 64.43; H, 4.23; N, 7.60.

Exact mass (MALDI) - m/z: 865.2393 for $[M]^+$ with (^{193}Ir).

^{1}H NMR (500 MHz, $CDCl_3$): δ 8.07 (d, *J* = 5.0, 1H), 7.93 (d, *J* = 6.7, 2H), 7.90 (d, *J* = 7.7, 2H, $C_{24}H_{18}N_3O$), 7.86 (d, *J* = 8.5, 2H, $C_{24}H_{18}N_3O$), 7.78 (m, 3H), 7.69 (d, *J* = 5.9, 1H), 7.62 (m, 3H), 7.54 – 7.44 (m, 5H), 7.12 (d, *J* = 7.1, 1H), 6.93 (m, 8H), 6.70 (d, *J* = 4.5, 2H), 6.63 (d, *J* = 5.6, 1H), 6.47 (d, *J* = 7.1, 1H), 4.98 (s, 2H, CH_2).

^{13}C NMR (126 MHz, $CDCl_3$): δ 178.38 (1C, $C_{quat.}$), 175.06 (1C, $C_{quat.}$), 170.59 (1C, $C_{quat.}$), 168.12 (1C, $C_{quat.}$), 167.98 (1C, $C_{quat.}$), 161.55 (1C, $C_{quat.}$), 159.14 (1C, $C_{quat.}$), 153.35 (1C, CH), 152.91 (1C, $C_{quat.}$), 151.34 (1C, CH), 147.88 (1C, CH), 146.87 (1C, $C_{quat.}$), 145.49 (1C, $C_{quat.}$), 144.84 (1C, $C_{quat.}$), 142.32 (1C, $C_{quat.}$), 137.24 (1C, CH), 137.22 (1C, $C_{quat.}$), 136.62 (1C, CH), 135.61 (1C, CH), 134.15 (1C, CH), 132.81 (1C, CH), 130.59 (1C, CH), 130.36 (1C, CH), 130.07 (1C, CH), 129.76 (1C, CH), 129.13 (2C, CH, , $C_{12}H_9N_2$), 124.66 (2C, CH, , $C_{12}H_9N_2$), 124.50 (1C, CH), 124.21 (1C, CH), 124.11 (1C, CH), 122.60 (2C, CH, , $C_{12}H_9N_2$), 122.45 (1C, CH), 122.13 (1C, CH), 121.29 (1C, CH), 120.98 (1C, CH), 120.68 (1C, CH), 119.18 (1C, CH), 119.01 (1C, CH), 118.67 (1C, CH), 118.48 (1C, CH), 115.44 (2C, CH, $C_{12}H_9N_2$), 71.04 (1C, CH_2).

UV/Vis (CH_3CN, λ, nm (ε, L mol^{-1} cm^{-1})): 345 ($3.2 \cdot 10^4$), 454 ($4.0 \cdot 10^3$).

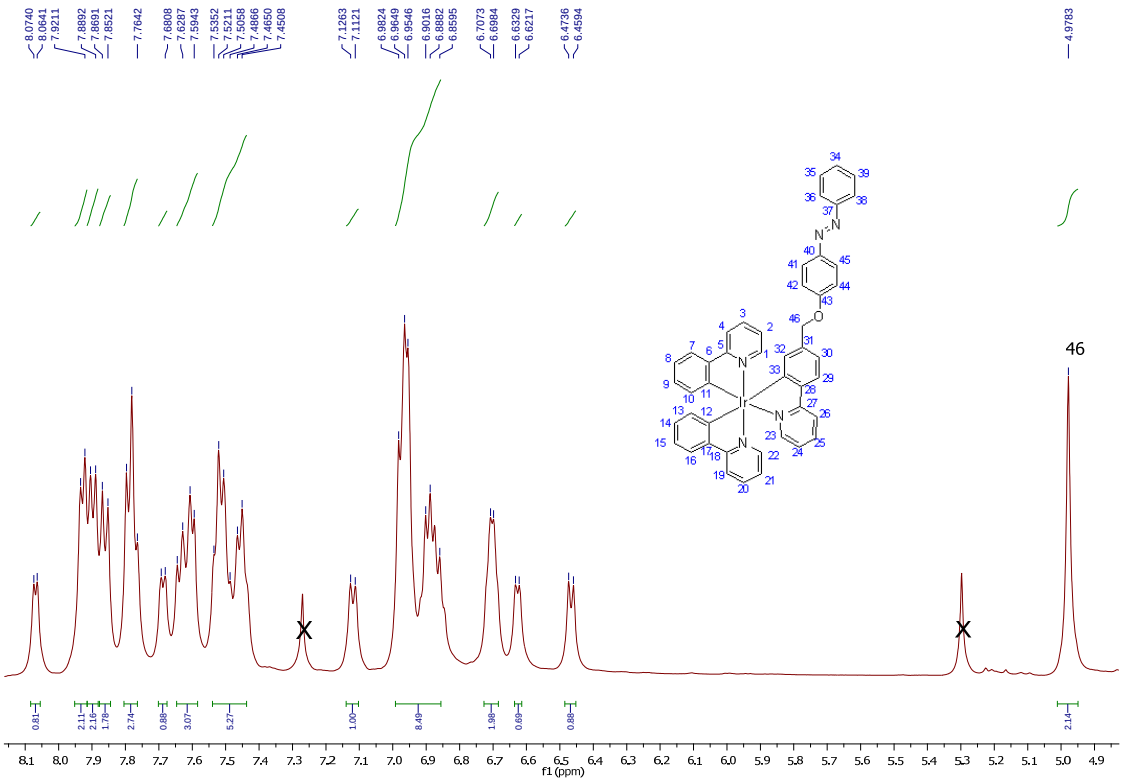

Fig. S47. ^{1}H NMR spectrum of [Ir(ppy)$_2$(**1**)] in $CDCl_3$, 500 MHz.

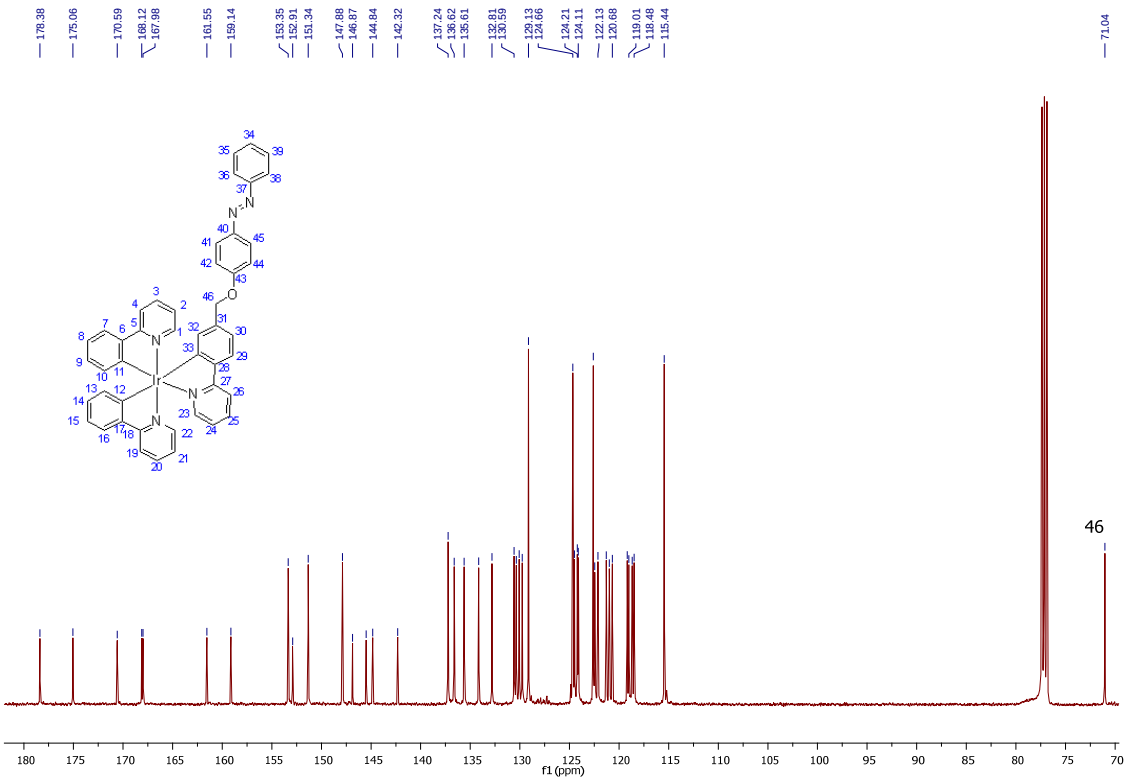

Fig. S48. ^{13}C NMR spectrum of [Ir(ppy)$_2$(**1**)] in $CDCl_3$, 126 MHz.

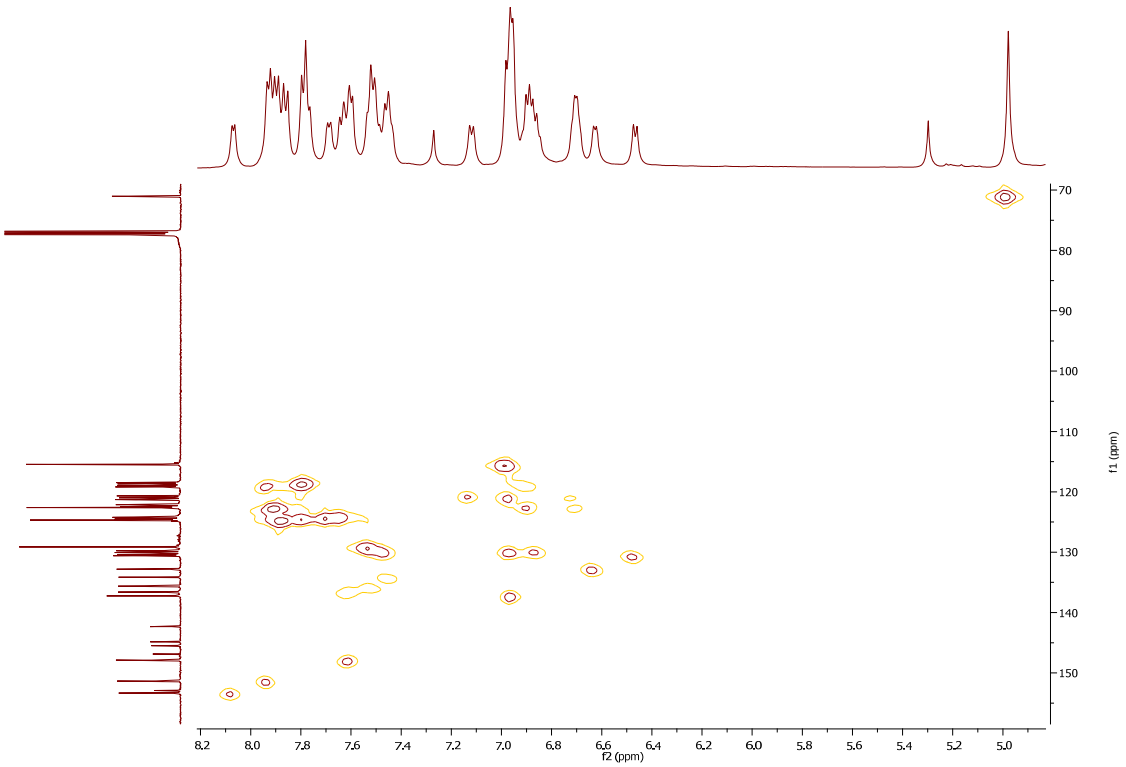

Fig. S49. HSQC NMR spectrum of [Ir(ppy)$_2$(**1**)] in $CDCl_3$.

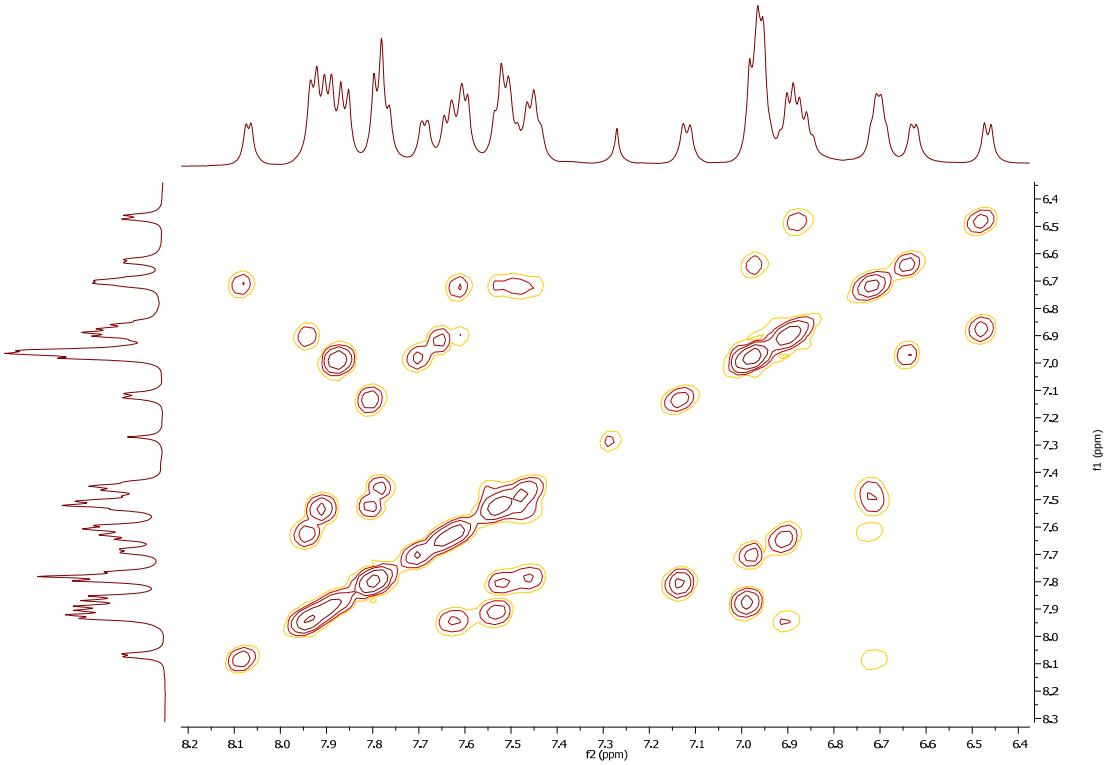

Fig. S50. COSY NMR spectrum of [Ir(ppy)$_2$(**1**)] in $CDCl_3$.

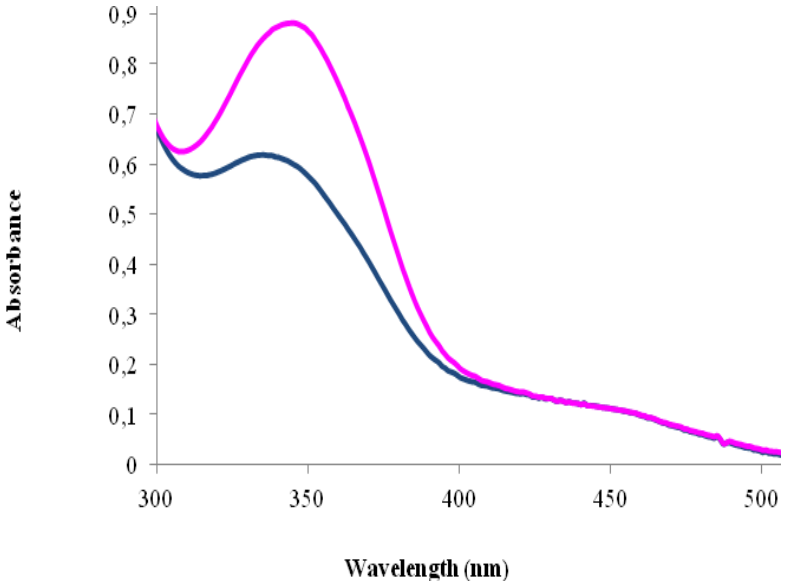

Fig. S51. UV/Vis spectra of [[Ir(ppy)$_2$(**1**)] in CH_3CN. Before (pink line) and after (blue line) irradiation at 349 nm, 2.50×10^{-5} M.

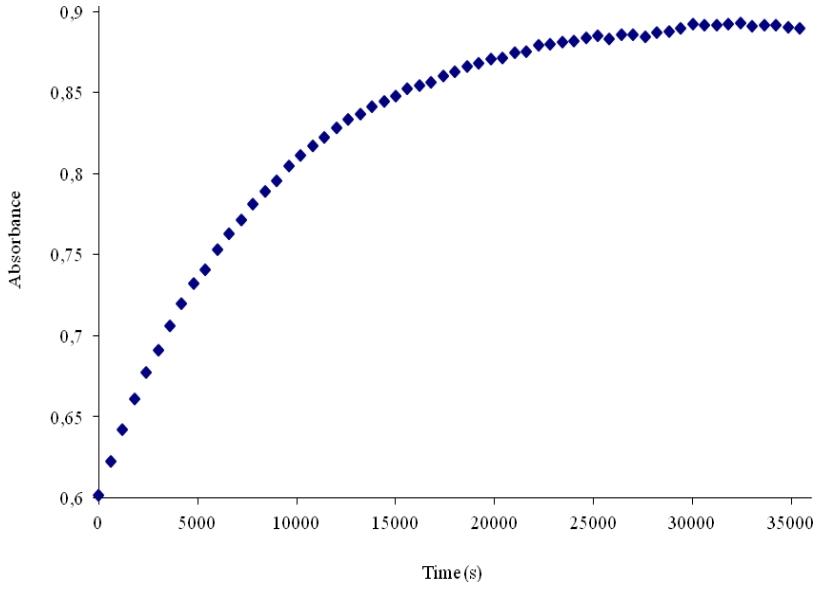

Fig. S52. *Cis* to *trans* thermal isomerization kinetics of [Ir(ppy)$_2$(**1**)]. Absorption change of the band 345 nm at 328 K in CH_3CN after irradiation at 349 nm (2.50×10^{-5} M).

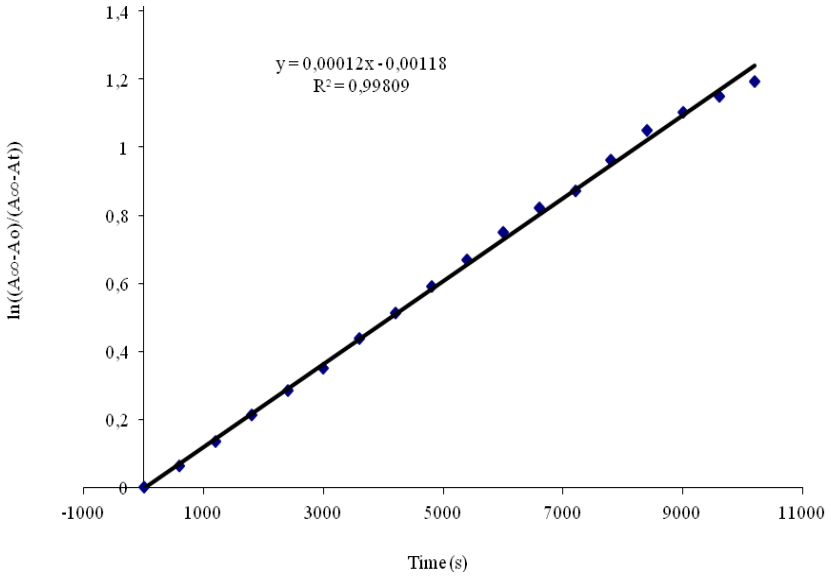

Fig. S53. *Cis* to *trans* thermal isomerization kinetics of [Ir(ppy)$_2$(**1**)]. First-order plot. k (s^{-1}) = 1.2×10^{-4}. Half-life (s) = 5600.

[Ir(ppy)$_2$(2)]. Synthesis, characterization and photoisomerization studies.

SYNTHESIS

$[Ir(ppy)_2Cl]_2$ (150 mg, 0.14 mmol) and AgOTf (108 mg, 0.42 mmol) were dissolved in degassed acetone (8 mL) and refluxed under nitrogen for 2 h. The solution was cooled to room temperature and gravity-filtered to remove AgCl. The filtrate was refluxed under nitrogen (55 °C) for 1 h and added to a 1 h refluxed solution of ligand **2** (196 mg, 0.56 mmol) and NEt_3 (147 µL, 1.05 mmol) in degassed acetone (4 mL). The resulting solution was refluxed overnight (55 °C) under nitrogen. After removing the solvent, the residue was purified by column chromatography: silica/CH_2Cl_2 (Rf = 0.8). It was obtained as an orange powder (100 mg, 42%).

Elemental Analysis: calculated for $C_{46}H_{34}IrN_5 \cdot C_3H_6O$: C, 64.88; H, 4.44; N, 7.72. Found: C, 64.75; H, 4.21; N, 7.59.

Exact mass (MALDI) - m/z: 849.2443 for $[M]^+$ with (^{193}Ir).

^{1}H NMR (300 MHz, $CDCl_3$): δ 8.15 (dd, *J* = 5.8, 0.9, 1H), 7.98 (dd, *J* = 8.2, 1.5, 2H, $C_{12}H_9N_2$), 7.87 – 7.72 (m, 7H), 7.70 – 7.63 (m, 3H), 7.61-7.43 (m, 6H), 7.10 (d, *J* = 8.4, 2H, $C_{12}H_9N_2$), 7.02 – 6.84 (m, 7H), 6.72 (d, *J* = 1.3, 1H), 6.72 (dddd, *J* =7.1, 5.8, 2.4, 1.2, 1H), 6.63-6.61 (m, 1H), 6.56 (dd, *J* = 7.4, 1.3, 1H), 3.80 (s, 2H, CH_2).

^{13}C NMR (75 MHz, $CDCl_3$): δ 177.31 (1C, $C_{quat.}$), 175.10 (1C, $C_{quat.}$), 170.52 (1C, $C_{quat.}$), 167.85 (1C, $C_{quat.}$), 166.65 (1C, $C_{quat.}$), 159.40 (1C, $C_{quat.}$), 153.17 (1C, 1CH), 152.67 (1C, $C_{quat.}$), 151.22 (1C, $C_{quat.}$), 150.95 (1C, CH), 147.77 (1C, CH), 145.18 (1C, $C_{quat.}$), 144.62 (1C, $C_{quat.}$), 142.58 (1C, $C_{quat.}$), 142.25 (1C, $C_{quat.}$), 137.89 (1C, CH), 136.75 (1C, CH), 135.40 (1C, CH), 134.63 (1C, $C_{quat.}$), 133.90 (1C, CH), 132.57 (1C, CH), 130.96 (1C, CH), 130.60 (1C, CH), 130.04 (1C, CH), 129.69 (1C, CH), 129.48 (1C, CH), 129.30 (2C, CH, $C_{12}H_9N_2$), 129.10 (2C, CH, $C_{12}H_9N_2$), 124.13 (1C, CH), 123.98 (1C, CH), 123.91 (1C, CH), 123.19 (2C, CH, $C_{12}H_9N_2$), 122.77 (2C, CH, $C_{12}H_9N_2$), 121.86 (1C, CH), 121.15 (1C, CH), 121.12 (1C, CH), 120.96 (1C, CH), 118.74 (1C, CH), 118.71 (1C, CH), 118.42 (1C, CH), 118.29 (1C, CH), 38.45 (1C, CH_2).

UV/Vis (CH_3CN, λ, nm (ε, L mol^{-1} cm^{-1})): 324 ($3.5 \cdot 10^4$), 436 ($5.0 \cdot 10^3$).

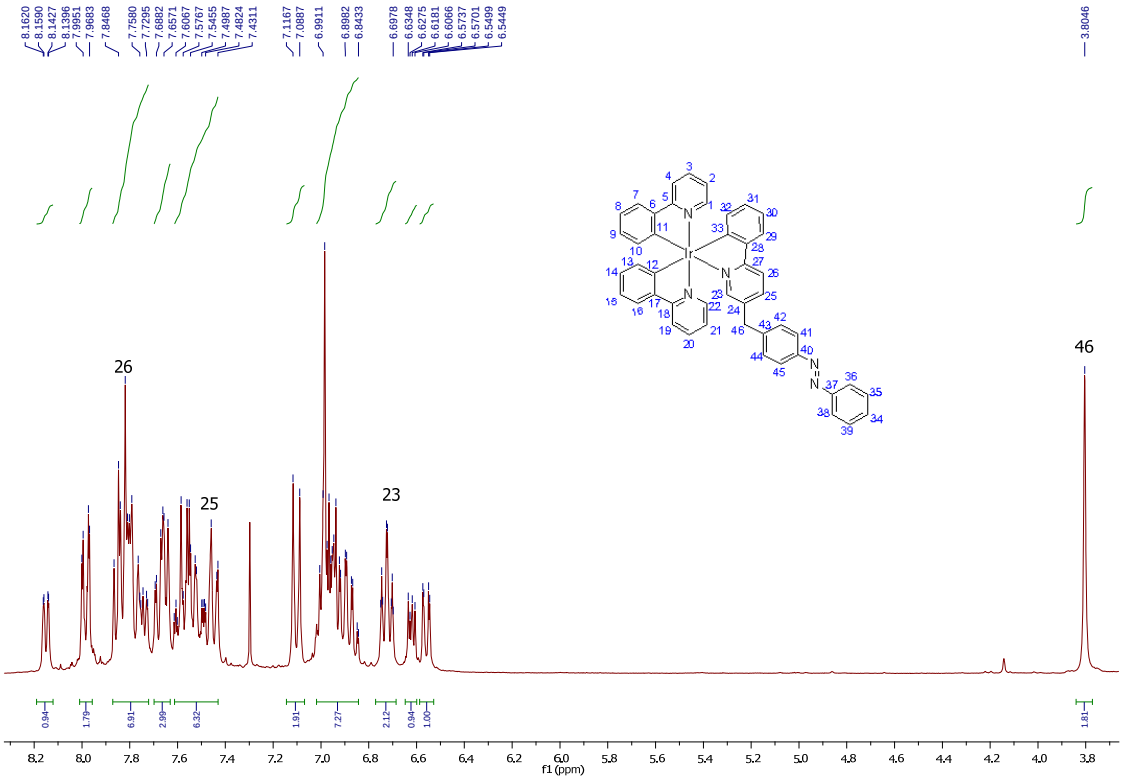

Fig. S54. ^{1}H NMR spectrum of [Ir(ppy)$_2$(**2**)] in $CDCl_3$, 300 MHz.

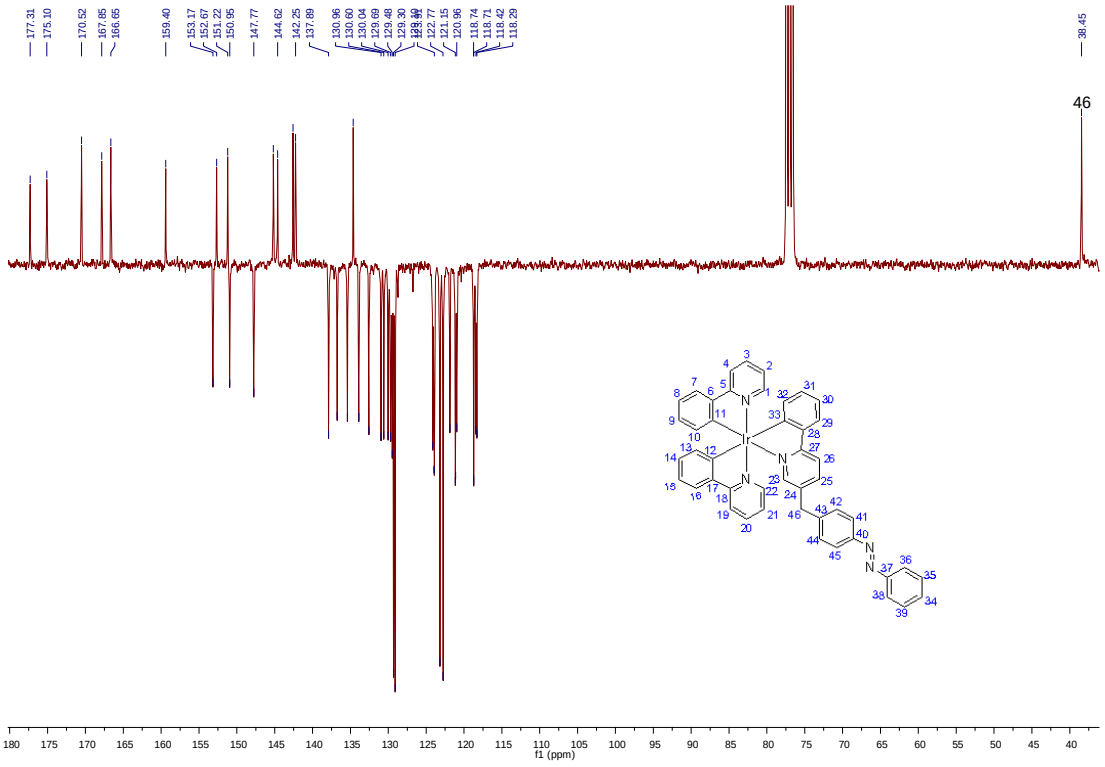

Fig. S55. ^{13}C APT NMR spectrum of [Ir(ppy)$_2$(**2**)] in $CDCl_3$, 75 MHz.

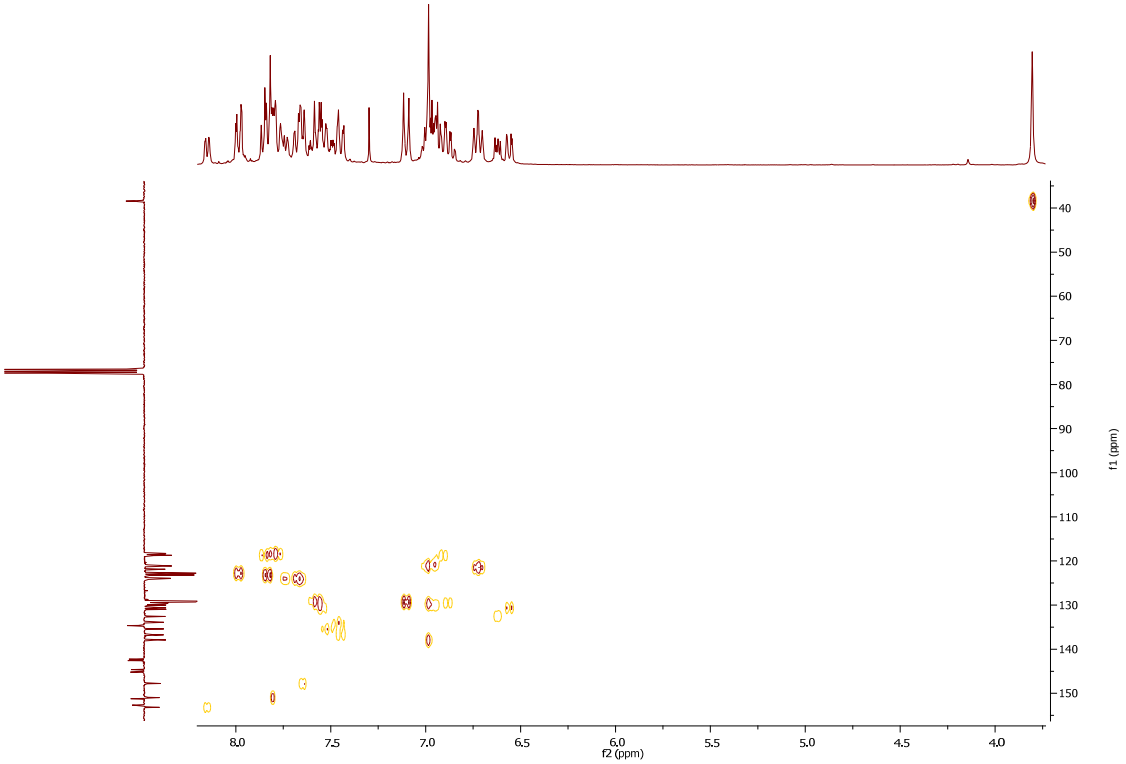

Fig. S56. HSQC NMR spectrum of [Ir(ppy)$_2$(**2**)] in $CDCl_3$.

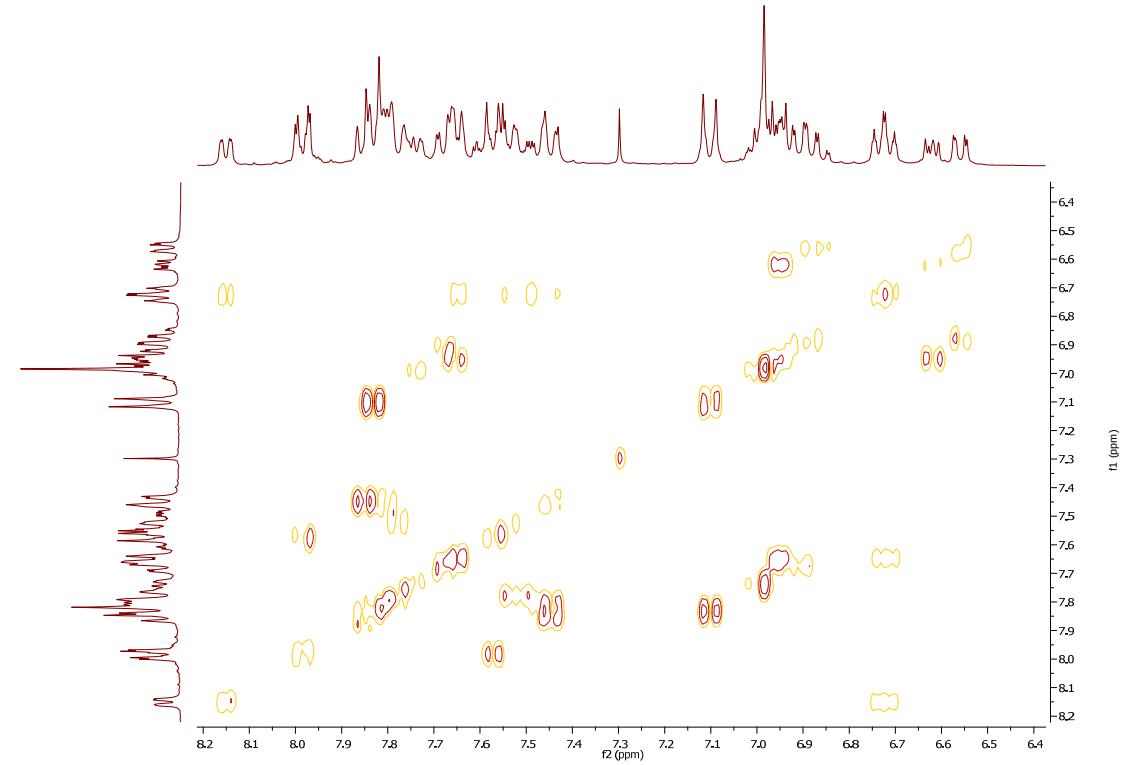

Fig. S57. COSY NMR spectrum of [Ir(ppy)$_2$(**2**)] in $CDCl_3$.

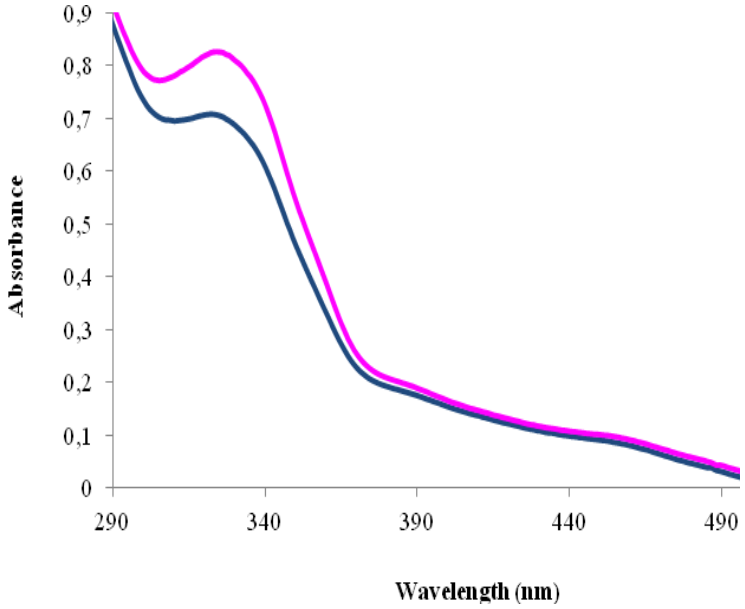

Fig. S58. UV/Vis spectra of [Ir(ppy)$_2$(**2**)] in CH_3CN. Before (pink line) and after (blue line) irradiation at 328 nm, 2.50×10^{-5} M.

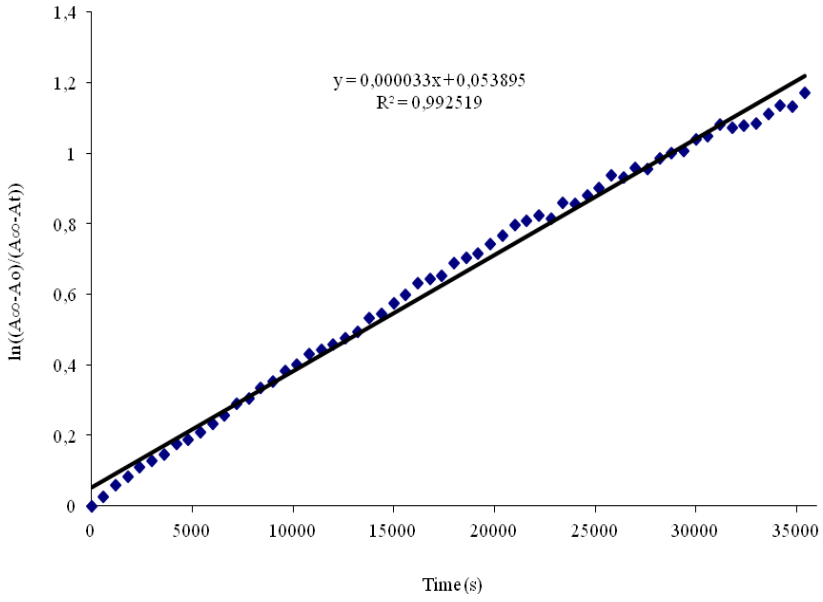

Fig. S59. *Cis* to *trans* thermal isomerization kinetics of [Ir(ppy)$_2$(**2**)]. All k values were calculated from the first-order plots of absorption change of the band 324 nm at 328 K in CH_3CN after irradiation at 328 nm (2.50×10^{-5} M). *Cis* to *trans* thermal isomerization of this complex is slow, and the A_∞ (0.789) value obtained in the kinetic measure does not correspond to A_∞ value (0.826) obtained as maximum of absorbance before the photoisomerization. We have used A_∞ = 0.826 as maximum of absorbance corresponding to *trans* isomer. k (s^{-1}) = 0.3×10^{-4}. Half-life (s) = 21000.

[Ir(ppy)$_2$(3)]. Synthesis, characterization and photoisomerization studies.

SYNTHESIS

$[Ir(ppy)_2Cl]_2$ (150 mg, 0.14 mmol) and AgOTf (108 mg, 0.42 mmol) were dissolved in degassed acetone (8 mL) and refluxed under nitrogen for 2 h. The solution was cooled to room temperature and gravity-filtered to remove AgCl. The filtrate was refluxed under nitrogen (55 °C) for 1 h and added to a 1 h refluxed solution of ligand **3** (157 mg, 0.56 mmol) and NEt_3 (147 µL, 1.05 mmol) in degassed acetone (4 mL). The resulting solution was refluxed overnight (55 °C) under nitrogen. After removing the solvent, the residue was purified by column chromatography: alumina/CH_2Cl_2 (Rf = 0.7). It was obtained as an orange powder (50 mg, 23%).

Elemental Analysis: calculated for $C_{39}H_{31}IrN_4O_2$: C, 60.06; H, 4.01; N, 7.18. Found: C, 59.85; H, 3.84; N, 7.05.

Exact mass (MALDI) - m/z: 780.2056 for $[M]^+$ with (^{193}Ir).

^{1}H NMR (300 MHz, $CDCl_3$): δ 8.71 (dd, *J* = 5.7, 0.7, 2H, $C_{11}H_8N$), 7.98 – 7.89 (m, 6H), 7.83 (ddd, J= 8.1, 7.4, 1.5, 2H, $C_{11}H_8N$), 7.62 (dd, *J* = 7.7, 1.0, 2H, $C_{11}H_8N$), 7.59 – 7.47 (m, 3H, $C_{12}H_9N_2$), 7.33 (d, J= 8.9, 2H, $C_{12}H_9N_2$), 7.27 (ddd, J= 7.2, 5.8, 1.4, 2H, $C_{11}H_8N$), 6.86 (td, *J* = 7.5, 1.2, 2H, $C_{11}H_8N$), 6.74 (td, *J* = 7.4, 1.3, 2H, $C_{11}H_8N$), 6.33 (dd, *J* = 7.6, 0.9, 2H, $C_{11}H_8N$), 1.61 (s, 6H, CH_3).

^{13}C NMR (75 MHz, $CDCl_3$): δ 182.99 (2C, $C_{quat.}$), 168.35 (2C, $C_{quat.}$), 152.33 (1C, $C_{quat.}$), 150.74 (1C, $C_{quat.}$), 147.72 (2C, CH, $C_{11}H_8N$), 147, 63 (2C, $C_{quat.}$), 146.15 (1C, $C_{quat.}$), 144.26 (2C, $C_{quat.}$), 136.50 (2C, CH, $C_{11}H_8N$), 132.69 (4C, CH), 130.44 (1C, CH, $C_{12}H_9N_2$), 128.65 (2C, CH), 128.62 (2C, CH), 123.45 (2C, CH, $C_{11}H_8N$), 122.61 (2C, CH), 122.33 (2C, CH), 120.88 (2C, CH, $C_{11}H_8N$), 120.19 (2C, CH, $C_{11}H_8N$), 118.03 (2C, CH), 114.56 (1C, $C_{quat.}$), 29.18 (2C, CH_3).

UV/Vis (CH_3CN, λ, nm (ε, L mol^{-1} cm^{-1})): 327 ($3.0 \cdot 10^4$), 455 ($3.7 \cdot 10^3$).

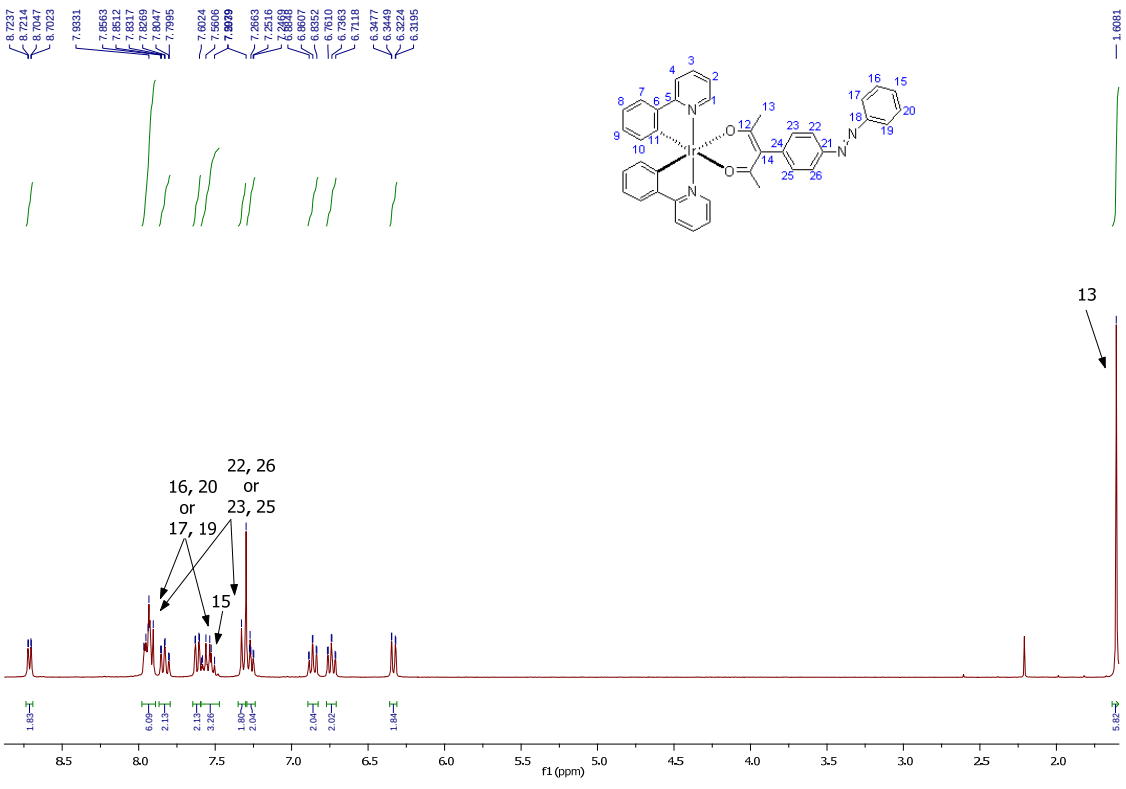

Fig. S60. ^{1}H NMR spectrum of [Ir(ppy)$_2$(**3**)] in $CDCl_3$, 300 MHz.

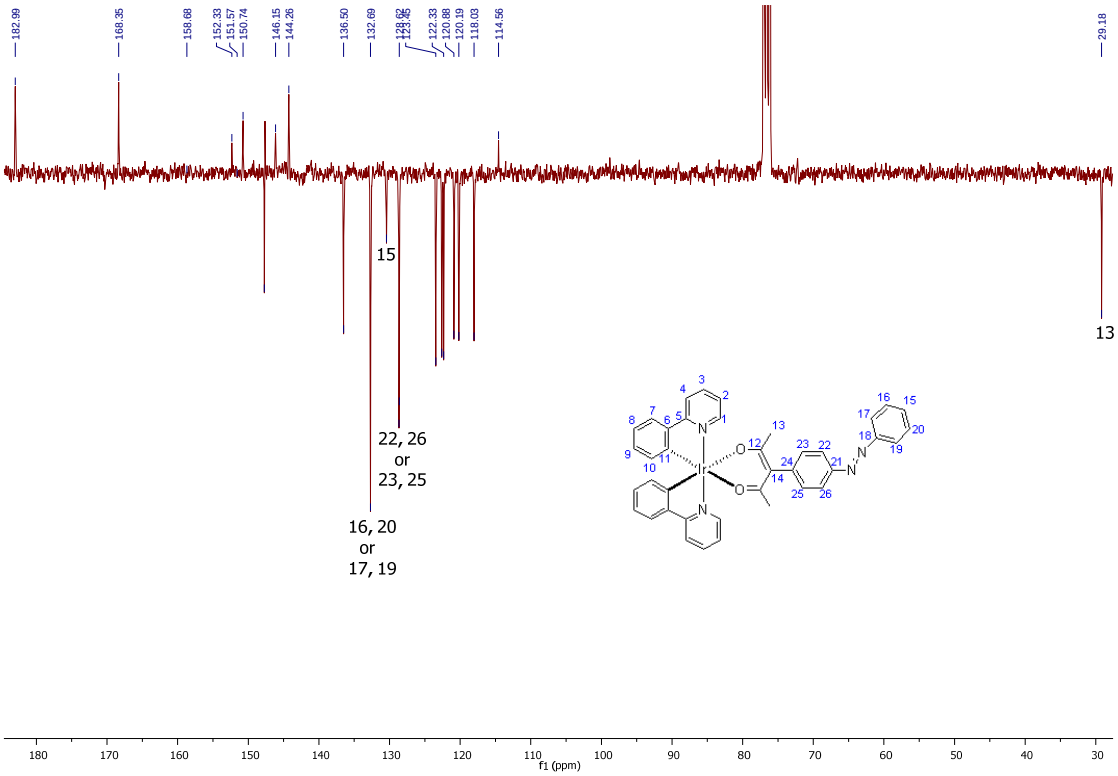

Fig. S61. ^{13}C NMR spectrum of [Ir(ppy)$_2$(**3**)] in $CDCl_3$, 75 MHz.

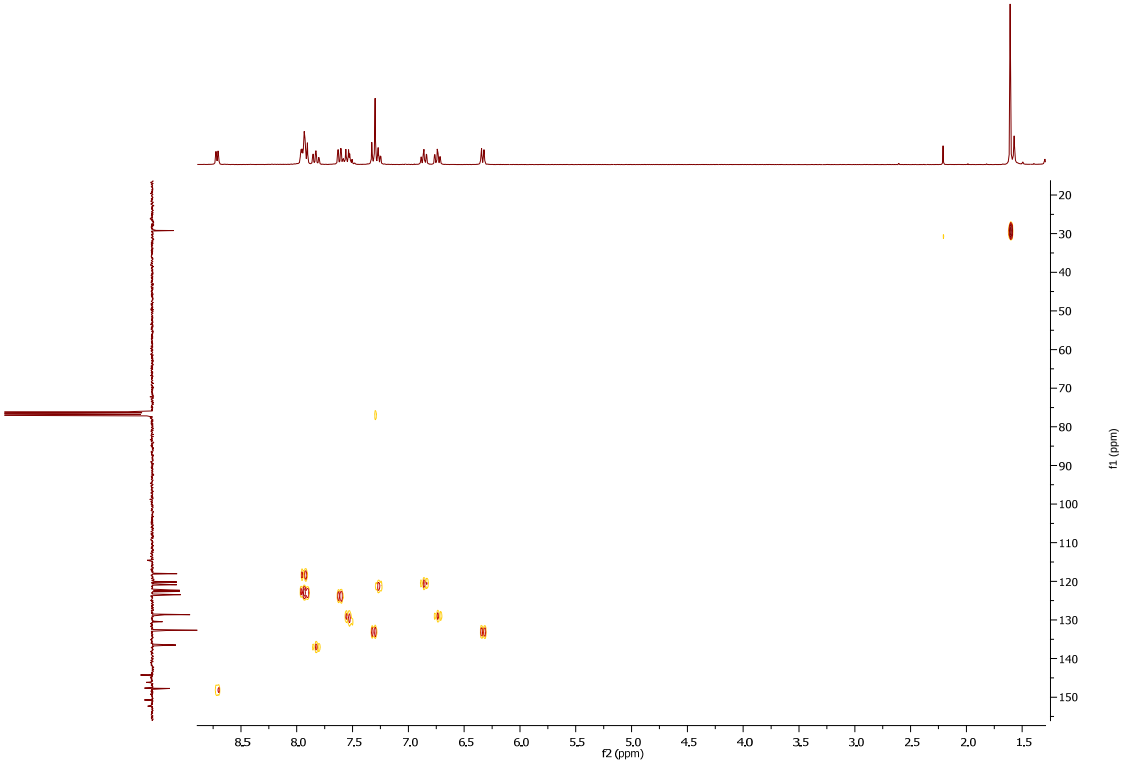

Fig. S62. HSQC NMR spectrum of [Ir(ppy)$_2$(**3**)] in $CDCl_3$.

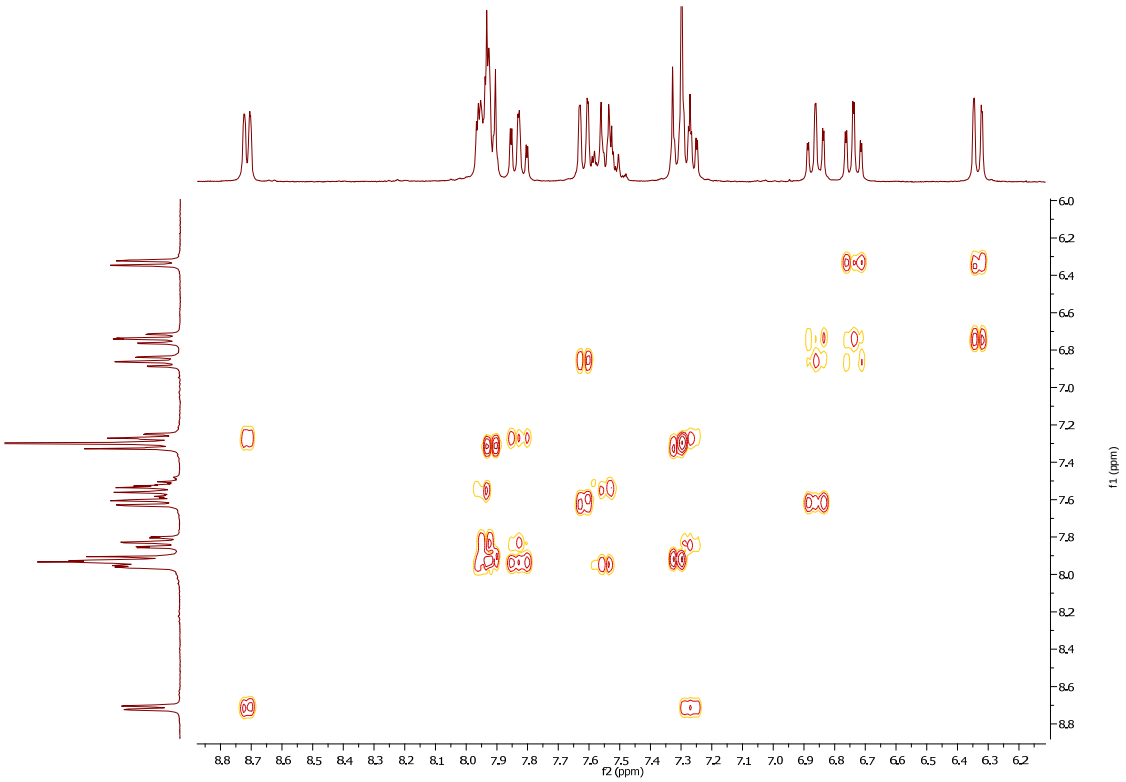

Fig. S63. COSY NMR spectrum of [Ir(ppy)$_2$(**3**)] in $CDCl_3$.

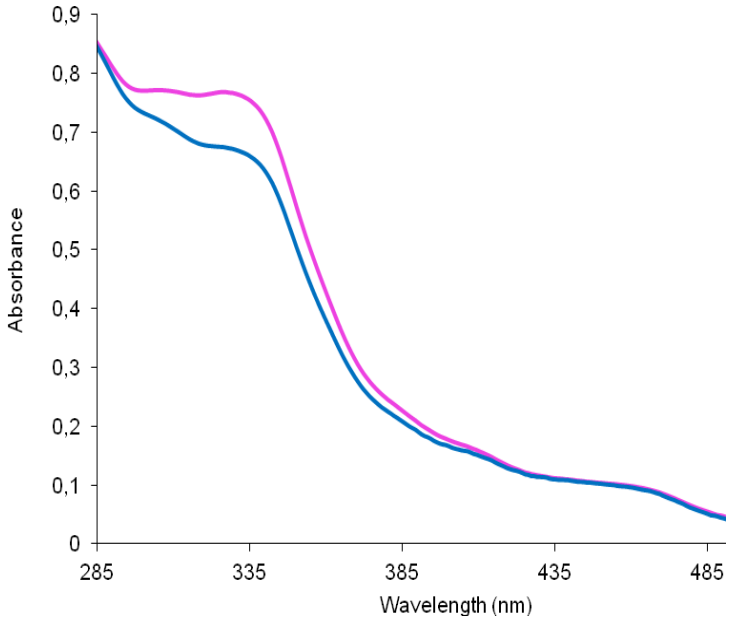

Fig. S64. UV/Vis spectra of [Ir(ppy)$_2$(**3**)] in CH_3CN. Before (pink line) and after (blue line) irradiation at 331 nm, 2.50×10^{-5} M.

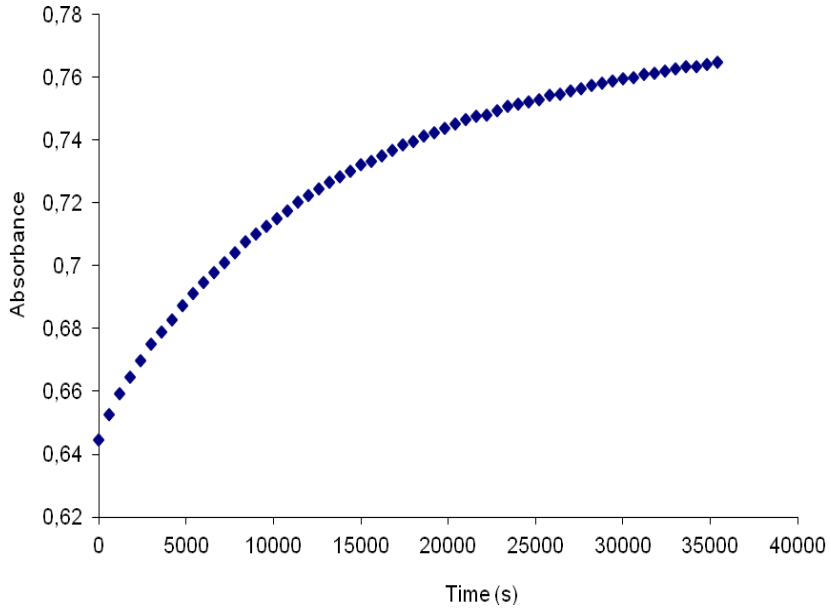

Fig. S65. *Cis* to *trans* thermal isomerization kinetics of [Ir(ppy)$_2$(**3**)]. Absorption change of the band 327 nm at 328 K in CH_3CN after irradiation at 331 nm (2.50×10^{-5} M).

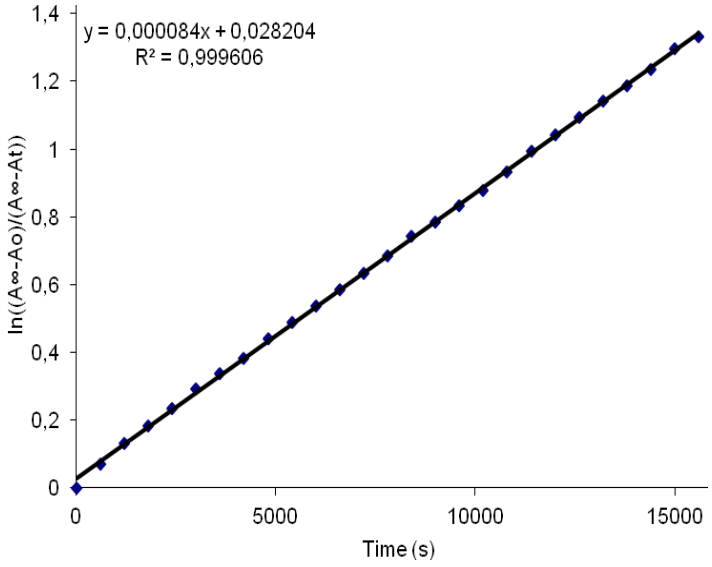

Fig. S66. *Cis* to *trans* thermal isomerization kinetics of [Ir(ppy)$_2$(**3**)]. First-order plot. k (s^{-1}) = 0.8×10^{-4}. Half-life (s) = 8300.

[Ir(Fppy)$_2$(1)]. Synthesis, characterization and photoisomerization studies.

SYNTHESIS

$[Ir(Fppy)_2Cl]_2$ (150 mg, 0.12 mmol) and AgOTf (95 mg, 0.37 mmol) were dissolved in degassed acetone (8 mL) and refluxed under nitrogen for 2 h. The solution was cooled to room temperature and gravity-filtered to remove AgCl. The filtrate was refluxed under nitrogen for 1 h and added to a 1 h refluxed solution of **1** (180 mg, 0.49 mmol) and NEt_3 (130 µL, 0.93 mmol) in degassed acetone (4 mL). The resulting solution was refluxed overnight under nitrogen. After removing the solvent, the residue was purified by column chromatography: silica/CH_2Cl_2 (Rf = 0.8). [Ir(Fppy)$_2$(**1**)] was obtained as a light orange powder (92 mg, 40%).

Elemental Analysis: calculated for $C_{46}H_{30}F_4IrN_5O \cdot C_3H_6O$: C, 59.15; H, 3.65; N, 7.04. Found: C, 59.17; H, 3.69; N, 6.80.

Exact mass (EI) - m/z: 938.2110 for $[M+H]^+$ with (^{193}Ir).

^{1}H NMR (300 MHz, $CDCl_3$): δ 8.22 (t, *J* = 9.1, 2H, $C_5H_4N(C_{11}H_6NF_2)$), 8.04 (dd, *J* = 5.8, 1.0, 1H, $C_5H_4N(C_{11}H_6NF_2)$), 7.98 (d, J=8.16, 1H, $C_5H_4N(C_{24}H_{18}N_3O)$), 7.95 – 7.88 (m, 5H), 7.81 (d, *J* = 8.1, 1H, C_6H_3), 7.70 (td, *J* = 8.0, 1.5, 1H, $C_5H_4N(C_{24}H_{18}N_3O)$), 7.62 – 7.48 (m, 6H), 7.18 (dd, *J* = 8.0, 1.8, 1H, C_6H_3), 7.06 – 6.97 (m, 3H), 6.93 (d, *J* = 1.5, 1H, C_6H_3), 6.77 (ddd, *J* = 6.9, 6.0, 1.3, 1H, $C_5H_4N(C_{11}H_6NF_2)$), 6.76 (ddd, *J* = 7.1, 5.9, 1.3, 1H, $C_5H_4N(C_{11}H_6NF_2)$) 6.52 – 6.42 (m, 2H, $C_6H_4F_2$), 6.05 (dd, *J* = 7.5, 2.3, 1H, $C_6H_4F_2$), 5.84 (dd, *J* = 9.2, 2.3, 1H, $C_6H_4F_2$), 5.06 (s, 2H, CH_2).

^{13}C NMR (75 MHz, $CDCl_3$): δ 180.51 (1C, $C_{quat.\ C11H6NF2}$), 175.19 (1C, $C_{quat.\ C24H18N3O}$), 167.75 (1C, $C_{quat.\ C24H18N3O}$), 166.89 (d, J=8.1, 1C, $C_{quat.\ C11H6NF2}$), 164.87 (dd, J=10.1, J=257, 1C, $C_{quat.C-F}$), 164.59 (d, J=6.8, 1C, $C_{quat.\ C11H6NF2}$), 163.84 (dd, J=12.4, J= 253, 1C, $C_{quat.C-F}$), 162.78 (d, J= 6.0, 1C, $C_{quat.\ C11H6NF2}$), 162.27 (dd, J=10.9, J=262, 1C, $C_{quat.C-F}$), 161.66 (dd, J=13.1, J=258, 1C, $C_{quat.C-F}$), 161.26 (1C, $C_{quat.\ C24H18N3O}$), 153.10 (1C, CH, $C_5H_4N(C_{11}H_6NF_2)$), 152.82 (1C, $C_{quat.\ C24H18N3O}$), 150.90 (1C, CH, $C_5H_4N(C_{24}H_{18}N_3O)$), 147.68 (1C, CH), 146.88 (1C, $C_{quat.\ C24H18N3O}$), 144.89 (1C, $C_{quat.\ C24H18N3O}$), 137.76 (1C, $C_{quat.\ C24H18N3O}$), 137.13 (1C, CH, C_5H_4N ($C_{24}H_{18}N_3O$)), 136.55 (1C, CH, C_6H_3), 136.45 (1C, CH), 135.22 (1C, CH), 130.27 (1C, CH, C_6H_5), 129.01 (2C, CH, $C_{12}H_9N_2$), 127.88 (1C, $C_{quat.\ C11H6NF2}$), 126.41 (1C, $C_{quat.\ C11H6NF2}$), 124.63 (1C, CH, C_6H_3), 124.57 (2C, CH, $C_{12}H_9N_2$), 122.80 (d, J= 21.3, 1C, CH, $C_5H_4N(C_{11}H_6NF_2)$), 122.66 (1C, CH, $C_5H_4N(C_{24}H_{18}N_3O)$), 122.58 (d, J=19.0, 1C, CH, $C_5H_4N(C_{11}H_6NF_2)$), 122.51 (2C, CH, $C_{12}H_9N_2$), 122.29 (1C, CH, $C_5H_4N(C_{11}H_6NF_2)$), 121.48 (1C, CH, $C_5H_4N(C_{11}H_6NF_2)$), 121.17 (1C, CH, C_6H_3), 119.43 (1C, CH, $C_5H_4N(C_{24}H_{18}N_3O)$), 115.32 (2C, CH, $C_{12}H_9N_2$),113.71 (d, J=14.1, 1C, CH, $C_6H_4F_2$), 111.93 (d, J=16.3, 1C, CH, $C_6H_4F_2$), 97.42 (pst, J=27.2, 1C, CH, $C_6H_4F_2$), 95.47 (pst, J=27.1, 1C, CH, $C_6H_4F_2$), 70.67 (1C, CH_2).

UV/Vis (CH_3CN, λ, nm (ε, L mol^{-1} cm^{-1})): 346 (3.1×10^4), 436 (4.0×10^3).

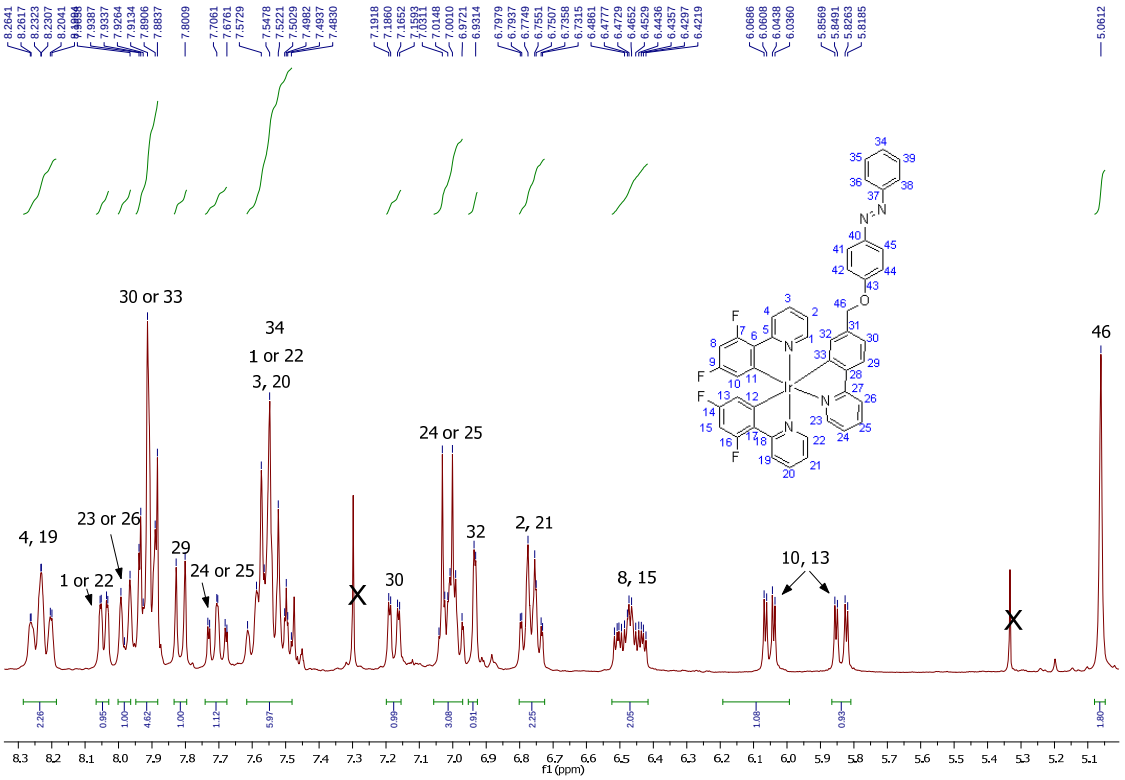

Fig. S67. ^{1}H NMR spectrum of [Ir(Fppy)$_2$(**1**)] in $CDCl_3$, 300 MHz.

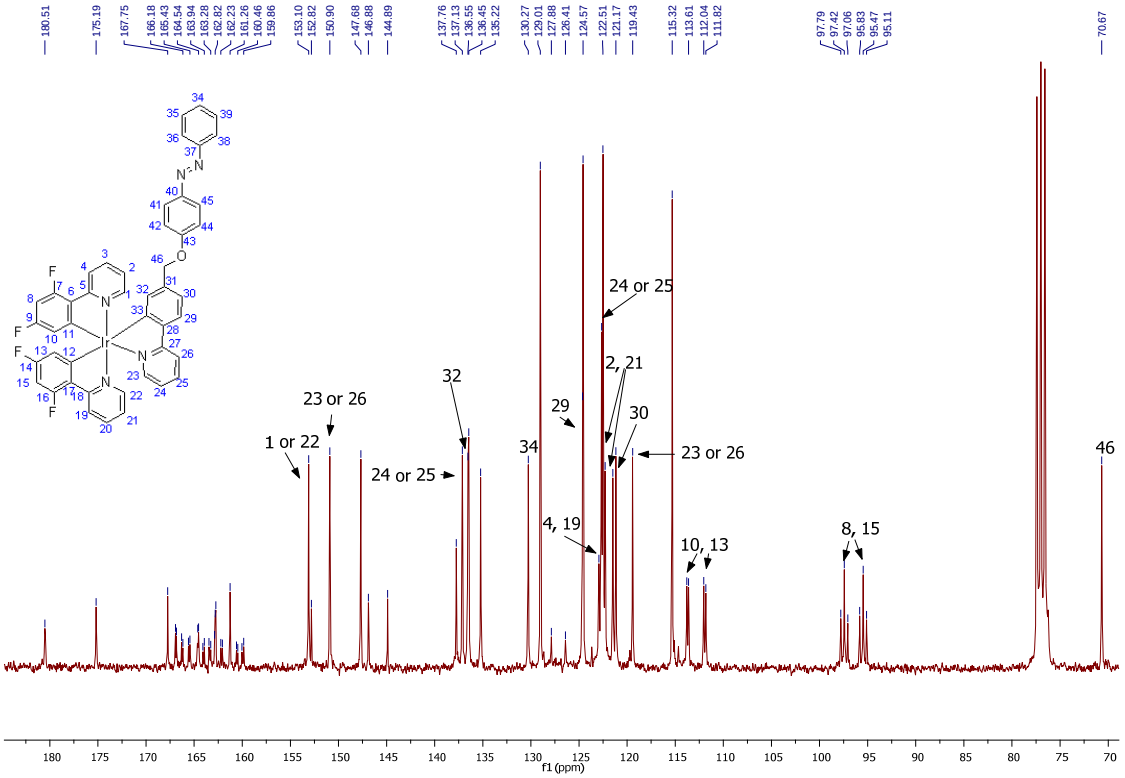

Fig. S68. ^{13}C NMR spectrum of [Ir(Fppy)$_2$(**1**)] in $CDCl_3$, 75 MHz.

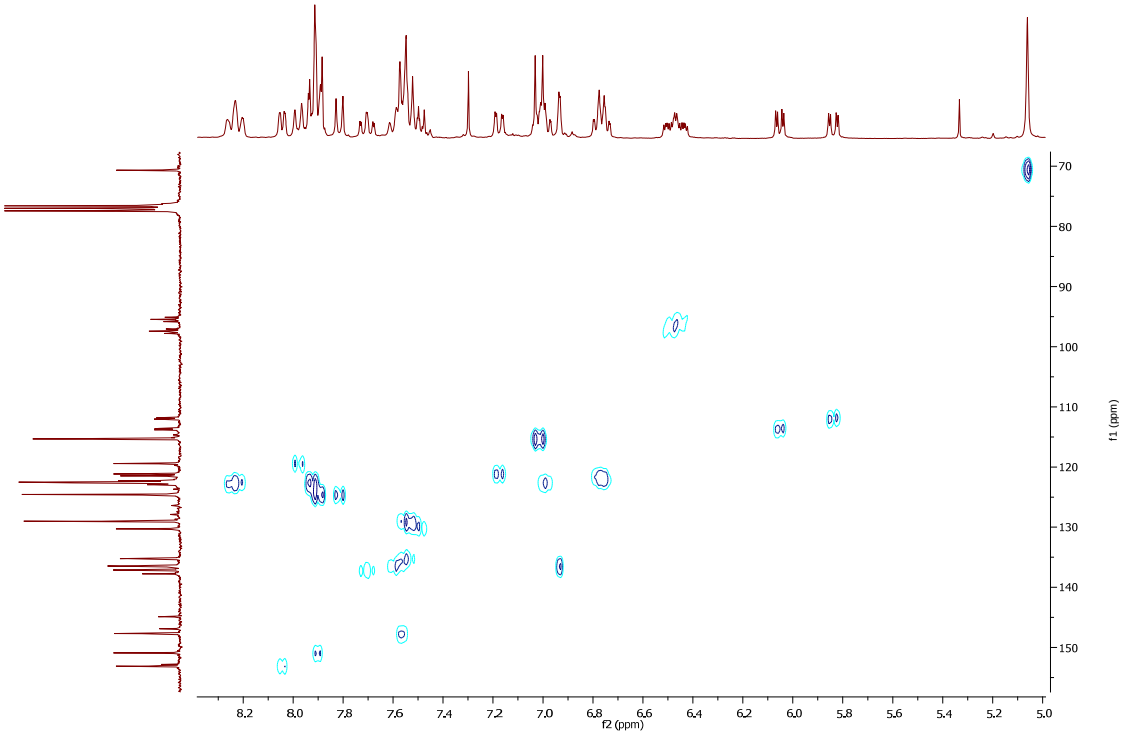

Fig. S69. HSQC NMR spectrum of [Ir(Fppy)$_2$(**1**)] in $CDCl_3$.

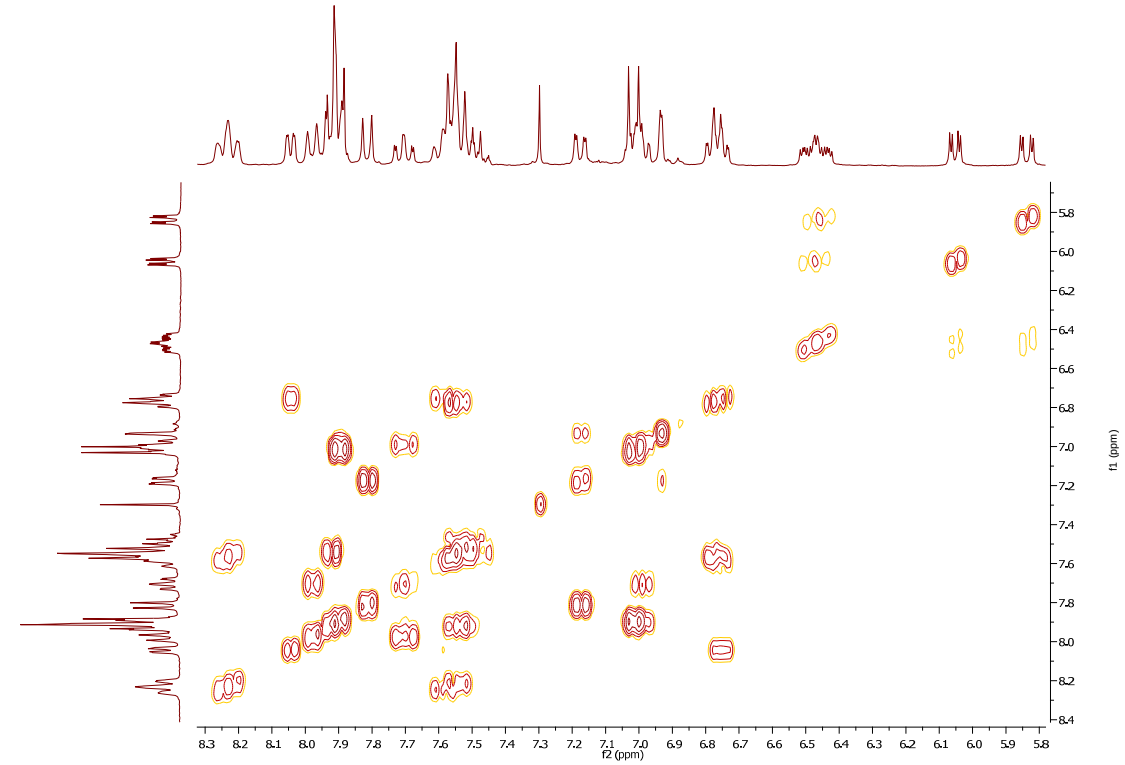

Fig. S70. COSY NMR spectrum of [Ir(Fppy)$_2$(**1**)] in $CDCl_3$.

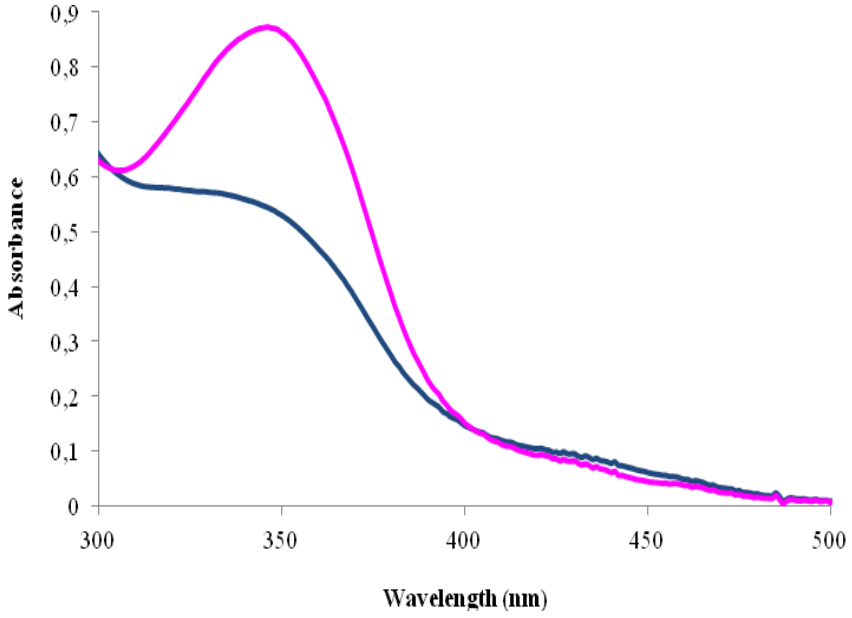

Fig. S71. UV/Vis spectra of [Ir(Fppy)$_2$(**1**)] in CH_3CN. Before (pink line) and after (blue line) irradiation at 349 nm, 2.50×10^{-5} M.

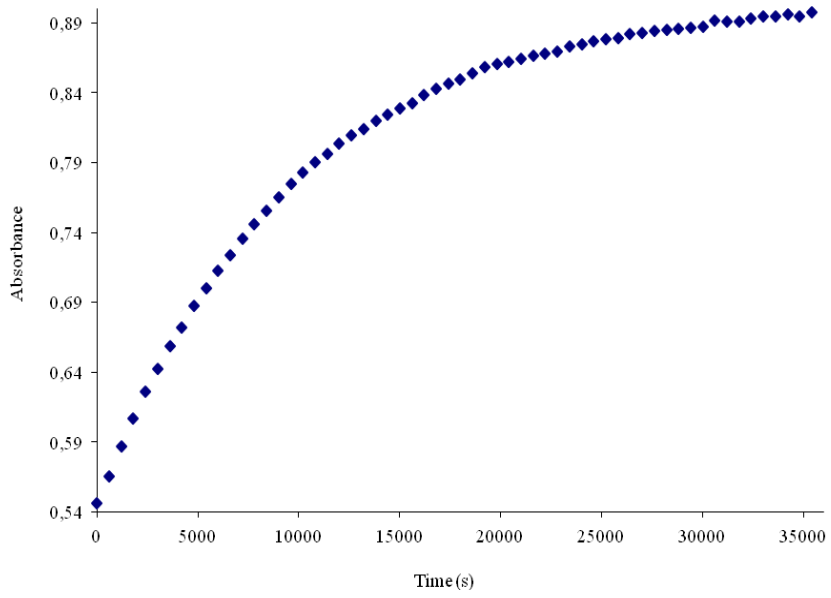

Fig. S72. *Cis* to *trans* thermal isomerization kinetics of [Ir(Fppy)$_2$(**1**)]. Absorption change of the band 346 nm at 328 K in CH_3CN after irradiation at 349 nm (2.50×10^{-5} M).

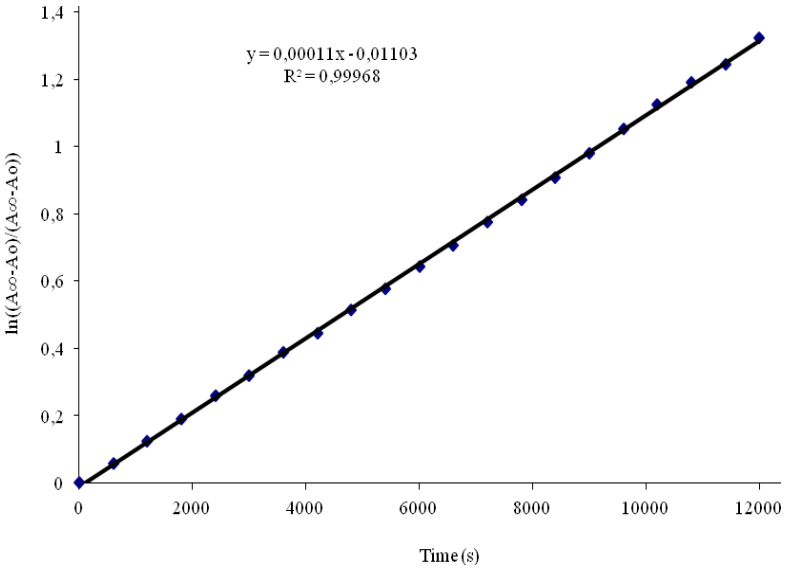

Fig. S73. *Cis* to *trans* thermal isomerization kinetics of [Ir(Fppy)$_2$(**1**)]. First-order plot. k (s^{-1}) = 1.1×10^{-4}. Half-life (s) = 6300.

[Ir(Brppy)$_2$(1)]. Synthesis, characterization and photoisomerization studies.

SYNTHESIS

[Ir(Brppy)$_2$Cl]$_2$, (150 mg, 0.11 mmol) and AgOTf (84 mg, 0.32 mmol) were dissolved in degassed acetone (8 mL) and refluxed under nitrogen for 2 h. The solution was cooled to room temperature and gravity-filtered to remove AgCl. The filtrate was refluxed under nitrogen for 1 h and added to a 1 h refluxed solution of **1** (158 mg, 0.43 mmol) and triethylamine (113 µL, 0.81 mmol) dissolved in degassed acetone (4 mL). The resulting solution was refluxed overnight under nitrogen. After removing the solvent, the residue was purified by column chromatography: silica/CH_2Cl_2 (Rf = 0.9). It was obtained as an orange powder (74 mg, 35%).

Elemental Analysis: calculated for $C_{46}H_{32}Br_2IrN_5O \cdot C_3H_6O$: C, 54.45; H, 3.54; N, 6.48. Found: C, 54.24; H, 3.65; N, 6.17.

Exact mass (MALDI) - m/z: 1021.0578 for $[M]^+$ with (^{193}Ir)(^{79}Br).

^{1}H NMR (300 MHz, $CDCl_3$): δ 7.99-7.88 (m, 7H), 7.81-7.74 (m, 3H), 7.67 (td, *J* = 7.7, 1.5, 1H), 7.60 – 7.47 (m, 8H), 7.18-7.09 (m, 3H), 7.03 – 6.95 (m, 3H), 6.93 (d, J=1.1, 1H, C_6H_3) 6.80 – 6.71 (m, 2H), 6.69 (d, *J* = 2.0, 1H, C_6H_4Br), 6.50 (d, *J* = 1.9, 1H, C_6H_4Br), 5.05 (d, *J* = 2.2, 2H, CH_2).

^{13}C NMR (75 MHz, $CDCl_3$): δ 177.52 (1C, $C_{quat.}$), 175.78 (1C, $C_{quat.}$), 169.23 (1C, $C_{quat.}$), 167.86 (1C, $C_{quat.}$), 166.77 (1C, $C_{quat.}$), 161.30 (1C, $C_{quat.}$), 160.77 (1C, $C_{quat.}$), 153.10 (1C, CH), 152.84 (1C, $C_{quat.}$), 151.16 (1C, CH), 147.76 (1C, CH), 146.87 (1C, $C_{quat.}$), 145.05 (1C, $C_{quat.}$), 143.56 (1C, $C_{quat.}$), 141.41 (1C, $C_{quat.}$), 137.55 (1C, $C_{quat.}$), 136.90, (1C, CH) 136.69 (1C, CH, C_6H_3), 136.02 (1C, CH), 135.12 (1C, CH, C_6H_4Br), 134.67 (1C, CH), 132.79 (1C, CH, C_6H_4Br), 130.26 (1C, CH), 129.02 (2C, CH, $C_{12}H_9N_2$), 126.75 (1C, $C_{quat.}$), 125.84 (1C, CH), 125.53 (1C, CH), 125.19 (1C, $C_{quat.}$), 124.57 (2C, CH, $C_{12}H_9N_2$), 124.51 (1C, CH), 124.31 (1C, CH), 122.63 (1C, CH), 122.51 (3C, 2CH $C_{12}H_9N_2$ + CH), 122.39 (1C, CH), 121.80 (1C, CH), 120.95 (1C, CH), 119.24 (1C, CH), 118.99 (1C, CH), 118.79 (1C, CH), 115.46 (2C, CH, $C_{12}H_9N_2$), 70.70 (1C, CH_2).

UV/Vis (CH_3CN, λ, nm (ε, L mol^{-1} cm^{-1})): 343($2.8 \cdot 10^4$), 448 ($4.0 \cdot 10^3$).

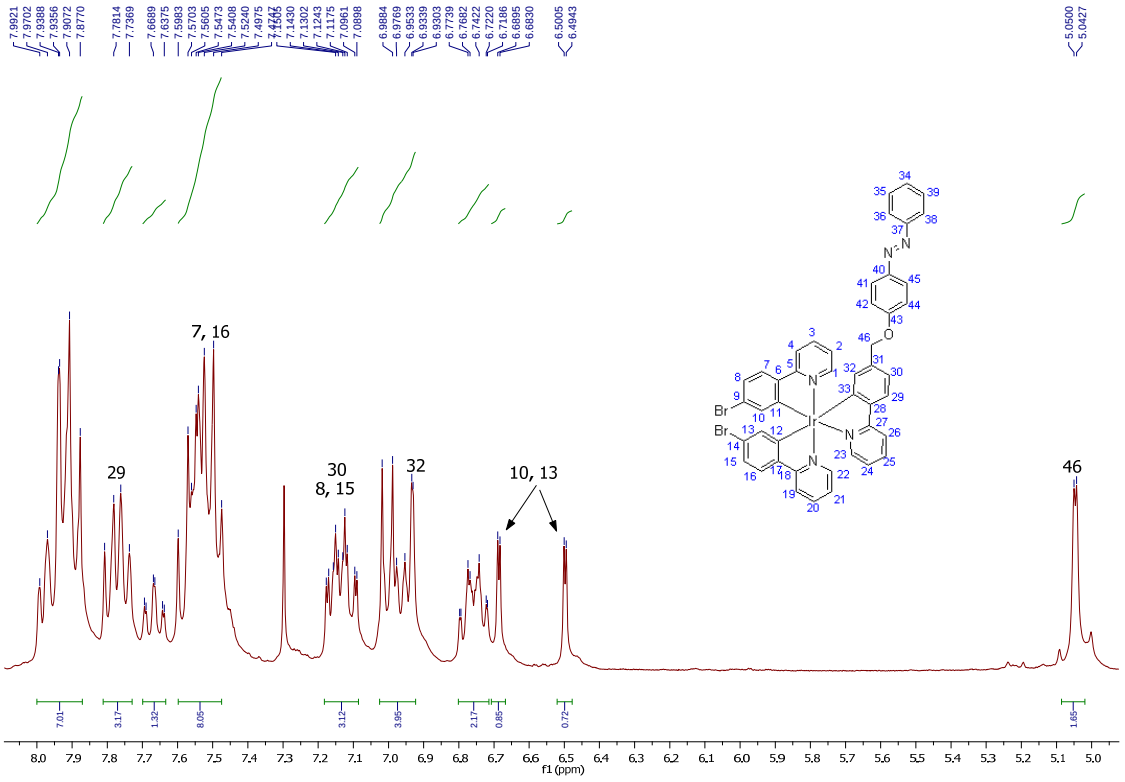

Fig. S74. ^{1}H NMR spectrum of [Ir(Brppy)$_2$(**1**)] in $CDCl_3$, 300 MHz.

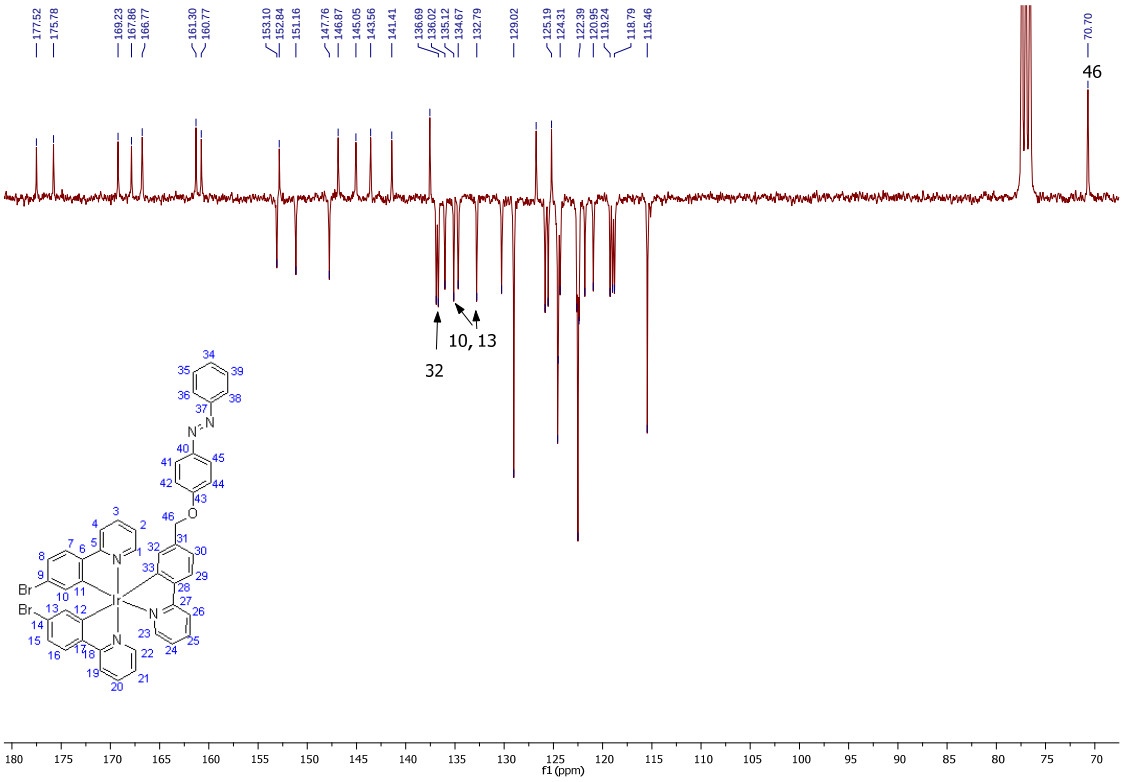

Fig. S75. ^{13}C NMR spectrum of [Ir(Brppy)$_2$(**1**)] in $CDCl_3$, 75 MHz.

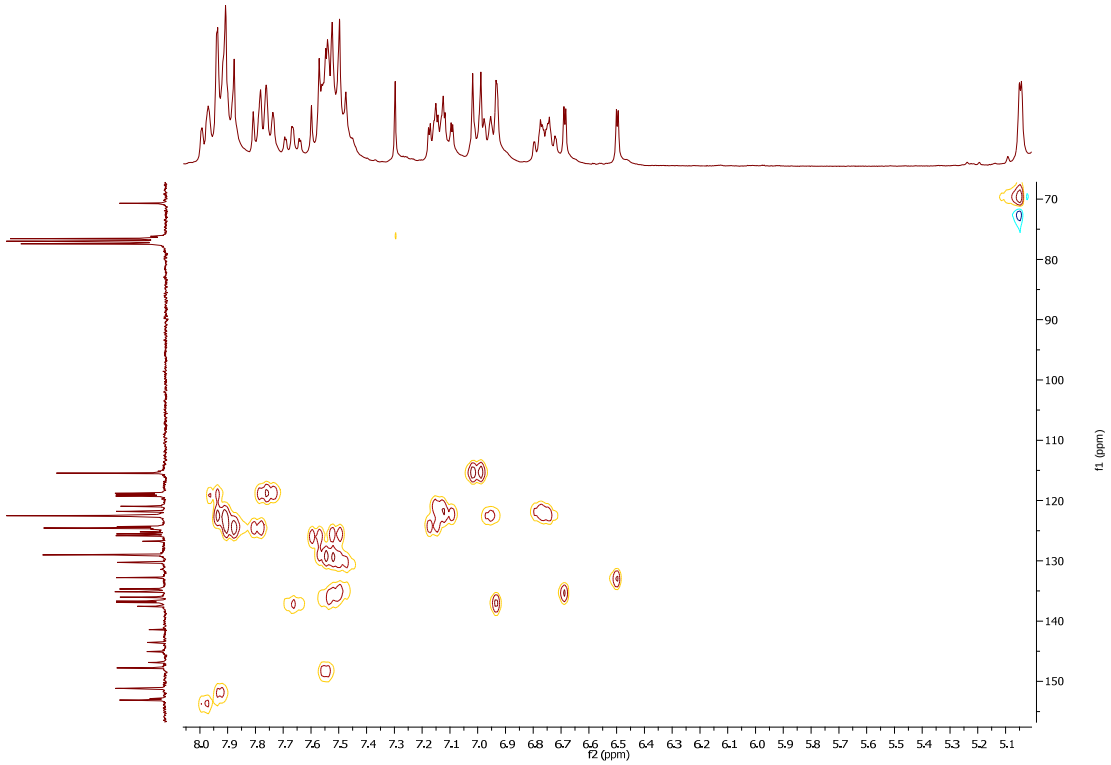

Fig. S76. HSQC NMR spectrum of [Ir(Brppy)$_2$(**1**)] in $CDCl_3$.

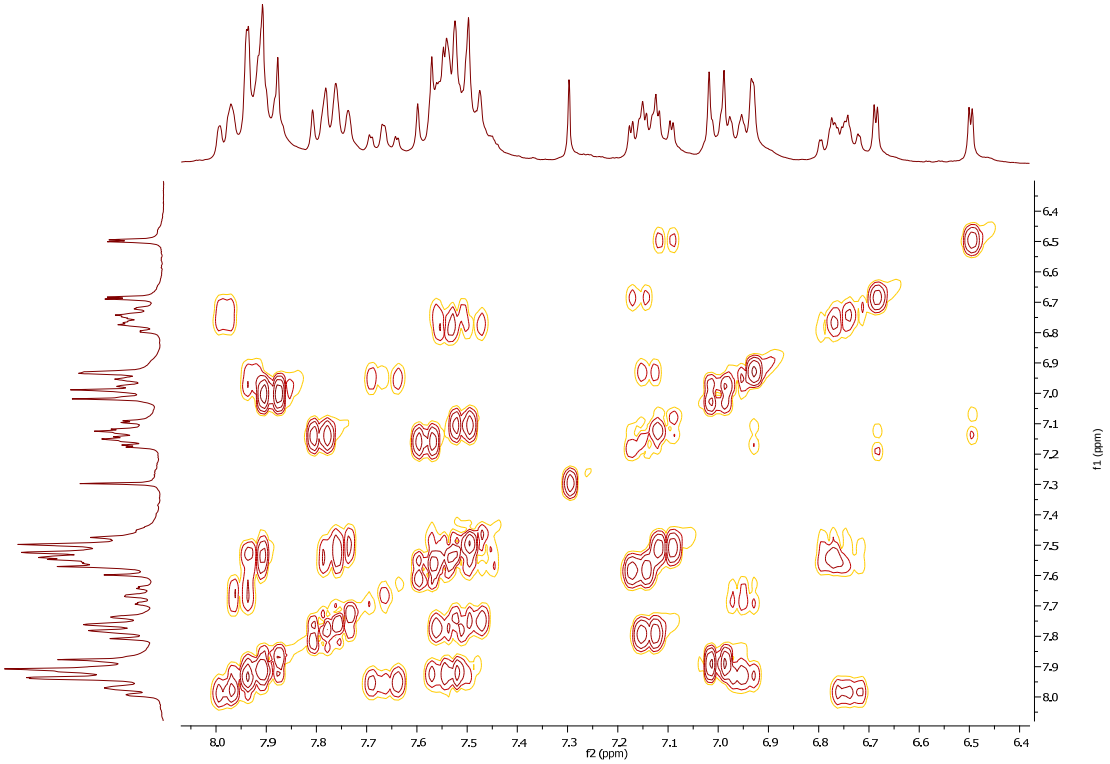

Fig. S77. COSY NMR spectrum of [Ir(Brppy)$_2$(**1**)] in $CDCl_3$.

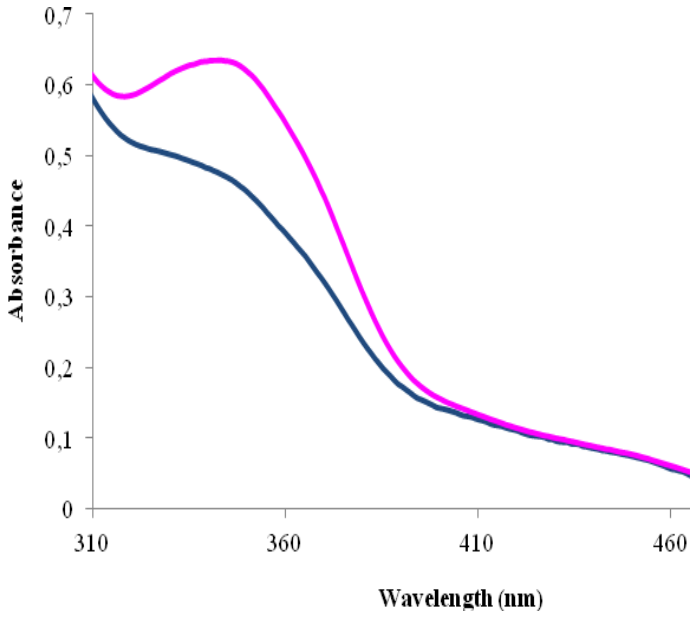

Fig. S78. UV/Vis spectra of [Ir(Brppy)$_2$(**1**)] in CH_3CN. Before (pink line) and after (blue line) irradiation at 349 nm, 2.50×10^{-5} M.

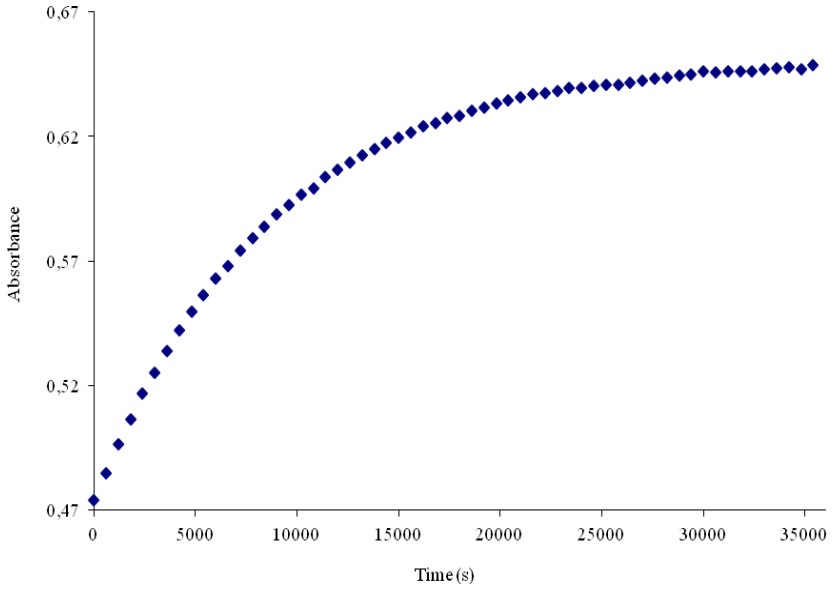

Fig. S79. *Cis* to *trans* thermal isomerization kinetics of [Ir(Brppy)$_2$(**1**)]. Absorption change of the band 343 nm at 328 K in CH_3CN after irradiation at 349 nm (2.50×10^{-5} M).

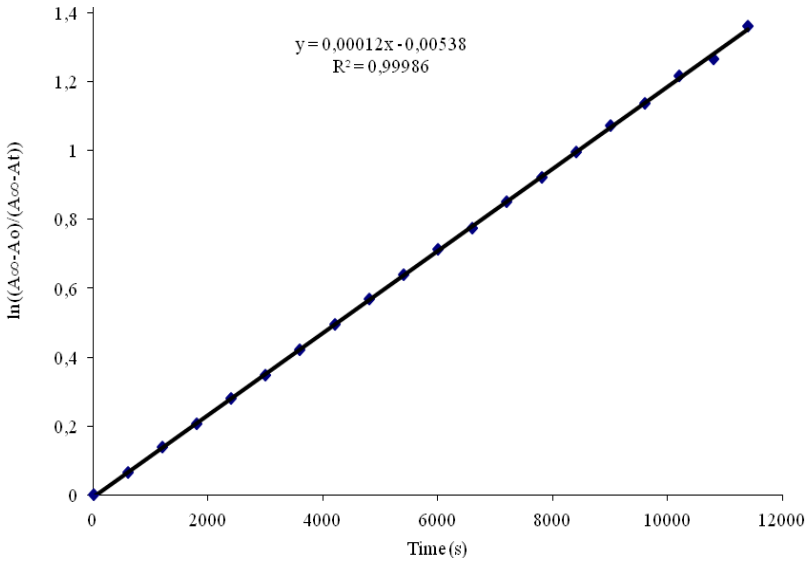

Fig. S80. *Cis* to *trans* thermal isomerization kinetics of [Ir(Brppy)$_2$(**1**)]. First-order plot. k (s^{-1}) = 1.2×10^{-4}. Half-life (s) = 5800.

[Ir(4)$_2$(1)]. Synthesis and characterization.

SYNTHESIS

[Ir(Brppy)$_2$(**1**)] (60 mg, 0.058 mmol) was dissolved in 4 mL of degassed THF. To this mixture, 4-(phenylazo)phenyl boronic acid pinacol ester (40 mg, 0.129 mmol), Pd(PPh$_3$)$_4$ (2 mol%, 3 mg, 0.002 mmol), and Na_2CO_3 (1 M aq., 2 mL) were added successively under nitrogen. The reaction mixture was heated overnight at 80 °C with continuous stirring. The reaction was cooled to room temperature and 50 mL of water were added to precipitate the formed compound. The solution was gravity filtered and the solid was washed with hexane (20 mL) and dichloromethane (10 mL). The compound was obtained as a dark-orange powder (70 mg, 92%), rather insoluble in all the solvents assayed (i.e. solubility is less than 0.8 mg in 10 mL of $CDCl_3$). Low solubility hampered a complete NMR characterization.

Elemental Analysis: calculated for $C_{70}H_{50}IrN_9O \cdot 2CH_2Cl_2 \cdot 1C_6H_{14}$: C, 63.24; H, 4.63; N, 8.51. Found: C, 63.34; H, 4.09; N, 8.55.

Exact mass (MALDI) - m/z: 1225.3766 for $[M]^+$ with (^{193}Ir).

UV/Vis (CH_3CN, λ, nm (ε, L mol^{-1} cm^{-1})): 351 ($6.5 \cdot 10^4$), 465 ($6.6 \cdot 10^3$).

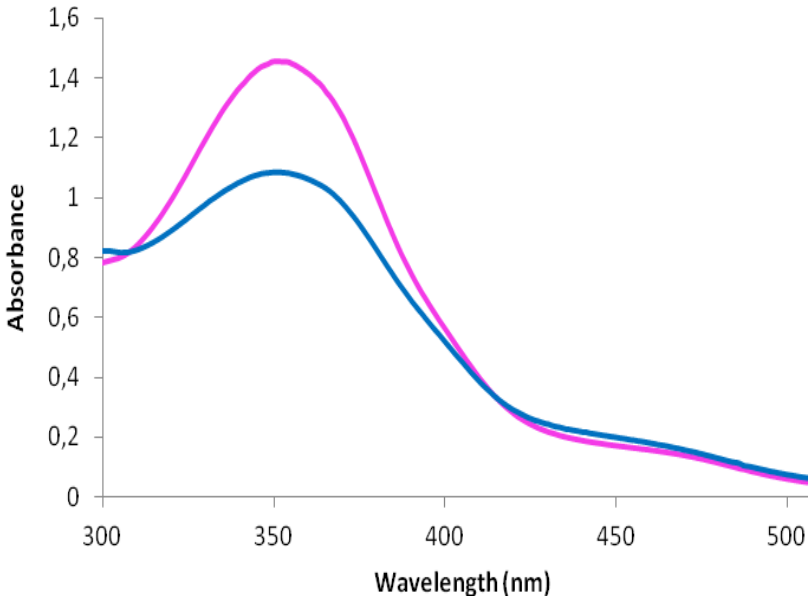

Fig. S81. UV/Vis spectra of [Ir(**4**)$_2$(**1**)] in CH_2Cl_2. Before (pink line) and after (blue line) irradiation at 354 nm, 0.90×10^{-5} M.

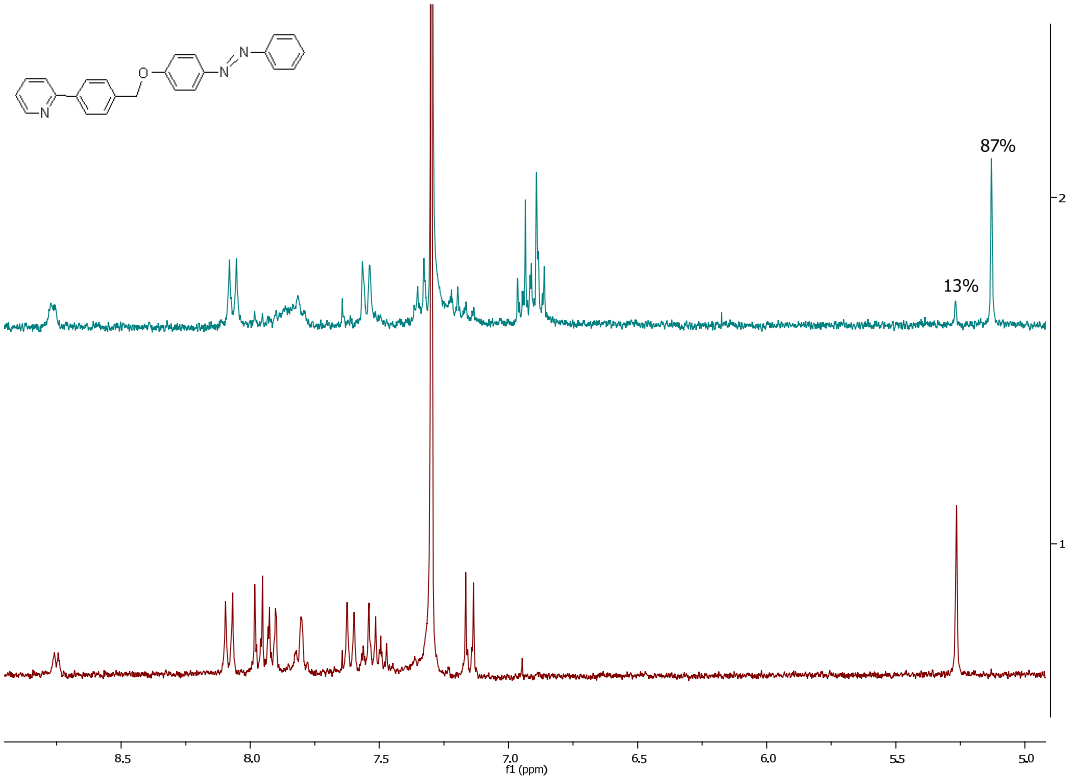

Fig. S82. ^{1}H-NMR spectra of ligand **1** in $CDCl_3$, 300 MHz. Before (red line) and after (blue line) irradiation at 365nm, 2.50×10^{-3} M.

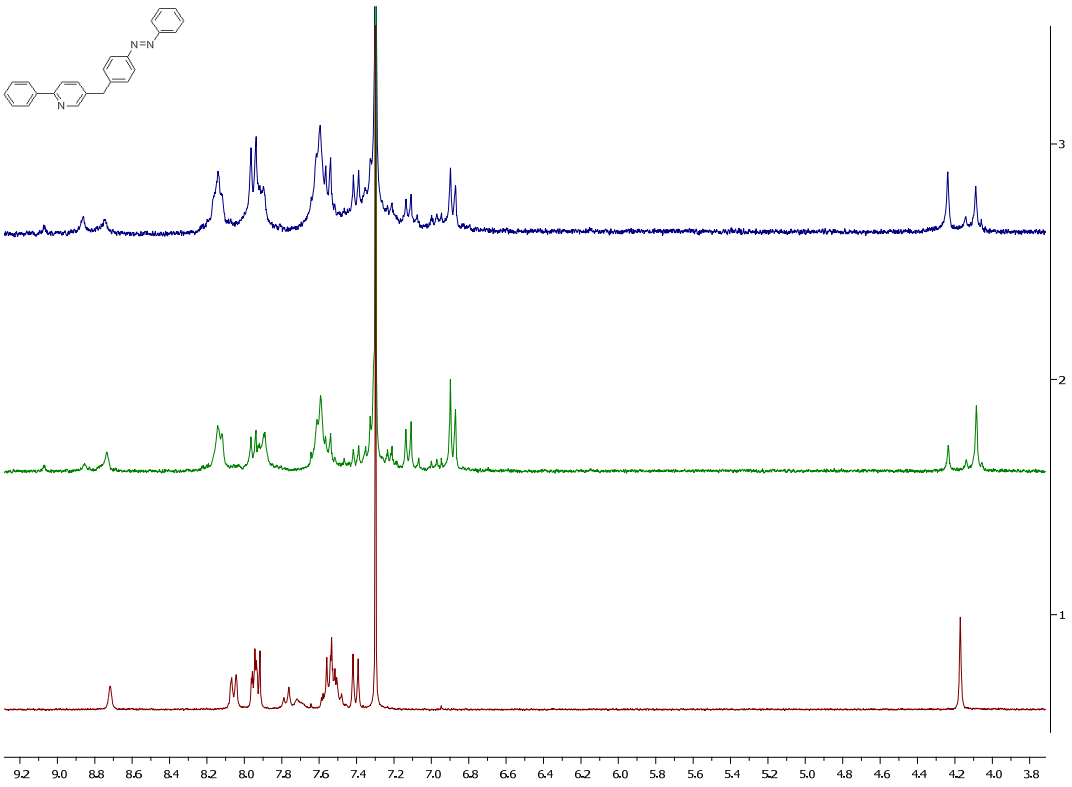

Fig. S83. ^{1}H-NMR spectra of ligand **2** in $CDCl_3$, 300 MHz. Before (red line) and after (green line) irradiation at 365nm, 2.50×10^{-3} M. After heating overnight at 55ºC (blue line).

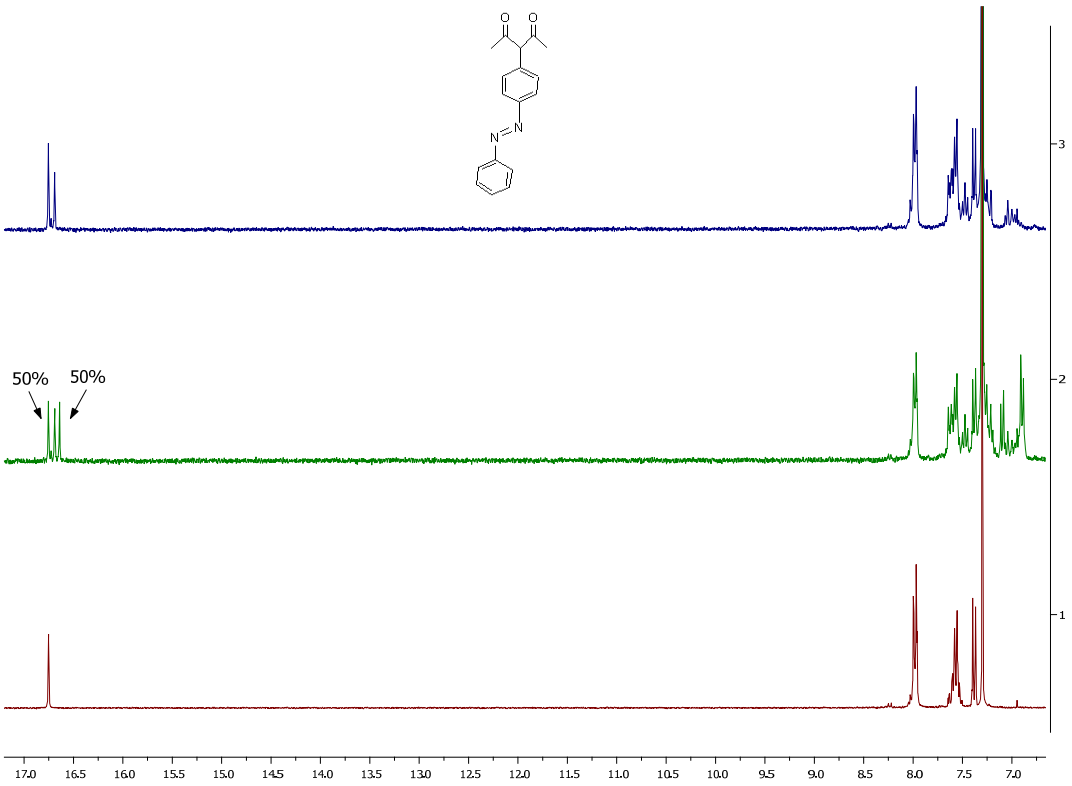

Fig. S84. ^{1}H-NMR spectra of ligand **3** in $CDCl_3$, 300 MHz. Before (red line) and after (green line) irradiation at 365nm, $2.50 \cdot 10^{-3}$ M. After heating overnight at 55 ºC (blue line).

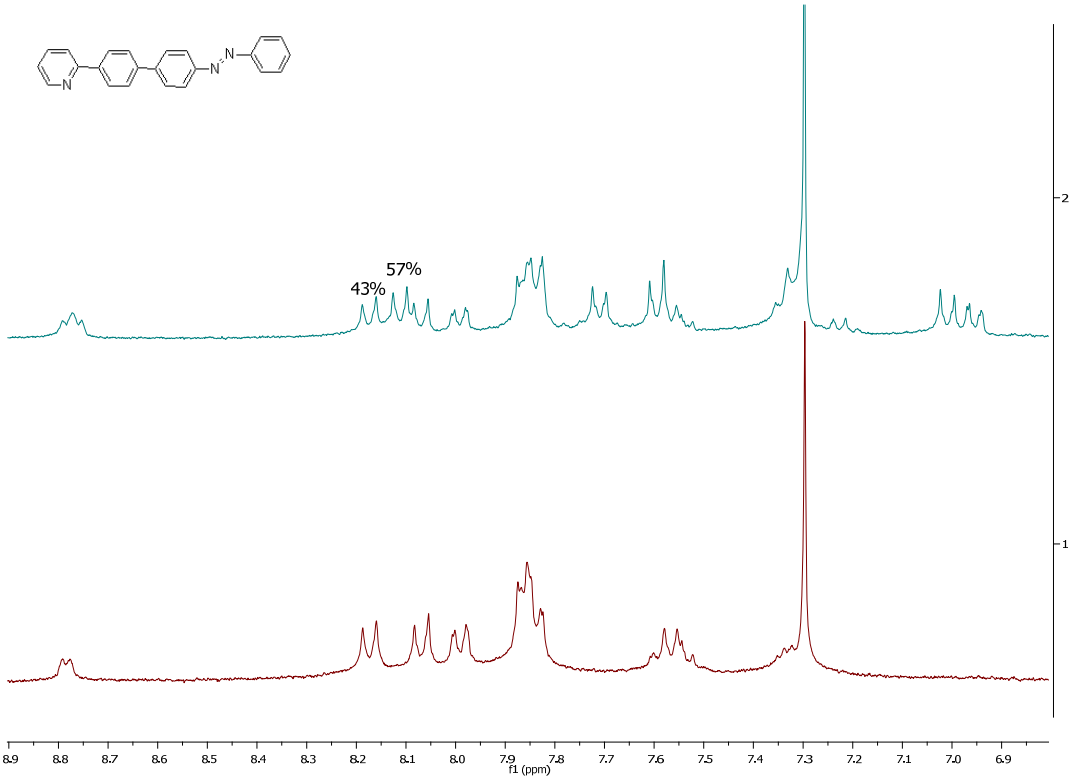

Fig. S85. ^{1}H-NMR spectra of ligand **4** in $CDCl_3$, 300 MHz. Before (red line) and after (blue line) irradiation at 365nm, 2.50×10^{-3} M.

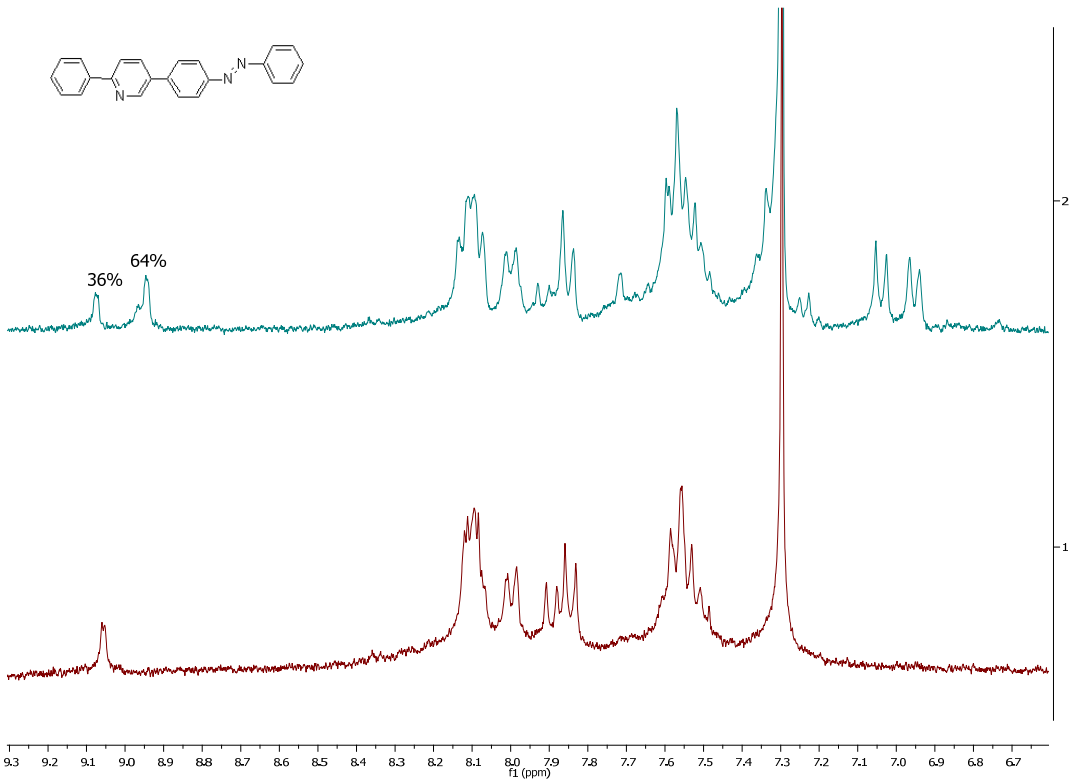

Fig. S86. ^{1}H-NMR spectra of ligand **5** in $CDCl_3$, 300 MHz. Before (red line) and after (blue line) irradiation at 365nm, 2.50×10^{-3} M.

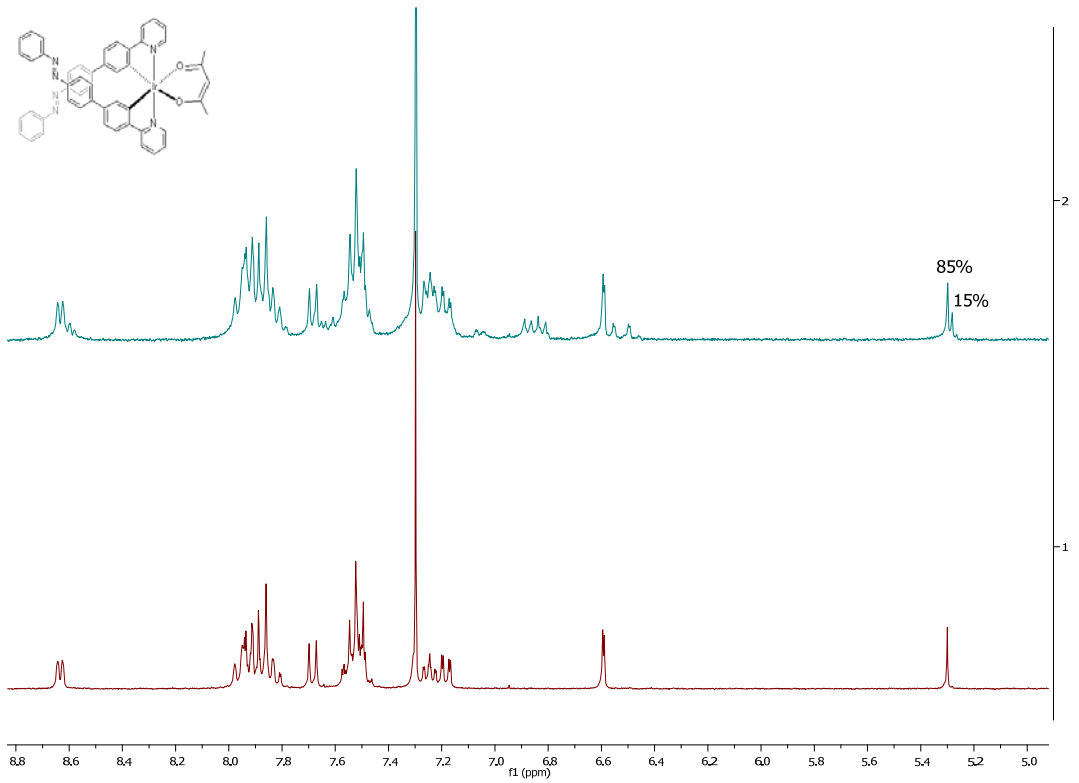

Fig. S87. ^{1}H-NMR spectra of [Ir(**4**)$_2$(acac)] in $CDCl_3$, 300 MHz. Before (red line) and after (blue line) irradiation at 365nm, 2.50×10^{-3} M.

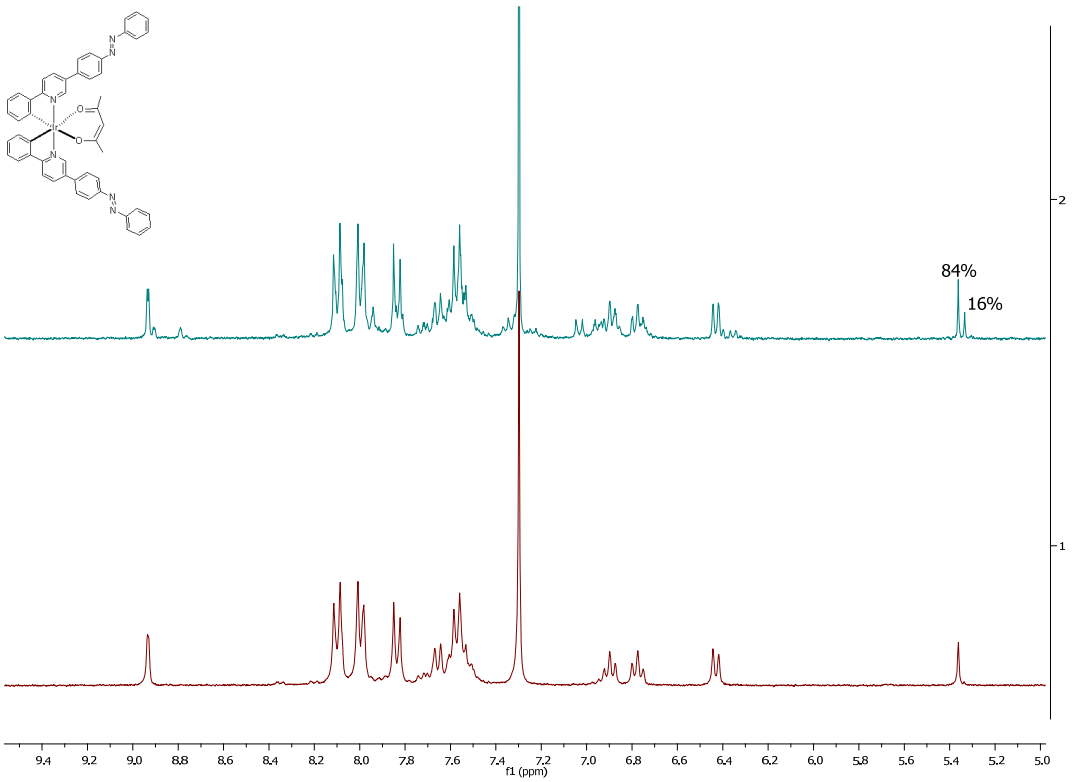

Fig. S88. ^{1}H-NMR spectra of [Ir(**5**)$_2$(acac)] in $CDCl_3$, 300 MHz. Before (red line) and after (blue line) irradiation at 365nm, 2.50×10^{-3} M.

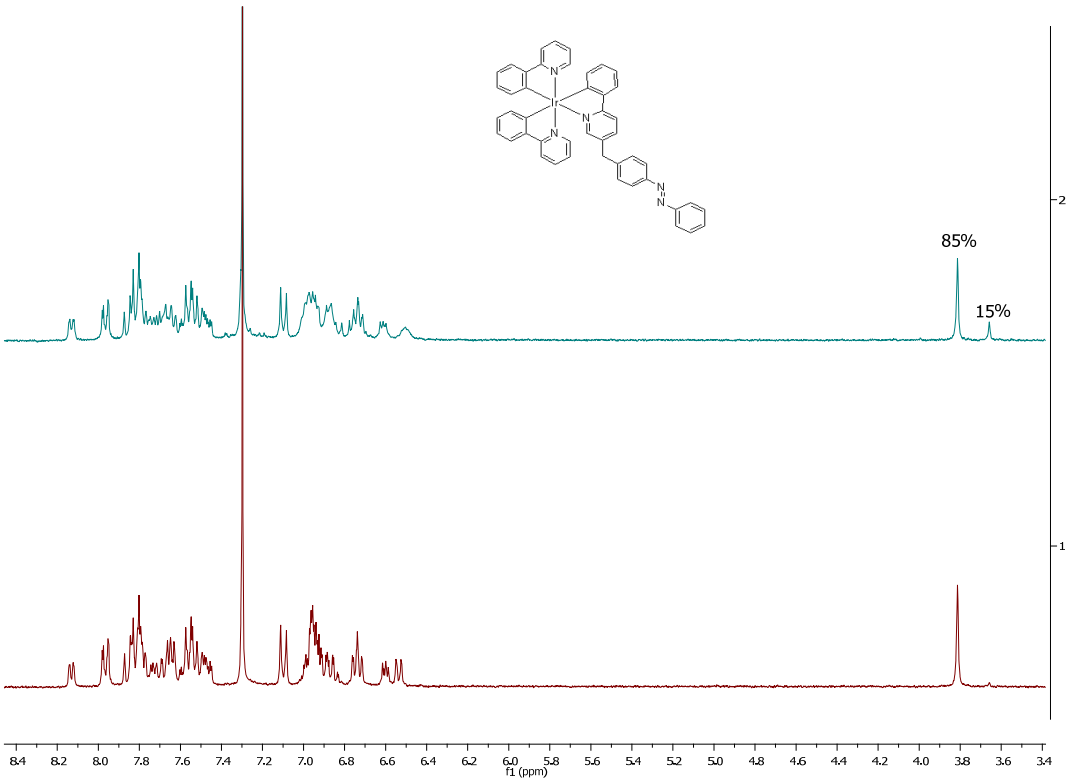

Fig. S89. ^{1}H-NMR spectra of [Ir(ppy)$_2$(**2**)] in $CDCl_3$, 300 MHz. Before (red line) and after (blue line) irradiation at 365nm, 2.50×10^{-3} M.

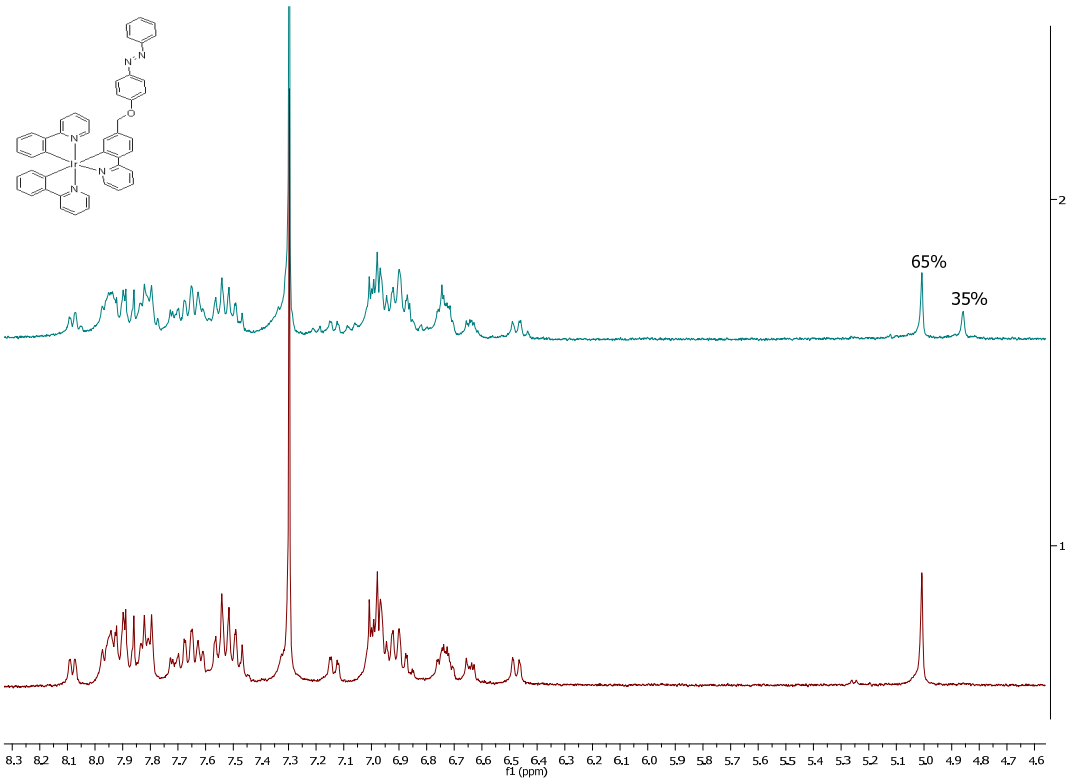

Fig. S90. ^{1}H-NMR spectra of [Ir(ppy)$_2$(**1**)] in $CDCl_3$, 300 MHz. Before (red line) and after (blue line) irradiation at 365nm, 2.50×10^{-3} M.

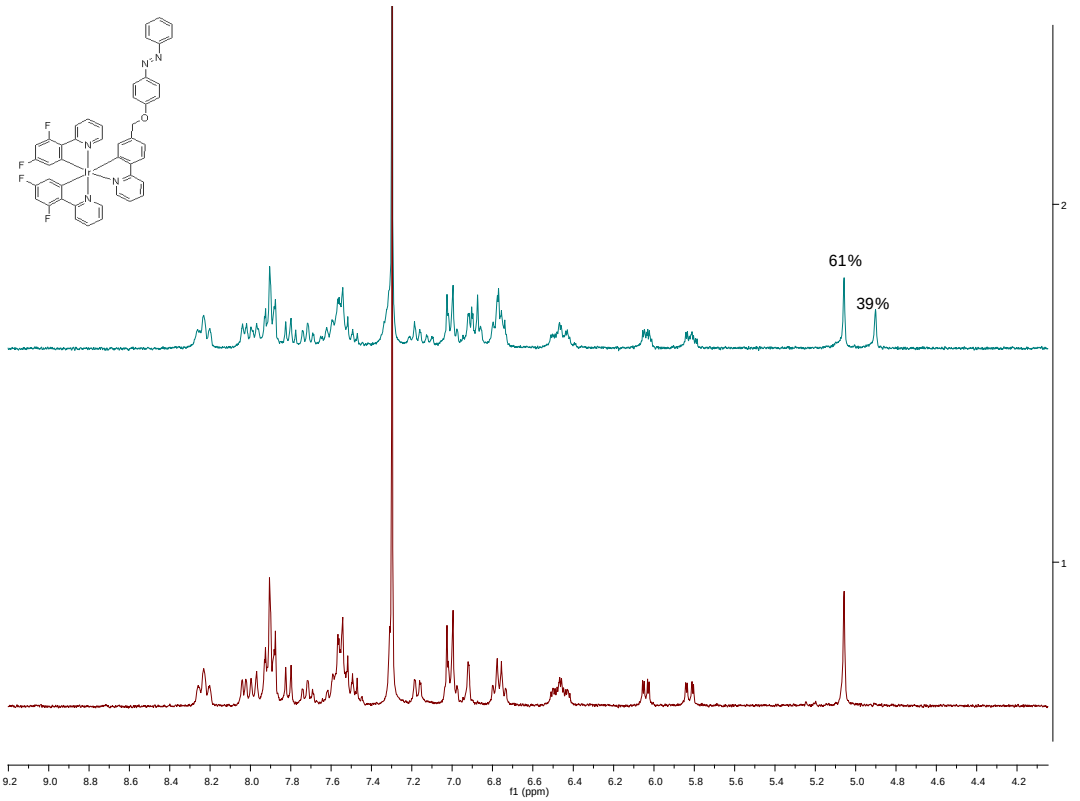

Fig. S91. ^{1}H-NMR spectra of [Ir(Fppy)$_2$(**1**)] in $CDCl_3$, 300 MHz. Before (red line) and after (blue line) irradiation at 365nm, 2.50×10^{-3} M.

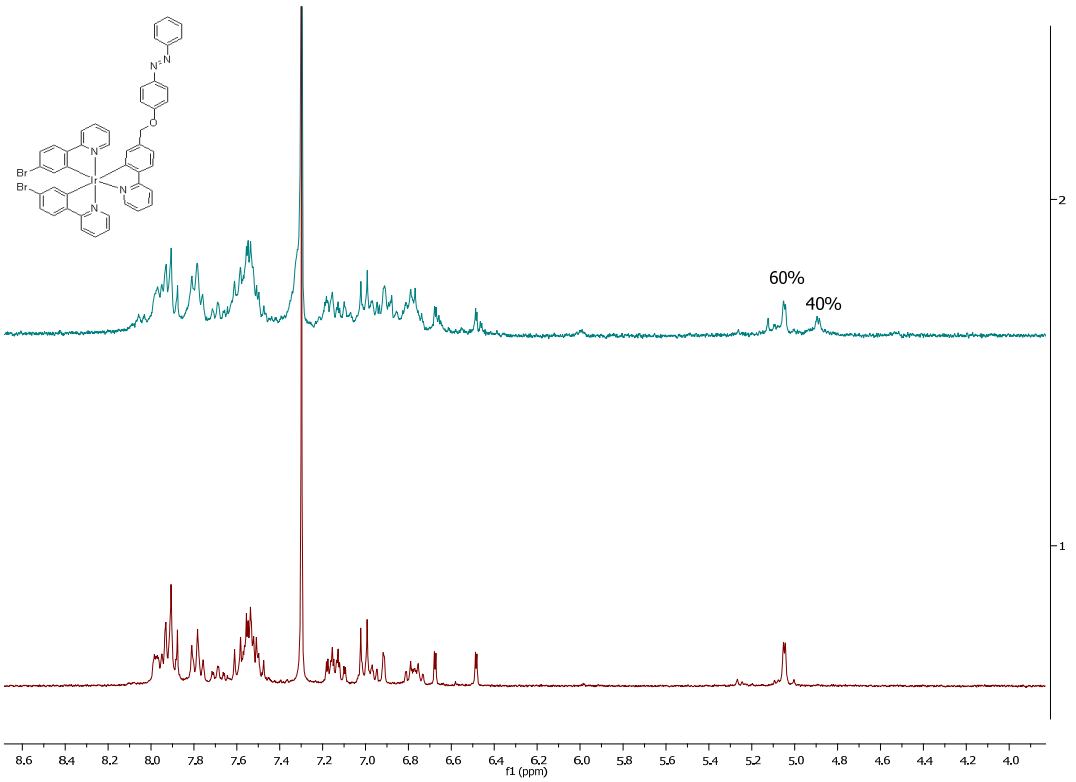

Fig. S92. ^{1}H-NMR spectra of [Ir(Brppy)$_2$(**1**)] in $CDCl_3$, 300 MHz.. Before (red line) and after (blue line) irradiation at 365nm, 2.50×10^{-3} M.

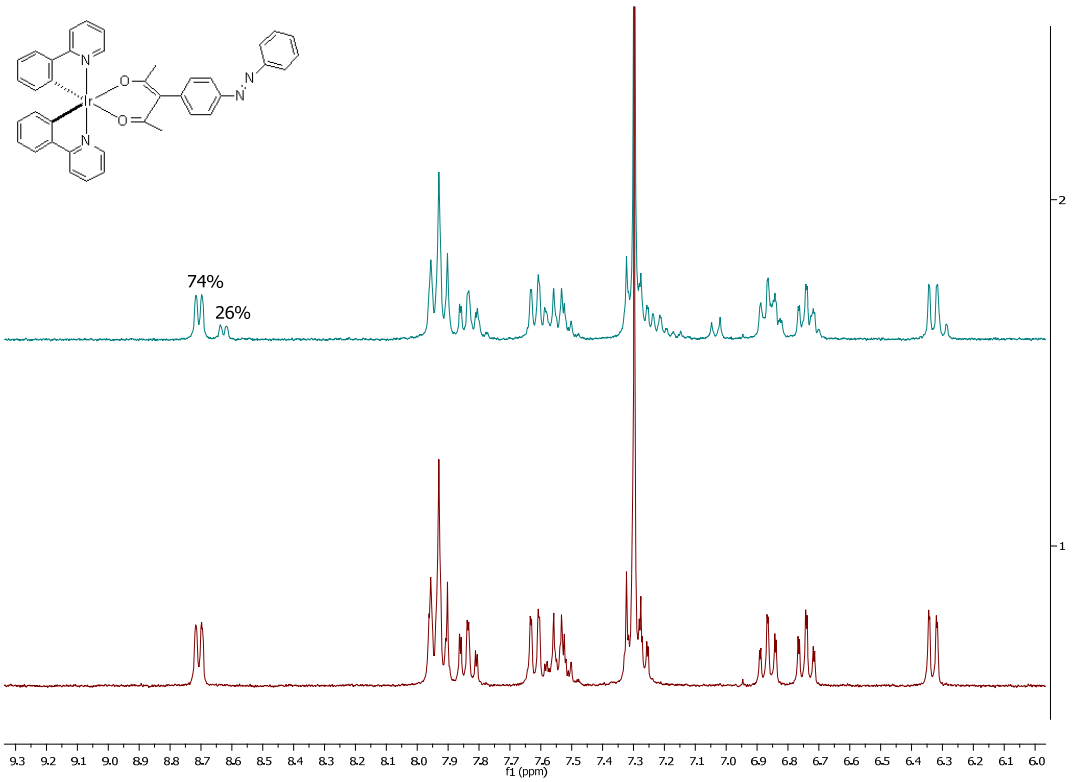

Fig. S93. ^{1}H-NMR spectra of [Ir(ppy)$_2$(**3**)] in $CDCl_3$, 300 MHz.. Before (red line) and after (blue line) irradiation at 365nm, 2.50×10^{-3} M.

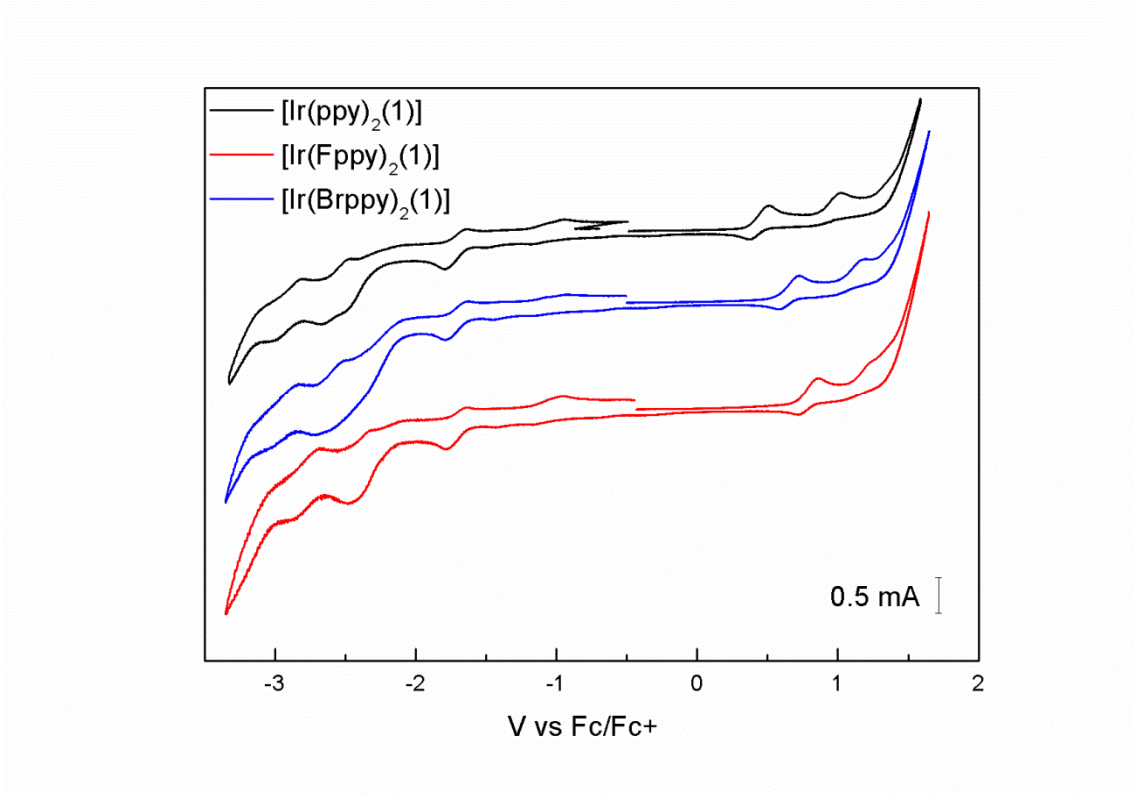

Figure S94. Cyclic voltammograms (10^{-3} M, dry DMF) of [Ir(ppy)$_2$(**1**)], [Ir(Fppy)$_2$(**1**)] and [Ir(Brppy)$_2$(**1**)] containing 0.1 M $TBAPF_6$ as the supporting electrolyte, scan rate of 100 mV s^{-1}.

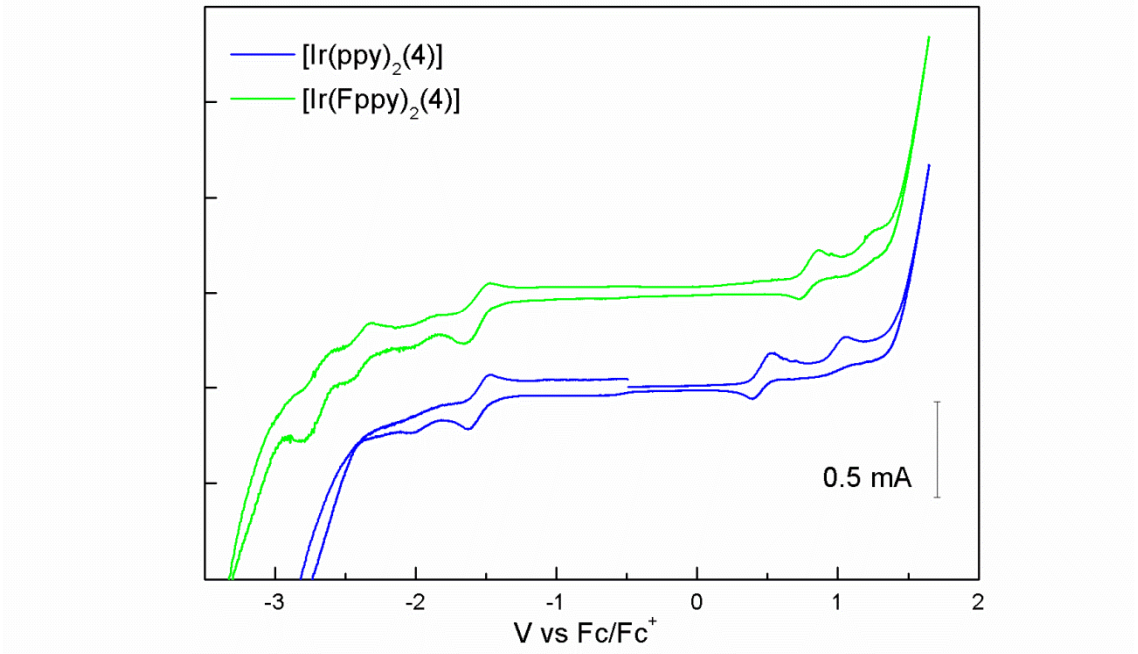

Figure S95. Cyclic voltammograms (10^{-3} M, dry DMF) of [Ir(ppy)$_2$(**4**)] and [Ir(Fppy)$_2$(**4**)] containing 0.1 M $TBAPF_6$ as the supporting electrolyte, scan rate of 100 mV s^{-1}.

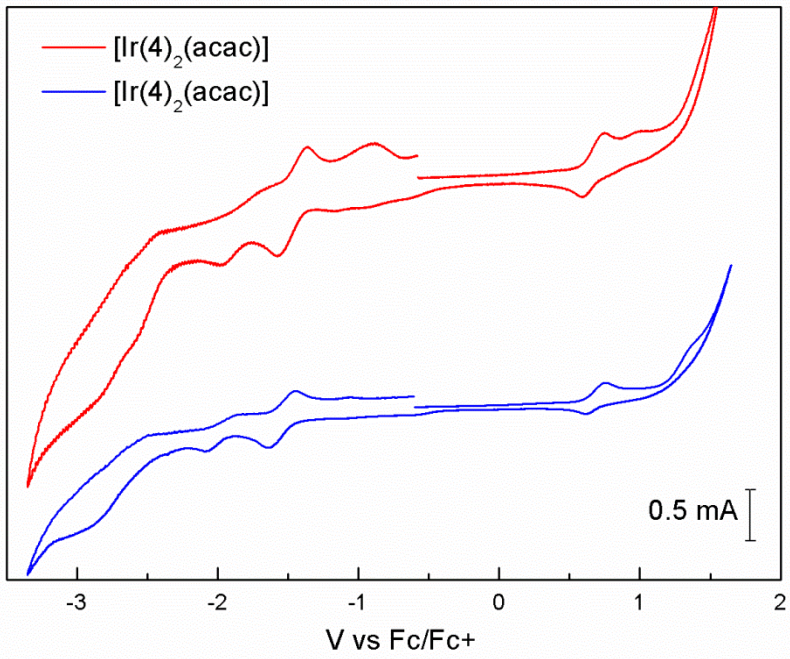

Figure S96. Cyclic voltammograms (10^{-3} M, dry DMF) of [Ir(**4**)$_2$(acac)] and [Ir(**5**)$_2$(acac)] containing 0.1 M $TBAPF_6$ as the supporting electrolyte, scan rate of 100 mV s^{-1}.

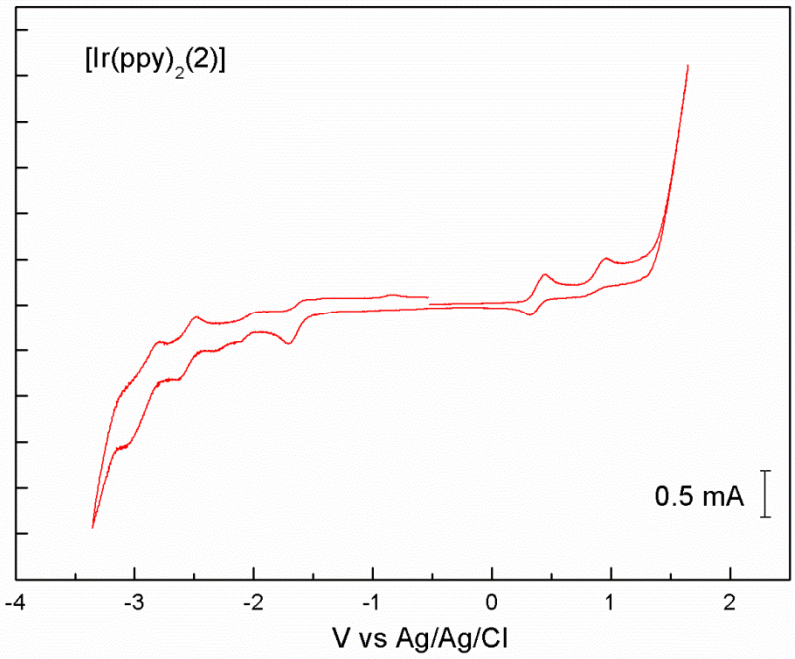

Figure S97. Cyclic voltammograms (10^{-3} M, dry DMF) of [Ir(ppy)$_2$(**2**)] containing 0.1 M $TBAPF_6$ as the supporting electrolyte, scan rate of 100 mV s^{-1}.

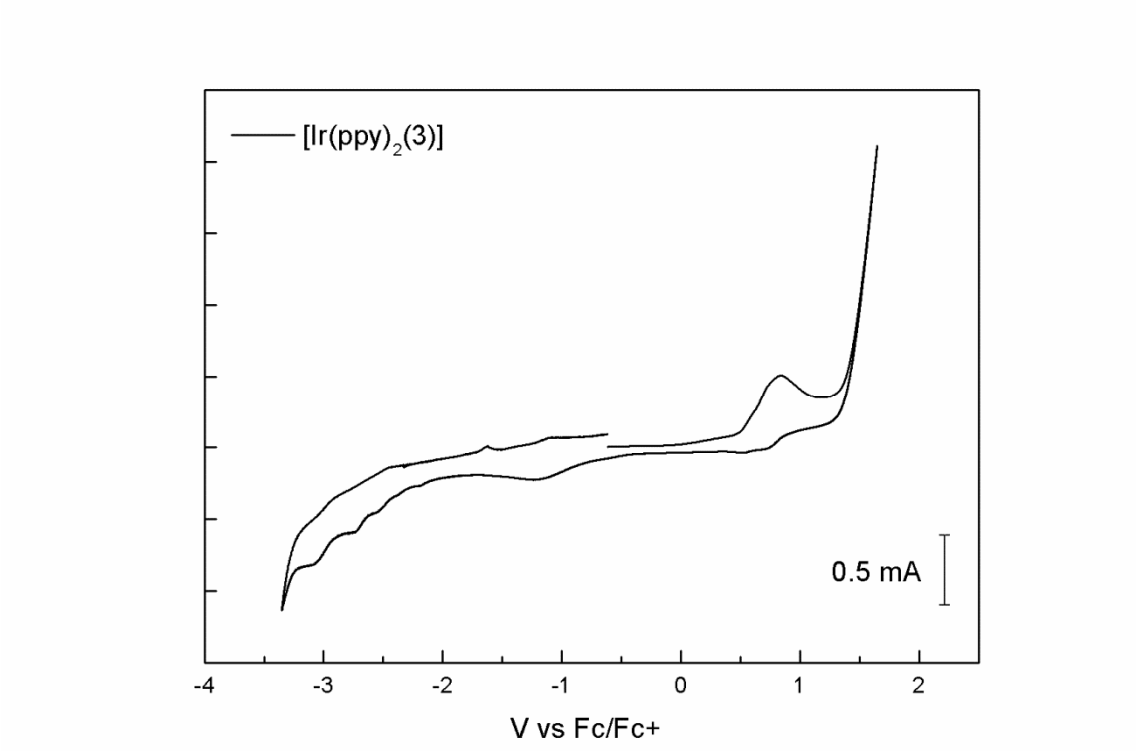

Figure S98. Cyclic voltammograms (10^{-3} M, dry DMF) of [Ir(ppy)$_2$(**3**)] containing 0.1 M $TBAPF_6$ as the supporting electrolyte, scan rate of 100 mV s^{-1}.

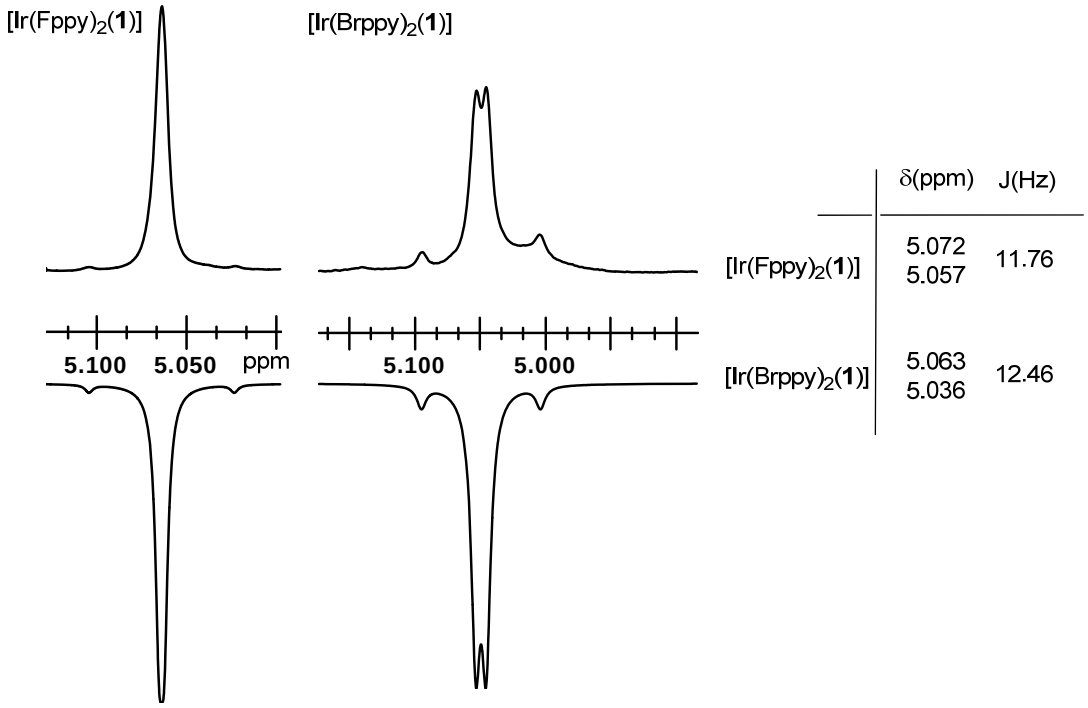

Figure S99. -OCH_2- signal of the ^{1}H-NMR spectra of compounds [Ir(Fppy)$_2$(**1**)] and [Ir(Brppy)$_2$(**1**)]. Top (experimental) bottom (simulated). Chemical shift and coupling constants used for the simulation are presented in the table.